Durability of Building and Construction Sealants and Adhesives

2nd Volume

Dr. Andreas T. Wolf
Editor

STP 1488

INTERNATIONAL
Standards Worldwide

STP 1488

Durability of Building and Construction Sealants and Adhesives: 2nd Volume

Andreas T. Wolf, editor

ASTM Stock Number: STP1488

ASTM
100 Barr Harbor Drive
PO Box C700
West Conshohocken, PA 19428-2959

Printed in the U.S.A.

Library of Congress Cataloging-in-Publication Data

Durability of building and construction sealants and adhesives / Andreas T. Wolf, ed.
p. cm. – (STP 1488)
ISBN: 0-8031-3414-2
ISBN: 978-0-8031-3414-0
1. Building materials-Testing-Congresses. 2. Sealing compounds-Testing-Congresses. 3. Sealing compounds-Deterioration-Congresses.
2. 4. Adhesives-Testing-Congresses. 5. Adhesives-Deterioration-Congresses. I. Wolf A. T. (Andreas T.) III Series: ASTM
3. special technical publication; 1488.

TA418.36.D87 2006

Peer Review Policy

Each paper published in this volume was evaluated by two peer reviewers and at least one editor. The authors addressed all of the reviewers' comments to the satisfaction of both the technical editor(s) and the ASTM International Committee on Publications.

The quality of the papers in this publication reflects not only the obvious efforts of the authors and the technical editor(s), but also the work of the peer reviewers. In keeping with long-standing publication practices, ASTM International maintains the anonymity of the peer reviewers. The ASTM International Committee on Publications acknowledges with appreciation their dedication and contribution of time and effort on behalf of ASTM International.

Printed in Mayfield, PA
April, 2006

Foreword

This publication, *Durability of Building and Construction Sealants and Adhesives*, contains papers presented at the second symposium of the same name held in Reno, Nevada, on 15-16 June, 2005. The symposium was sponsored by the ASTM International Committee C24 on Building Seals and Sealants. The symposium chairman was Andreas T. Wolf of Dow Corning GmbH, Wiesbaden, Germany.

Contents

Overview

Introduction

The Second ASTM Symposium on Durability of Building and Construction Sealants and Adhesives (2005-DBCSA) was held on June 15-16, 2005 in Reno, Nevada. The symposium brought together architects, engineers, scientists – researchers and practitioners. Their aim was to transfer new ideas, gained from laboratory research and field work, to the study of sealant and adhesive durability and the development of new products and test methods.

Nineteen papers were presented at the symposium. This book contains a selection of twelve symposium papers published by the Journal of ASTM International (JAI) prior to February 2007. JAI is an online, peer-reviewed journal for the international scientific and engineering community. Publication in JAI allows rapid dissemination of the papers as soon as they become available, while publication in this Special Technical Publication (STP) is intended to provide easy access to the condensed information in a single volume for future reference.

Since the commercial introduction of the first elastomeric sealants and adhesives about fifty years ago, major advancements have been made in our understanding of their durability and the factors governing it. The progress of sealant and adhesive technology in building and construction structures has brought with it many new materials, products, systems, designs and concepts. It has also brought an awareness of new or formerly unrealized problems relating to the durability of building and construction sealants, which ASTM C 24 Committee on Buildings Seals and Sealants is addressing.

Against a background of national and international efforts to harmonize testing and approval of building materials and structures, ASTM C 24 Committee has been looking for ways of bringing together the experience of international experts gathered in the application and testing of building and construction sealants.

The current series of ASTM symposia on Durability of Building and Construction Sealants and Adhesives is a continuation of tri-annual symposia which were inaugurated by the RILEM Technical Committee 139-DBS Durability of Building Sealants in 1994. Today, this continuing series of symposia provides the best scientific forum globally in the building and construction industry for peer-reviewed papers on all aspects of sealant and adhesive durability.

As with most scientific disciplines, substantial advances often occur through a series of small steps, rather than in giant leaps. This is also the case for the papers presented at the ASTM Symposium on Durability of Building and Construction Sealants and Adhesives (2005-DBCSA). Many of the papers reflect progress reports on on-going research.

This volume contains twelve contributions reflecting the wide spectrum of current state-of-the-art research into sealant and adhesive durability. The symposium papers cover the following topics:

- Factors Influencing the Durability of Sealed Joints and Adhesive Fixations
- Durability Studies of Sealants and Adhesives
- Development of New Test Methods and Performance Based Specifications

Below is a short overview of the papers which were published in JAI in the above three categories.

Factors Influencing the Durability of Sealed Joints and Adhesive Fixations

While our understanding of the factors influencing the durability of sealed joints and adhesive fixations has progressed substantially over the past decades, there is still much to learn. A number of papers therefore focus on this topic.

The modulus of a sealant is a key property influencing the durability of weatherproofing joints that undergo movement. For sealants subjected to cyclic movements, formulation changes resulting in a reduction in modulus will provide higher durability, if sealant fatigue and other performance properties, such as adhesion, are not simultaneously degraded. J. M. Klosowski and J. E. Plott show the utility of a melamine resin additive in reducing the modulus of polyurethane and silicon-curable polyether sealants. The authors demonstrate that addition of relative small amounts of the melamine resin results in modulus reduction and improved adhesion in the specific sealants studied. However, the short-term nature of the study does not allow a sound assessment of the long-term durability of these sealants, since potential negative effects of the additive on the long-term behavior of physical properties were not studied.

Differential thermal movement between the spacer frame and the glass panes is a key contributor to the aging of the insulating glass edge seal and of the insulating glass unit (IGU) itself. Using finite element analysis, J. E. Stewart, W. R. O'Brien, and A. T. Wolf model the thermal movements occurring in the edge seal of a large IGU as a result of temperature variations (-30°C to +60°C) for three commercially available spacer bars of different material (aluminum, galvanized steel, and stainless steel) and corner design (corner keys or bent corners). As expected, at the low temperature, the corners are pulled inward, resulting in a bending angle >90°; while at the high temperature, the corners are pushed outwards, resulting in a bending angle <90°. Monitoring the changes occurring in the thickness of the polyisobutylene primary seal along the circumference of the IGU, the authors find that the stainless steel spacer has, by far, the least effect on the change in the cross-sectional area, while the aluminum spacer has the most substantial effect. This finding is in keeping with the expected performance based on the difference in thermal expansion coefficients between spacer material and float glass. Thus, changes in the effective cross-sectional area of the primary seal available for diffusion that arise from differential thermal movements are likely to account for the observed performance differences of IGUs manufactured with different spacer materials.

Any material, that is an effective catalyst for an equilibrium reaction, catalyzes both the straight reaction as well as the reversion of the reaction. This much can be gleaned from any basic chemistry textbook. What makes predicting the durability of sealants and adhesives complicated is the fact that under weathering exposure in general several reactions occur simultaneously. Y. Cai in his paper studies the effect of tin and aminosilane – both well-known silicone condensation catalysts – on the durability of a silicone elastomeric coating. The author shows that the tin catalyst has the strongest influence on detrimental changes in elastomeric properties and on chalking, but that the aminosilane also contributes to these changes.

Durability Studies of Sealants and Adhesives

The intent of this section is to present recent studies of the durability of sealant and adhesive materials and systems.

Customers increasingly challenge sealant formulators to develop high weatherability construction sealants with ever-higher performance. The trend towards higher service-life sealants is most visible in Japan and has led there to a gradual substitution of conventional sealants, such as polyurethanes, by higher performance sealants, such as silane curable organic sealants. Building on experience gained in Japan, C. Urban, T. Matsumoto, S. Tomari, and F. Adeleu in their paper discuss some of the factors that influence weatherability and durability of one-component sealants, such as binder, pigments, stabilizers, and catalysts. The authors compare conventional polyurethane sealants to silane curable sealants based on polypropylene oxide or polyacrylate backbones and mixtures of these two backbones. As expected, binder and stabilizer have the most notable influence on weathering resistance; however, catalyst, titanium dioxide, and plasticizer also affect the weathering behavior. For optimum weathering performance, all raw materials influences need to be carefully tested. Combinations of raw materials, especially in the case of stabilizers, may have synergistic effects, but may also reduce the weathering resistance. The authors also highlight the fact that a minimum of 1500–2000 hours of accelerated weathering should be used to assess the durability of construction sealants, and that for more demanding applications, 5000 hours, 10 000 hours, or an even longer duration of accelerated weathering may be required.

The second paper by Y. Masaoka, Y. Nakagawa, T. Hasegawa, and H. Ando also deals with the durability of silane curable organic sealants. In this paper, the authors discuss the durability and performance of sealants based on a novel telechelic silane curable acrylate polymer in contact with photocatalytic self-cleaning glass. Conventional sealants, when used in this application, often lack sufficient weatherability or involve the risk of hydrophobic staining of the self-cleaning glass. Sealants based on the novel telechelic silane curable acrylate polymer retain good adhesion to the self-cleaning glass even after more than 10 000 hours of exposure to UV irradiation in a super-accelerated xenon-arc weathering machine. Based on outdoor exposure of the test samples for two months and measurement of contact angles before and after exposure the authors conclude that these novel sealants have very low staining potential on photocatalytic coatings.

Since its introduction nearly four decades ago, structural silicone glazing (SSG) has become a popular glazing method for curtain wall construction. The major difference between SSG systems and the more widely used 'dry-glazed' systems is that glass lights or panels in SSG systems are adhered to the supporting glazing frame with structural silicone sealant along either two edges of the glass panel or all four edges. It is generally believed that SSG systems perform well in seismic regions due to the 'resilient attachment' of glass to the glazing frame. This notion has merits in four-sided SSG systems, but has not been previously substantiated for two-sided systems, wherein the top and bottom edges are typically captured in metal glazing pockets. The research presented by A. M. Memari, X. Chen, P. A. Kremer, and R. A. Behr in their paper therefore is aimed at characterizing the serviceability and ultimate behavior of two-sided SSG curtain walls under cyclic racking displacements. Serviceability drift capacities corresponding to damage states such as gasket distortion, weather-seal and structural seal failures leading to air leakage and glass cracking are identified. Based on the results obtained in this study and comparisons with data collected during comparable studies on dry-glazed curtain walls, the authors conclude that serviceability and ultimate drift capacities of two-sided SSG systems under seismic conditions are significantly higher than their dry-glazed counterparts.

Development of New Test Methods and Performance Based Specifications

The final section of the collated symposium papers reviews attempts at developing new test methods for assessing the durability of sealants and adhesives, and, at reaching the ultimate goal, the development of performance-based specifications.

Structural silicone sealants are used to attach glass or other panels to curtainwall framing systems. These sealants must possess sufficient structural strength to carry the wind-loads but must also have sufficient movement capability to resist the fatigue caused by cyclic shear movement. Cyclic shear movement is induced in the structural sealant by differences in the thermal expansion between the glazing panel and the curtainwall substructure undergoing variations in temperature. Temperature variations occur in response to changes in atmospheric conditions (clouds, rain, etc.), as well as diurnal or seasonal climate changes. Assuming the occurrence of a cyclic shear exposure event twice a day, a structural sealant is exposed to 36 525 cycles over a period of 50 years. In their paper, L. D. Carbary, E. D. Bull, and S. S. Mishra expose nine silicone sealants with rated movement capabilities of 12.5%, 20%, 25% and 50% to at least 36 000 cycles of cyclic shear movement with 15% strain at a rate of five cycles per minute. It should be noted that realistically, thermal movement displacements for in-service curtainwalls will rarely approach strains of 15%. Products with a movement capability of 12.5% have been performing without failure for many years lending credence to this point. While the tested structural silicone sealants experience degradation as a result of the cyclic shear exposure, the degradation is small enough not to induce rupture, if the sealants are not strained beyond their movement capability. The sealants with higher movement capability show less susceptibility to degradation than sealants with lower movement capability. The authors suggest that this test method can provide a basis and a model from which to further study fatigue and to provide some guidelines and understanding of how the structural silicone sealants react to repetitive loading. They also speculate that further development of this method may result in its inclusion in the ASTM C1184 Specification for Structural Silicone Sealants.

The expectations of building owners for waterproofing systems are simple. Waterproofing must prevent the passage of water (impermeability), must be capable of successful installation under typical construction conditions (constructability), and must continue to provide waterproofing for the life of the structure (durability). The realization of these expectations is thwarted, in part, by a lack of consensus on how these features are defined, tested, and compared to performance-based criteria. J. C. Strong, J. R. Kovach, and V. S. Eng in the first part of their paper investigate important properties of waterproofing materials commonly used on plazas and below-grade walls and review the acceptance criteria of ASTM International, Canadian General Standards Board (CGSB), and International Code Council (ICC) Evaluation Services (ES) standards for waterproofing systems. In order to overcome the discrepancies between these standards, the authors recommend an open dialogue between the groups responsible for waterproofing material specifications in ASTM, CGSB, and the ICC ES. In the second part of their paper, the authors contribute two exploratory studies on the initial leakage resistance of bentonite waterproofing and the water absorption in cold liquid-applied waterproofing. Based on this testing, the authors suggest specific improvements in the relevant standards.

In November 2000, the Architectural Institute of Japan (AIJ) established a subcommittee chartered with developing an accelerated weathering test method suitable for assessing the durability of sealants. In their paper, N. Enomoto, A. Ito, I. Shimizu, T. Matsumura, Y. Takane, and K. Tanaka report interim results obtained with the proposed test method. In this method, the weatherability of sealants is studied using newly developed test specimens, which enable exposure of the cured sealants to simultaneous compression and extension in a single test specimen. The study comprises twenty-four sealants of seven chemical types commercially available in Japan. Interim results are reported after twelve months of natural outdoor weathering at three exposure sites in Japan (north: Hokkaido, central: Chiba, and south: Okinawa) and 3500 hours of artificial accelerated weathering with xenon lamp and carbon flame weathering devices. The interim results confirm that the surface degradation of sealants is accelerated by the additional movement cycles, and that the differences in the degradation among the sealants are becoming observable after the current exposure durations.

In their paper, H. Miyauchi and K. Tanaka propose a new design and service life assessment method for sealed joints exposed to seismic events. The paper is the culmination of several years of research by the two authors. In this research, the fatigue resistance of sealed joints to relative story displacement movements caused by earthquakes was studied experimentally and analytically. The authors now propose a new joint design method, which provides adequate sealed joint performance over the joint's service life. The design method is based on three criteria, i.e., type of sealant, effect of cross-sectional size and shape of the sealed joint, and fatigue resistance of the sealant at intersectional zones of sealed joints to the sliding and rocking motions of curtain wall panels. The process of sealed joint design considers the relationship between the number of cyclic movements to which the sealed joint is exposed during its service life and the number of cycles to crack initiation in the sealed joint as observed in the fatigue test method developed by the authors. Finally, the approach suggested by the authors allows the calculation of the accumulated damage level and the expected service life of a sealed joint.

In their paper, A. T. Wolf, S. Sugiyama, and F. Lee report on the use of an optical imaging and image analysis system in the assessment of surface changes induced in sealants by outdoor weathering. The method allows quantification of four distinct surface defects in the samples, namely cracking (crazing), visual color change, spatial uniformity of deterioration (due to dirt pick-up and uneven color change, or both), and overall surface texture. Chalking and dirt pick-up, as rated visually prior to the evaluation, cannot be accurately assessed with the digital imaging technique employed. The analysis shows that surface cracking and crazing generally can be well characterized using the automated image analysis system. While this study represents a step in the right direction, the authors suggest that further investigations are needed to develop an automated surface characterization method for sealants.

With current expectations for building exteriors to prevent all air and water entry into the building interior, the need for a near perfect seal of weatherproofing sealant joints has reached new levels of intensity. The need for better field tests has increased accordingly. To reach these goals, ASTM C-1521-02a Standard Practice for Evaluating Adhesion of Installed Weatherproofing Sealant Joints has been developed and adopted. The practice outlines a nondestructive procedure. The advantage of this methodology is that it allows an unlimited amount of testing to be conducted. While the procedure does not specify a specific instrument to induce the strain on the sealant/substrate bond-line, a device able to accomplish this procedure in a uniform, controlled, and calibrated fashion has been developed. The paper by D. Huff outlines a description of the device and its capabilities. The paper also provides a discussion of the use of statistical sampling when the option of complete testing is not feasible or required.

Closure

As we publish this volume, I look forward to the next Symposium on Durability of Building and Construction Sealants and Adhesives (2008-DBCSA) and the associated flurry of papers in this dynamic industry. I encourage all readers to participate in the work of ASTM C24 committee, to attend the future symposia and to contribute new papers. Your participation and feedback help to advance the industry and, as a result, we will all benefit from improvements to our built environment.

In closing, I would like to gratefully acknowledge the outstanding quality of the contributions made by the authors as well as the dedicated efforts of the 2005 session chairpersons, the peer reviewers, and the staff of ASTM and AIP, who all helped to make the 2005 symposium and the publication of the associated papers possible.

Andreas T. Wolf
Wiesbaden, Germany

Factors Influencing the Durability of Sealed Joints and Adhesive Fixations

Journal of ASTM International, Vol. 3, No. 4
Paper ID JAI13415
Available online at www.astm.org

Jerome M. Klosowski[1] *and John E. Plott*[2]

Reducing Modulus of Sealants to Improve Durability

ABSTRACT: The premise is that if one reduces sealant fatigue by lowering modulus while leaving other characteristics of a sealant unchanged, its durability will improve. Reducing sealant fatigue is seen as a positive consequence of lowering the modulus of elasticity of a sealant. The data shows the effect of incorporating a modulus modifier in one- and two-part (standard curing) urethane sealants and a one-part silane curing polyether sealant. This approach lowers modulus with no or minimum reformulation.

KEYWORDS: sealant, additive, adhesion, modulus, elongation, movement, durability

Introduction

Most sealants are not used as structural adhesives. The majority of sealants are intended to fill holes and joints and move when the joint moves and adhere the whole time. Sealants that are somewhat softer but remain elastomeric are more suited for those applications having high joint movement like expansion joints, curtain walls, highway pavement joints, parking decks, and bridges. For example, a sealant that can take +/−25 % joint movement is considered more useful and can be used in more applications than a sealant +/−12.5 % or +/−20 % joint movement. That is true right up the line, with +/−30, 40, and 50 % joint movement all being more useful. Therefore, additives that lower the modulus of elasticity can be very useful if indeed they lower the modulus of elasticity and are accompanied by higher elongation. The key benefit seen is that they are more capable of handling higher joint movement while lessening stresses on the substrates resulting in greater durability and longevity. This is especially important if the substrate is relatively weak like Exterior Insulation Finished System (EIFS) or with many cementatious surfaces. In essence, the joint lasts longer when less stress is introduced. When joints last longer, buildings last longer.

To that end, a melamine type additive was evaluated in different concentrations and solvents with several sealant types to see if a beneficial change in performance could be achieved.

Procedure

A melamine type additive supplied by The C.P. Hall Company (Chicago, Illinois) was added at levels ranging from 0.3 to 6.0 % solids in solution to various sealants including a one- and two-part urethane sealant, and a one-part silane curing polyether sealant.

Solution concentrations were maintained at 85 % solids and 15 % solvent; solvent types included 2-ethylhexanol (2EH) and Methyl isobutyl ketone (MIBK). The study looked at changes in sealant physical properties and changes in substrate adhesion. Physical property testing included sealant resilience as measured with a plastometer, and the sealant stress/strain relationship as measured from stressing typical C 719 (or ISO 9047) configured sealant joints. The adhesion was studied after 21-day cure using the 90 deg peel test done at ambient conditions and then at 7-, 14- and 21-day 50°C water immersions. The peel test was appropriate for this study since it is comparing a product to itself and variations within a given formula.

Manuscript received May 23, 2005; accepted for publication October 20, 2005; published online February 2006. Presented at ASTM Symposium on Durability of Building and Construction Sealants and Adhesives, Second Symposium on 15–16 June 2005 in Reno, NV; A. T. Wolf, Guest Editor.

[1] President of Klosowski Scientific Inc., Chief Chemist—Engineering Diagnostics Inc., FASTM, Retired Senior Scientist, Dow Corning Corporation, Klosowski Scientific Inc., 3031 State Street Rd., Bay City, Michigan 48706.

[2] President, The Performance Strategy Group, www.performancestrategygroup.com, Registered Professional Engineer, Certified New Product Development Professional, John E. Plott, PE LLC, 6000 Woodpark Drive, Midland, MI 48640.

TABLE 1—*Additive adhesion testing of two-part urethane sealant (dry and 9 days wet).*

	Concrete[a]		Glass[a]		Kynar[a]		PVC[a]		Aluminum[a]	
	dry	9d wet	dry	9d wet	dry	9d wet	dry	9d wet	dry	9d wet
Control	5	4 to 5	5	5	2	0-1	5	5	5	5
2-EH (alcohol only) at 0.26 %	5	5	5 to 4	4 to 5	3	3	5	4	5	5
Resin 2-EH at 0.3 %	4	4 to 5	5	5	2	0-1	5	5	5	5
Resin in 2-EH at 0.65 %	4	4 to 5	5	5	2	1	5	5	5	5
Resin in 2-EH at 1.7 %	5	5	4 to 5	5	3	0-1	5	5	5	5

Note: The resin additive was 85 % solids, 15 % 2EH solvent. 5=cohesive failure, 4=partial cohesion, 3=strong adhesion but adhesive failure, 2=moderate adhesion, 1=weak adhesion, 0=no adhesion

[a]Unprimed

For one part sealants, 94 g of sealant was put into the disposable cups that go with the (DAC) 150 mixer and 0.65, 1.7, 4.0, 6.0 % additive solution was added. Each time it was mixed in gently by hand, and then mixed for 26 s, the top removed, scrapped down, and mixed again for 26 s. The head space was purged with an inert gas and the container was sealed and left to sit for 24 h to equilibrate. A 10 cc syringe with the bottom removed was used to draw the sealant and inject it into the test joints. The joints had Teflon®[3] spacers and were 12 mm by 12 mm by 50 mm ($\frac{1}{2}$ by $\frac{1}{2}$ by 2 in.). Separately, a 3 mm (1/8 in.) thick slab of the same sealant was prepared by tooling the sealant between 3 mm (1/8 in.) spacers to check cure rate and durometer. For each test, a control was made and handled in the same manner.

The two-part sealants were handled in a similar fashion with the additive introduced into the base, allowed to equilibrate for 24 h. The pigment and activator were then added, mixed 12 s, scrapped down, mixed again for 12 s and then placed into joints and into a slab as done with the one part sealants.

The additive in 2EH represented 0.3, 0.65, and 1.7 % of the total sealant formulation; the additive in MIBK represented 4.0, 5.0, and 6.0 % of the sealant formulation. The resin additive was 85 % solids and 15 % solvent in each case. In each set of experiments, a separate experiment was run using 2EH and MIBK in the amount that is present in the additive solution.

No attempt was made to optimize the order of addition, sealant equilibration time or other manufacturing variables.

With each sealant and additive combination, an adhesion study was done on concrete, EPDM, glass, Kynar, PVC, cold rolled steel, anodized aluminum and brass. For this study, the concrete was wiped free of dust; the EPDM was wiped with xylene; the glass cleaned with IPA/water; the Kynar was wiped with MIBK, and the cold rolled steel with toluene. In each case the surface was cleaned twice, using the two-rag method each time, one to wipe it on and the other to wipe it off. These were than coated with approximately $\frac{1}{4}$ in. thick by 1 in. wide sealant in strips and cured for 21 days. The adhesion was checked by forming a tab and pulling at 90 deg to the surface noting the resistance to the pull and the mode of failure. After the initial check, the samples were put into a 50°C water bath for one week, then checked, then re-immersed and rechecked on a periodic basis (e.g., 9-days wet (two-part urethane), 21-days wet (one-part urethane), 35-days wet (one-part silane curing polyether). These results were then compared to the control (without additive). Tables 1–3 represent the data generated from these experiments with various additive levels and solvent types.

Discussion

For purposes of this evaluation, adhesion data was based on the following number scale: 5 equals cohesive failure, 4 equals partial cohesion, 3 equals strong adhesion but adhesive failure, 2 equals moderate adhesion, 1 equals weak adhesion and 0 equals no adhesion, that is, the sealant almost falls off the substrate.

Tables 1–3 show the adhesion results for both one- and two-part urethane sealants and one-part silane curing polyether for the control and with various additive levels and solvent types.

In all cases, the additive did not hurt adhesion, and with several substrates, adhesion was improved. Pictures of actual samples tested are also shown in Figs. 1–3.

Standard cure, two-part urethane control on aluminum joint (left) showing 100 % adhesive failureand

[3]Teflon® is a registered trademark of the DuPont Corporation.0.

TABLE 2—*Additive adhesion testing of one-part urethane sealant (dry and 21 days wet).*

	Concrete[a]		EPDM[a]		Glass[a]		Kynar[a]		PVC[a]	
	dry	21d wet	dry	21d wet	dry	21d wet	dry	21d wet	dry	21d wet
Control	3	3	1	5	2	5	1	4	2	3
2-EH at 0.35 %	5	5	2	5	3	5	2	5	3	5
Resin in 2-EH at 0.65 %	3	5	1	5	2	4	1	3	3	4
Resin in 2-EH at 1.1 %	3	5	1	5	3	4	1	4	1	4
Resin in 2-EH at 1.7 %	3	5	1	5	3	5	1	4	1	5
Resin in 2-EH at 2.2 %	3	5	1	5	3	5	1	5	2	5
Resin in 2-EH at 2.8 %	5	5	2	5	5	5	2	5	2	5

Note: The resin additive was 85 % solids, 15 % 2EH solvent; 5=cohesive failure, 4=partial cohesion, 3=strong adhesion but adhesive failure, 2=moderate adhesion, 1=weak adhesion, 0=no adhesion

[a]Unprimed

1.7 % additive in 2EH (right) in the same formulation showing 100 % cohesive failure.

Standard one-part urethane control on concrete joint (left) showing 100 % adhesive failure; versus 1.7 % additive in 2EH in the same formulation (right) showing 100 % adhesive failure.

TABLE 3—*Additive adhesion testing of one-part silane curing polyether (dry and 35 days wet).*

	Concrete[a]		EPDM[a]		Glass[a]		Kynar[a]		PVC[a]		Steel[a]		Aluminum[a]		Brass[a]	
	dry	35d wet	dry	35d wet	dry	35d wet	dry	35d wet	dry	35d wet	dry	35d wet	dry	35d wet	dry	35d wet
Control	5	2	0-1	0	5	5	3	3	1	1	5	2	4	5	2	0
Resin in MIBK at 4.0 %	5	2	0-1	0	5	5	3	5	0	0	5	3-4	5	5	4-5	2
Resin in MIBK at 5.0 %	5	2	0	0	5	5	2	3	0	0	5	3-4	5	5	3	2
Resin in MIBK at 6.0 %	5	2-3	0	0	5	5	2	3-4	0	0	4-5	2	2-3	5	2-3	1-2

Note: The resin additive was 85 % solids, 15 % MIBK solvent. 5=cohesive failure, 4=partial cohesion, 3=strong adhesion but adhesive failure, 2=moderate adhesion, 1=weak adhesion, 0=no adhesion

[a]Unprimed

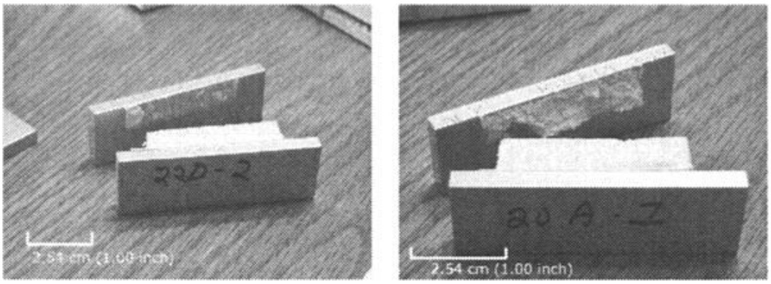

FIG. 1—*Two-part urethane on aluminum (left) and with additive (right).*

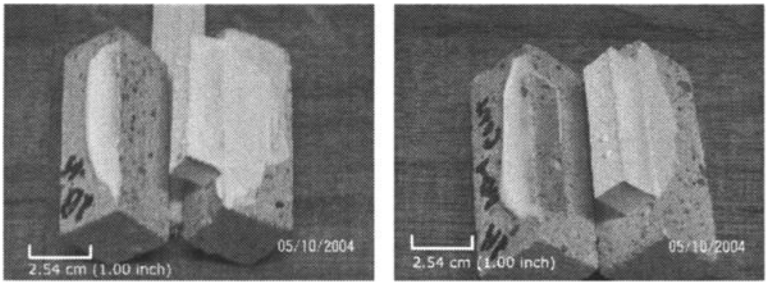

FIG. 2—*One-part urethane on concrete (left) and with additive (right).*

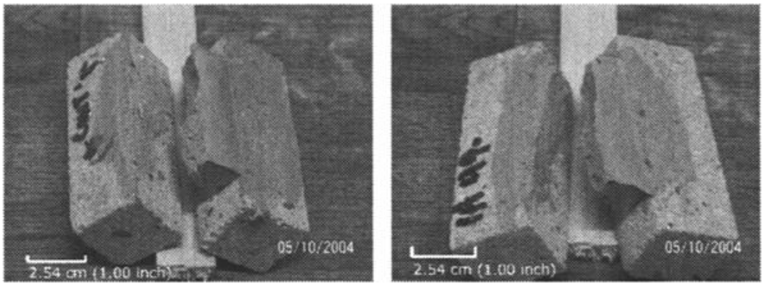

FIG. 3—*1-part silane curing polyether on concrete (left) and with additive (right).*

One-part silane curing polyether control on concrete joint (left) showing 40 % cohesive failure versus 4.0 % additive in MIBK (right) showing 70 % cohesive failure.

The photos reinforce the previous comment that the additive solution does not harm adhesion and may have some improvement.

Additional testing was done to validate the effect of the additive on sealant modulus. Within an optimum range of additive level—that is, 1.7 % in 2EH for one- and two-part urethane sealants, and 4.0 to 6.0 % in MIBK for one-part silane curing polyether sealant—the elongation increased approximately 60 % percent. When the equivalent amount of solvent was used without additive, tensile force was lowered but no resultant increase in elongation was seen. See Figs. 4–6.

Conclusions

The data indicates that relatively low levels of the additive—that is, 1.7 % in 2EH for one- and two-part urethanes, 6.0 % in MIBK for silane curing polyether sealants—lowers sealant modulus without negatively affecting substrate adhesion. 2EH (alcohol) by itself lowered the pull force but did not increase sealant elongation versus the additive in solvent which did. In separate controls, the additive in MIBK was also evaluated and found to be useful in lowering modulus and increasing sealant elongation in one-part silane curing polyether sealants. In data not shown in this paper, the additive in both 2EH and MIBK lowered the modulus in proportion to the concentration level used while increasing elongation to produce a very interesting product with enhanced joint movement abilities leading to increased sealant durability. In other

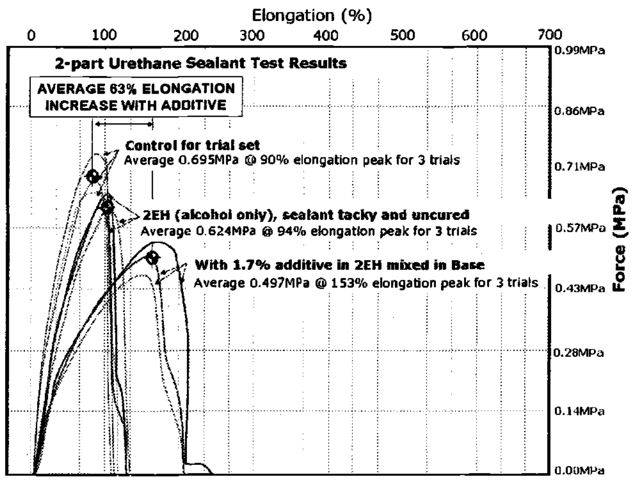

FIG. 4—*Elongation comparison of two-part, urethane sealant (unprimed) with and without additive.*

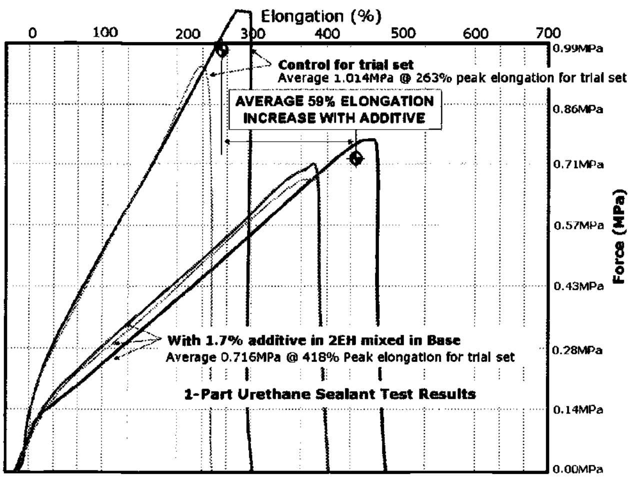

FIG. 5—*Elongation comparison of one-part, urethane sealant (unprimed) with and without additive.*

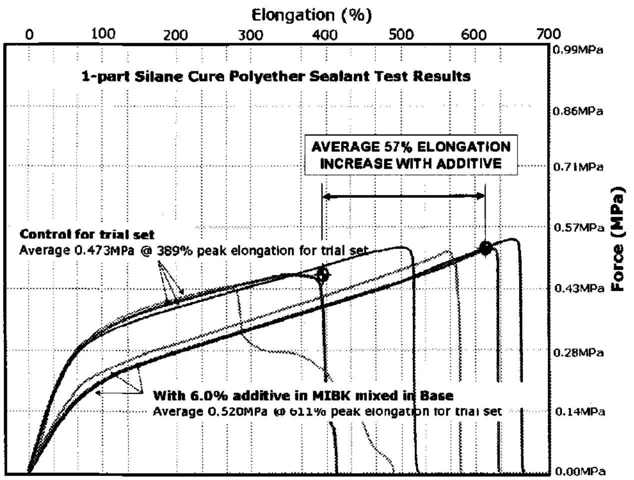

FIG. 6—*Elongation comparison of one-part, silane curing polyether sealant (unprimed) with and without additive*

data not shown in this paper, higher levels of 2EH (alcohol) inhibited cure rate and caused the surface to remain tacky for extended periods. For this reason, MIBK was substituted for 2EH when additive concentrations above 1.7 % were used. As shown in these tables, lower concentrations of additive were especially useful in one- and two-part urethane formulations in that they had little effect on cure rate or tackiness or adhesion but a significant effect on movement ability and modulus of elasticity. Also, higher concentrations of additive in MIBK were more useful in the silane curing polyether sealants again with little effect on cure rate, tackiness or adhesion but a significant effect on movement ability and modulus.

A key observation is that the melamine type additive, while having a pronounced effect on physical properties, had no detrimental effects on adhesion. These could be very useful in extending the sealants joint movement capabilities into the higher movement (+/−50 %) ranges.

To the extent that joint movement ability, enhanced by lowering sealant modulus and increasing elongation, is a factor in joint durability, an additive like this could contribute to increased durability and broaden the range of application.

Remarks

The melamine type additive is a proprietary material available from C. P. Hall Inc of Chicago, IL.
Urethane sealants were commercially available; suppliers did not wish to be identified at this time.
One-part silane curing polyether sealant was a proprietary product from a supplier also not wanting to be identified at this time.
Adhesion substrates of glass, aluminum, and concrete were the standard ASTM specimens. The others were commercially available both off the shelf.
The mixer used was a DAC 150, an early version of the centrifugal mixers available from Flacktek Inc. of Landrum, South Carolina.
All solvents were commercial grade from local hardware stores.
Stress/strain testing was done on an Instron run at a crosshead speed of 2 in. per minute.

Journal of ASTM International, Vol. 3, No. 8
Paper ID JAI13121
Available online at www.astm.org

James E. Stewart,[1] *William R. O'Brien,*[2] *and Andreas T. Wolf*[3]

Quantification of Differential Thermal Movement in Insulating Glass Edge Seals Using Finite Element Analysis

ABSTRACT: Differential thermal movement between the spacer frame and the glass panes is a key contributor to the aging of insulating glass edge seal and of the insulating glass unit (IGU) itself. Using finite element analysis (FEA) the authors modeled the thermal movements occurring in the edge seal of a large IGU (1.5×2.1 m^2) as a result of temperature variations (−30°C to +60°C) for three commercially available spacer bars of different material and design. The model was based on nylon corner keys for the aluminum and galvanized steel spacers and bent corners for the stainless steel spacers. The nylon corner keys were assumed to be solid and firmly bonded to the spacers; whereas the bent corners were modeled as solid, bent metal corner keys, also firmly bonded to the spacers. Since actual bent corners are hollow, the model tends to overestimate the stresses for this corner design. As expected, at the low temperature, the corners are pulled inward, resulting in a bending angle >90°; while at the high temperature, the corners are pushed outwards, resulting in a bending angle <90°. Monitoring the changes occurring in the thickness of the polyisobutylene primary seal along the circumference of the IGU, the authors found that the stainless steel spacer had, by far, the least effect on the change in the cross-sectional area, while the aluminum spacer had the most substantial effect. This finding is in keeping with the expected performance based on the difference in thermal expansion coefficients between spacer material and float glass. Thus, changes in the effective cross-sectional area of the primary seal available for diffusion that arise from differential thermal movements, are likely to account for the observed performance differences of IGUs having different spacer materials.

KEYWORDS: Insulating glass unit, differential thermal movement, spacer, finite element analysis

Introduction

Insulating glass units (IGUs) are exposed to a variety of environmental factors, such as temperature and atmospheric pressure fluctuations, wind loads, working loads, sunlight, water, and water vapor that negatively affects their service life [1]. During service, the edge seal of the glazed IGU is exposed to a microclimate within the window frame or curtain-wall construction that strongly deviates from the ambient climate. Two major studies have been conducted in an effort to monitor this microclimate in terms of edge-seal temperature, moisture, and presence of liquid water over a period of several years [2,3]. Whereas in Central Europe edge-seal temperatures of clear glass IGUs seldom exceed 40–50°C, for tinted or coated glass units or in warm climates service temperatures may well reach 80°C and above for prolonged periods of time [4].

In order to withstand these environmental loads, an IGU edge seal must have the following properties:

- Durability, i.e., resistance against environmental factors (both in terms of physical properties and adhesion).
- Structural strength that constrains movement in the edge-seal to minimize changes in the effective cross-sectional area of the primary seal available for diffusion.
- Low moisture- and gas-permeability under service conditions.

Differential thermal movement between the spacer and the glass panes is a key contributor to the aging of the insulating glass edge seal and of the IGU itself. Repetitive shear and tensile cycling induces a pumping effect in the polyisobutylene (PIB) primary seal that over time displaces the primary seal and

Manuscript received May 5, 2005; accepted for publication May 4, 2006; published online June 2006. Presented at ASTM Symposium on Durability of Building and Construction Sealants and Adhesives on 15–16 June 2005 in Reno, NV; A. T. Wolf, Guest Editor.

[1] Senior Engineer, Dow Corning Corporation, Midland, MI 48686.
[2] Marketing Specialist, Dow Corning Corporation, Midland, MI 48686.
[3] Scientist, Dow Corning GmbH, 65201Wiesbaden, Germany.

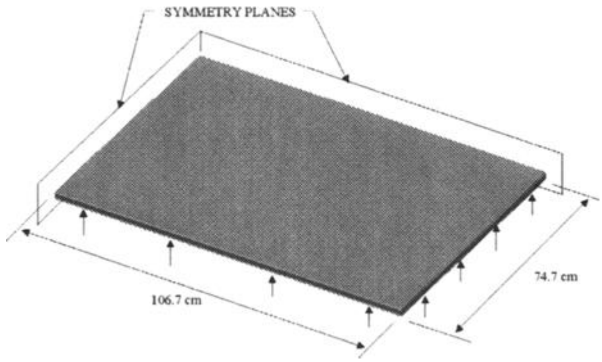

FIG. 1—*Glass pane element modeled.*

generates voids, resulting in an increased leakage rate of the IGU. Depending on the physical properties of the secondary seal, the mechanical cycling may also induce fatigue aging in the edge seal. Finally, the differential thermal movement also affects the opening of the primary and secondary seals and, therefore, the effective cross section through which diffusion of water vapor and fill gases occurs. Therefore, a quantitative evaluation of the magnitude of differential thermal movements in an IGU edge-seal configuration is essential in predicting the service life of an IGU.

Finite Element Analysis (FEA) Evaluation

Using finite element analysis (FEA) the authors modeled the thermal movements occurring in the edge seal of a large IGU as a result of temperature variations for three commercially available spacer bars of different material and design.

Modeling Considerations

An IGU window size of 1.49 m (58.8 in.) by 2.13 m (84 in.) was chosen for the FEA modeling. This size simulates a large sliding glass door, with the same aspect ratio (1.42857) as the 0.35 m (14 in.) by 0.50 m (20 in.) test panes. Taking advantage of symmetry, the model needs only to take one quarter of the full size into account. In the model, the pane is supported along the bottom perimeter edge as shown by the arrows in Fig. 1. Element nodes on symmetry planes are constrained to remain on the symmetry planes.

Galvanized steel and aluminum spacers are modeled with dimensions 12.3 mm (0.485 in.) wide and 8 mm (0.315 in.) deep and a wall thickness of 0.4 mm (0.016 in.) for aluminum and 0.5 mm (0.020 in.) for galvanized steel. Corner keys for galvanized steel and aluminum spacers are modeled as solid polyamide (Nylon® 6) keys that are "bonded" to the spacers (the model does not allow for any slippage between the spacer and the corner keys). Figure 2 shows the spacer and corner key designs and dimensions chosen.

The stainless steel spacer is modeled with dimensions of 11.5 mm (0.454 in.) wide and 6 mm (0.235 in.) deep with a wall thickness of 0.2 mm (0.01 in.). The corner key is modeled as "bonded" to the spacers and as a solid. The actual corner key is hollow and the metal is split at the inner radius, therefore the stress predicted by the model is much higher than the actual stress expected in service. Figure 3 shows the stainless steel spacer and corner key designs and dimensions chosen.

The edge seal of the galvanized steel and aluminum spacer is modeled with the secondary seal constrained by "bonding" to the spacer and the glass panes, but not to the nylon corner key, reflecting the fact that secondary sealants generally have poor adhesion to plastic corner keys. For the stainless steel spacer, the edge seal is modeled with the secondary seal constrained by "bonding" to the glass panes and the spacer, as was the case for the galvanized steel and aluminum spacers. However, the corner keys in this instance are bonded to the secondary seal as well as the edges in contrast to that described for the other two spacer types.

The secondary sealant thickness—measured as coverage above the spacer—is assumed as 6 mm. The glass thickness is modeled as 6 mm (0.236 in.) and a 0.3 mm (0.019 in.) gap is assumed for the primary

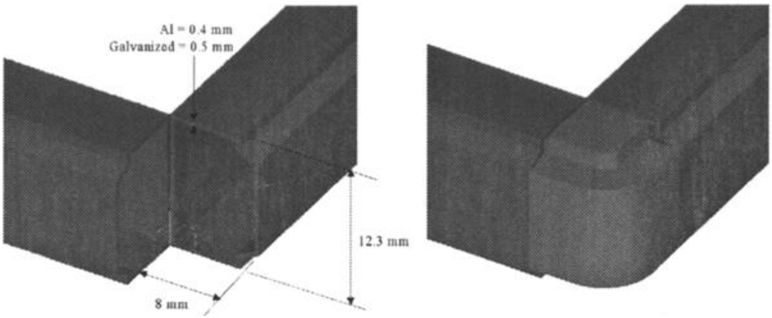

FIG. 2—*Spacer (aluminum and galvanized steel) and corner key designs and dimensions.*

seal. The polyisobutylene (PIB) material itself was not modeled, due to the low strength of the material. Figure 4 shows the edge-seal configurations for the aluminum and galvanized steel spacers and the stainless steel spacer.

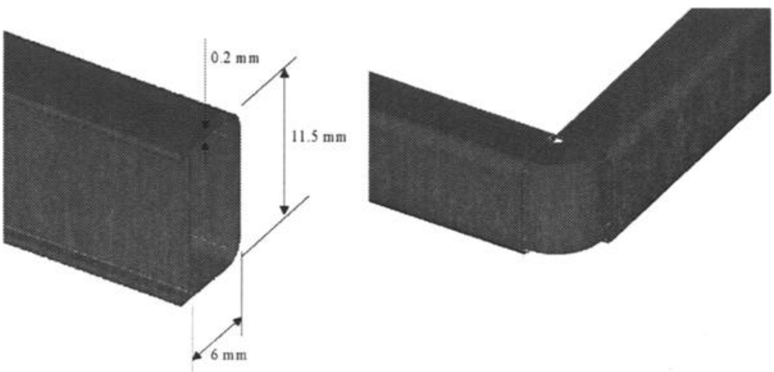

FIG. 3—*Stainless steel spacer and corner key designs and dimensions.*

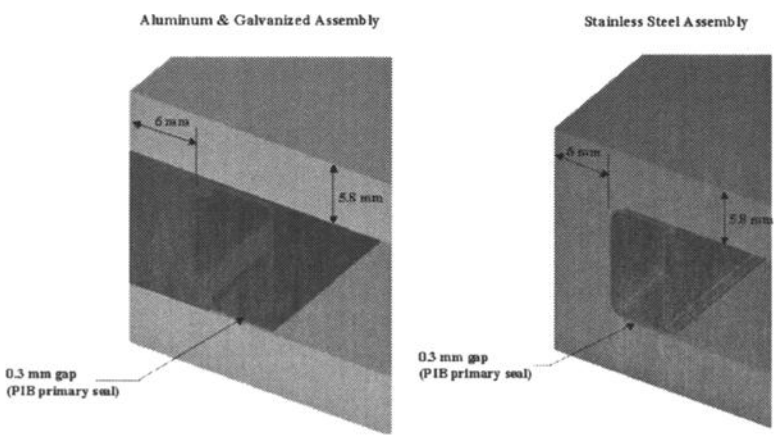

FIG. 4—*Edge-seal configurations for aluminum and galvanized steel and stainless steel spacers.*

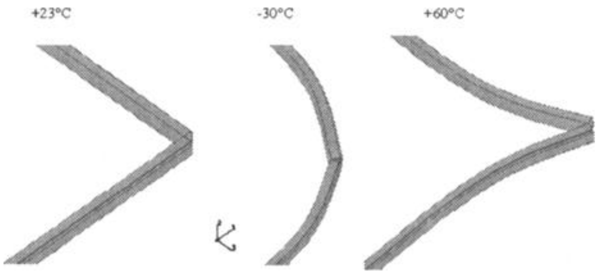

FIG. 5—*Corner deflection of aluminum spacer frame (exaggerated by factor of 100).*

Characterization of Material Properties

For materials that display an almost linear stress-strain response within the given range of loads, such as glass, aluminum, and steel, the key physical properties required for FEA modeling—Young's modulus of elasticity and Poisson's ratio—are available in a number of engineering handbooks [5]. The response of elastomeric seals and sealants, however, generally is nonlinear, even at lower strains. For silicone sealants, which by nature are closer in behavior to ideal elastomers, nonlinear response must be considered once strains exceed the range of about −15 % to +30 %. Linear FEA modeling becomes fairly inaccurate outside this limited range; therefore, a nonlinear stress-strain curve is required for the characterization of sealant behavior.

Uniaxial tensile and compressive stress relaxation testing was used to determine the behavior of two silicone insulating glass sealants (DOW CORNING 982 and DOW CORNING 3-0117)[4] within the functional range of strain of the materials. These tests characterize the stress-strain behavior of the sealant at a specific temperature and after the sealant has had time to relax under strain. This approach is more representative of a quasistatic design condition where the applied sealant strains occur slowly, providing sufficient time for the sealant to relax and reach a uniform temperature [6]. The tensile and compressive stress-strain curves are used with a curve fit program to create coefficients for a material constitutive equation. The constitutive equation provides strain energy density material functions for the elastomer portion of the model.

FEA Calculations

FEA is a numerical method for predicting the deformation of a part. Essentially, the part is broken down into a number of discrete entities or elements. A simultaneous analysis is performed on each individual element and the effect an element has on the neighboring elements. ABAQUS™, a commercially available finite element analysis (FEA) software program,[5] was used for the modeling. FEA calculations were carried out to simulate the deformation of the edge seal for IGUs exposed to temperatures of −30°C (−22°F) and +60°C (+140°F). IGUs with galvanized steel and aluminum spacers were modeled with DOW CORNING 982 as the secondary sealant; units with stainless steel spacer were modeled with DOW CORNING 3-0117 sealant.

Results and Discussion

As expected, at the low temperature, the corners are pulled inward, resulting in a bending angle greater than 90°; whereas at the high temperature, the corners are pushed outward, resulting in a bending angle less than 90°. Figure 5 shows, as an example, the deformed corner shapes for the aluminum spacer at the low and high temperatures exaggerated by a factor of 100.

Simultaneously, the primary seal (PIB) cross section decreases at the low temperature and increases at the high temperature. Figure 6 shows the "pumping" effect occurring in the PIB primary seal as a result of the thermal cycling. The aluminum spacer, having a larger coefficient of thermal expansion (c.t.e.), com-

[4]Dow Corning Corporation, West Salzburg Road, Midland, MI 48686.
[5]ABAQUS™ Software, HKS Michigan, 14500 Sheldon Road, Suite 160, Plymouth, MI 48170-2408.

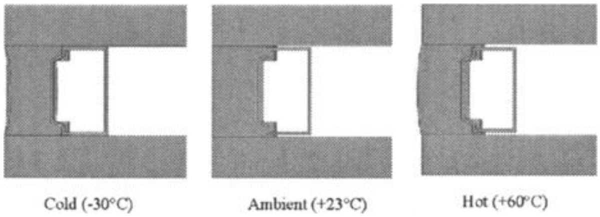

FIG. 6—*Pumping of PIB primary seal as a result of thermal cycling.*

bined with the sealant (DOW CORNING 982) having a high modulus and larger coefficient of thermal expansion, has the greatest effect on the corner of the IGU resulting in a large change in cross-sectional area during the change from hot to cold. Monitoring the changes occurring in PIB primary seal thickness around the circumference of the IGU, the authors found that the stainless steel spacer had, by far, the least effect on the change in cross-sectional area, while the aluminum spacer had the largest effect, see Table 1.

The spacer design and the material choices (spacer, sealant) also have a pronounced effect on the nominal strain distribution in the edge-seal. Figures 7–9 show the nominal strain distribution in the edge seal for the aluminum, galvanized steel, and stainless steel spacers at the cold (−30°C) and hot (+60°C) temperatures.

As can be seen, the maximum strain for the aluminum and galvanized steel spacers occurs in the primary seal region, while the stainless steel spacer results in a more even strain distribution. This finding is in keeping with the expected performance based on the difference in thermal expansion coefficients between spacer material and float glass. Thus, changes in the effective cross-sectional area of the primary seal available for diffusion that arise from differential thermal movements, are likely to account for the observed performance differences of IGUs having different spacer materials.

TABLE 1—*Deformation of PIB primary seal as a function of spacer material.*

	Deformation of PIB seal, %, for spacer material		
Temperature, °C	aluminum	galvanized	stainless steel
+60°C	+51%	+42%	+6%
−30°C	−60%	−36%	−4%

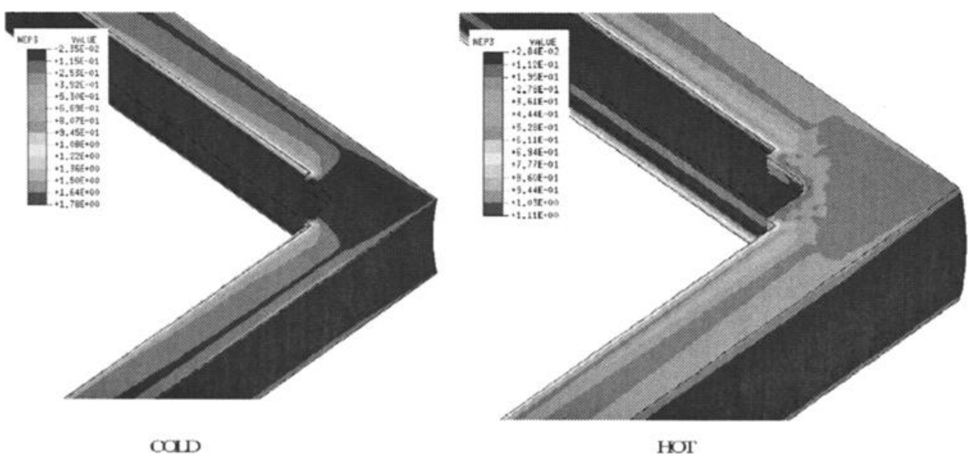

FIG. 7—*Nominal strain distribution in edge seal (aluminum spacer, DOW CORNING 982).*

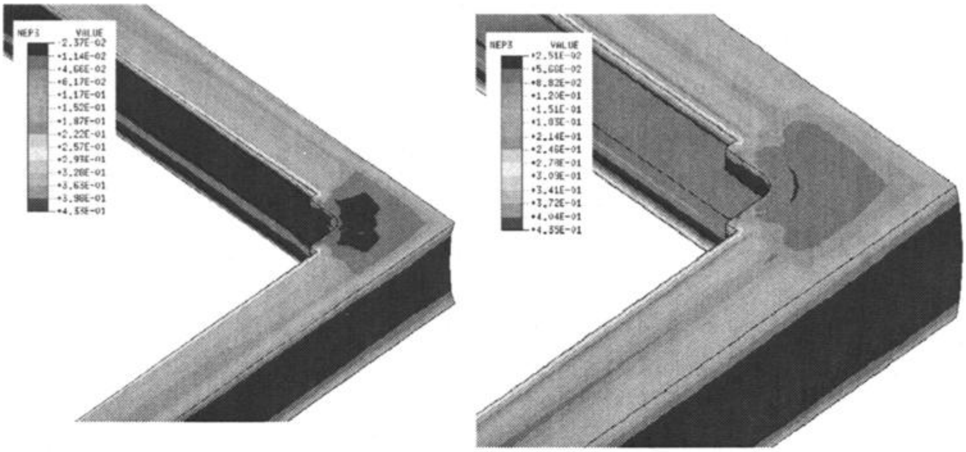

COLD HOT

FIG. 8—*Nominal strain distribution in edge seal (galvanized steel spacer, DOW CORNING 982).*

Summary and Conclusions

Differential thermal movement between the spacer frame and the glass panes is a key contributor to the aging of insulating glass edge seal and of the insulating glass unit (IGU) itself. Repetitive shear and tensile cycling induces a pumping effect in the polyisobutylene (PIB) primary seal. This pumping effect may over time displace the primary seal and generate voids, resulting in an increased leakage rate of the IGU, as has been observed on IG units exposed to accelerated testing or in-service conditions (see references cited in [1]). Depending on the physical properties of the secondary seal, the mechanical cycling may also induce fatigue aging in the edge seal. Finally, the differential thermal movement also affects the opening of the primary and secondary seals and, therefore, the effective cross section through which diffusion of water vapor and fill gases occurs.

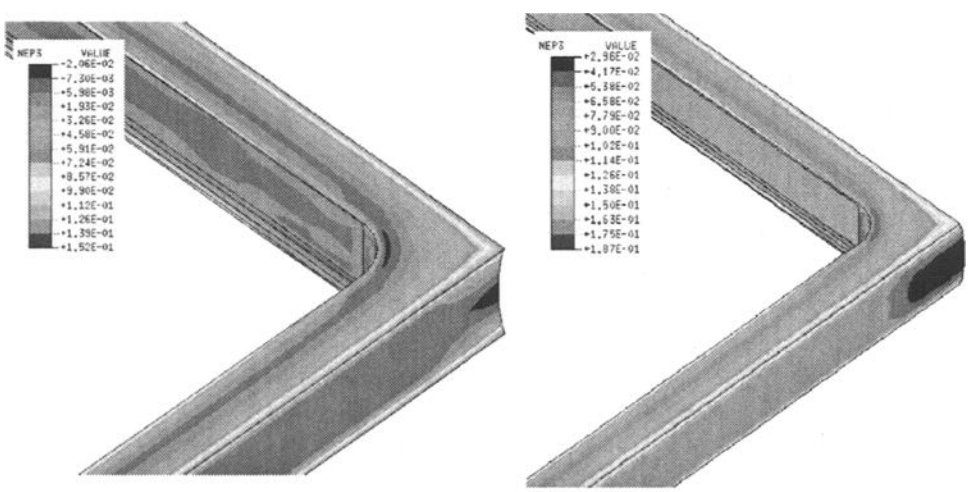

COLD HOT

FIG. 9—*Nominal strain distribution in edge seal (stainless steel spacer, DOW CORNING 3-0117).*

The FEA modeling performed by the authors confirmed that, as expected, at the low temperature, the corners of the spacer frame are pulled inward, resulting in a bending angle greater than 90°; whereas at the high temperature, the corners are pushed outward, resulting in a bending angle less than 90°. Monitoring the changes occurring in PIB primary seal thickness along the circumference of the IGU, the authors found that the stainless steel spacer had, by far, the least effect on the change in the cross-sectional area, whereas the aluminum spacer had the most substantial effect. This finding is in keeping with the expected performance based on the difference in thermal expansion coefficients between spacer material and float glass. Thus, changes in the effective cross-sectional area of the primary seal available for diffusion that arise from differential thermal movements, are likely to account for the observed performance differences of IGUs having different spacer materials.

References

[1] Wolf, A. T., "Studies into the Life-Expectancy of Insulating Glass Units," *Build. Environ.*, Vol. 27, No. 3, 1992, pp. 305–319.

[2] Feldmeier, F., Heinrich, R., Hepp, B., Schmid, J., and Stiell, W., *The Aging Behavior of Insulating Glass (in German)*, Institute for Window Technology (IFT), Rosenheim, Germany, 1984.

[3] Gravin, S. L., and Wilson, J., "Environmental Conditions in Window Frames with Double-Glazed Units," *Constr. Build. Mater.*, Vol. 12, 1998, pp. 289–302.

[4] Jacob, L., and D'Cruz, J., "Fundamental Concepts for the Design, Manufacture and Testing of IG Units for Warm Climate," *Glass Processing Days 13–16 June 1999*, Tamglass Ltd. Oy, J. Vitkala, ed., Tampere, Finland, 1999.

[5] *Chemical Engineers' Handbook*, 5th ed., R. H. Perry and C. H. Chilton, eds., McGraw-Hill Book Company, New York, 1973.

[6] Wolf, A. T., and Cleland-Host, H. L., "Material Properties for Use in FEA Modeling: Sealant Behavior with Ambient Laboratory Climate Aging," *Durability of Building and Construction Sealants and Adhesives, ASTM STP 1453*, ASTM International, A. T. Wolf, ed., West Conshohocken, PA, 2004, pp. 372–384.

Journal of ASTM International, November/December 2005, Vol. 2, No. 10
Paper ID JAI13126
Available online at www.astm.org

Yuhao Cai[1]

Reducing Tin and Aminosilane Concentration in Silicone Elastomeric Coating to Improve Its Durability

ABSTRACT: This study evaluated the impacts of tin and amino-functional silane on the long-term durability of a silicone coating material.

An experimental design was applied. Tin and aminosilane's concentrations were the variables. Laboratory-made samples were tested for initial mechanical properties. Samples were further placed in the QUV accelerated weathering chamber (fluorescent UV and condensation method) and tested periodically for tensile and elongation properties within the durability evaluation.

Based on the observations of the material and the measurements of mechanical properties, the concentration of tin in the formulation has the most influential impact on durability. The higher the concentration of tin, the faster the chalking. The concentration of the aminosilane also showed similar impacts on the durability, but not as significant as tin.

This study suggested that it is feasible to reduce both tin and aminosilane's amount by 30 % without significant impacts on the material's properties, and this may improve the coating's durability by more than 50 %. This finding may also apply to silicone sealant and adhesives.

KEYWORDS: Silicone coating, durability, QUV, mechanical property, tin catalyst, aminosilane

Introduction

Silicone materials have an unusual combination of properties that are retained over a wide temperature range (–100 to 250 °C). They have good low temperature flexibility. They are very stable at high temperature, during oxidation, in chemical and biological environments, and when subject to weathering. Silicones also have good dielectric strength and water repellency. Silicone materials are produced in the forms of fluids, resins, and elastomers. Among them, elastomer applications include sealants, coatings, adhesives, gaskets, tubing, hoses, electrical insulation, and a variety of medical applications [1].

This study evaluated the impacts of two formulation components, tin and amino-functional silane, on the long-term durability of a silicone coating (sealer) material.

Previous studies by Dow Corning indicated the coating might chalk over time after application, and there were several components in the formulation that may affect the coating's durability. Among them, tin and the aminosilane were the focus in this study.

Manuscript received 10 January 2005; accepted for publication 20 April 2005; published November 2005.
Presented at ASTM Symposium on Durability of Building and Construction Sealants and Adhesives on 15-16 June 2005 in Reno, NV.

[1] E-mail:y.cai@dowcorning.com.

Experiments

In the study, an experimental design [2] (DOE) was applied. The concentrations of organotin catalyst and aminosilane adhesion promoter were chosen as the two variables in the design. Eight samples were prepared with different tin and aminosilane's concentrations in the formulation. The silicone coating samples were made using a laboratory mixer. Table 1 lists the tin and aminosilane's levels in the eight samples.

TABLE 1—*Tin and aminosilane levels in the DOE design samples.*

Sample ID	Tin (ppm)	Aminosilane (ppm)
1	1800	1800
2	1800	1800
3	2700	2700
4	750	750
5	750	2700
6	1800	1800
7	1800	1800
8	2700	750

In sample #3, the amount of tin and aminosilane were the same as the coatings that had been demonstrated to perform well. So sample #3 represented the normal coating formulation, while other samples had either or both tin and aminosilane levels at lower than normal concentrations. All samples were tested for viscosity and cure rate (using tack free time). Viscosity was measured using a Carrimed Rheometer (Model CSL 500). Tack free time was determined using ASTM C 679-03: *Standard Test Method for Tack-Free Time of Elastomeric Sealants*. Table 2 summarizes the viscosity and cure rate for all the samples.

TABLE 2—*Samples' initial properties.*

Sample ID	Viscosity (poise)	Tack free time (min)
1	620	44
2	588	44
3	631	28
4	587	240
5	732	150
6	624	44
7	615	43
8	525	29

Samples made with the lowest concentration of tin (#4 and 5) need much longer time to cure. Samples # 1, 2, 6, and 7, which had about 33 % less in tin also had a bit longer cure time, but were still within an acceptable range. Aminosilane's level did not seem to impact cure time, considering that the sample #8 had the same cure time as the normal sample #3. Viscosity results also had some variations, but all in acceptable range. Samples #5 and 8 had viscosities on the high and the low side, respectively, which could be explained by the low levels of tin or aminosilane.

All samples were left on a plastic sheet at ambient temperature, 50 % humidity to cure for 28 days. The cured samples were tested for the mechanical properties (tensile strength and elongation). Then they were put into QUV [3] chamber (fluorescent UV and condensation method) and were periodically checked for chalking and measured for the mechanical properties. The QUV chamber was used as an accelerated weathering tester to reproduce the damage caused by sunlight, rain, and dew. ASTM G 154-04: *Standard Practice for Operating Fluorescent Light Apparatus for UV Exposure of Nonmetallic Materials* describes the basic principles and operating procedures for using fluorescent UV light and water apparatus. The QUV tests materials by exposing them to alternating cycles of UV light (340 nm lamp) and moisture at controlled, elevated temperatures. The specific weathering cycles employed in this study consisted of 4 h of UV light at 60°C followed by 4 h of condensation at 50°C [3].

In a few days or weeks, the QUV reproduces the damage that occurs over months or years outdoors [3]. Table 3 summarizes the observations on the chalking of the samples. Tables 4 and 5 summarize the tensile and elongation [4] results of the samples during the QUV exposure. The test method employed for determining tensile strength and elongation was ASTM D 412-98a(2002)e1: *Standard Test Methods for Vulcanized Rubber and Thermoplastic Elastomers-Tension.* In Figs. 1 and 2, the tensile strength and elongation data of the samples are plotted versus QUV exposure hours.

TABLE 3—*Chalking observations during QUV study.*

Sample ID	Time to chalk (h)	10 000 h QUV	17 000 h QUV
1	~ 10 000	Minor chalk	Chalk
2	10 000–17 000	No chalk	Chalk
3	~ 3000	Chalk	Chalk badly
4	No chalk up to 17 000	No chalk	No chalk
5	No chalk up to 17 000	No chalk	No chalk
6	~ 10 000	Minor chalk	N/A
7	10 000–17 000	No chalk	Minor chalk
8	5000–10 000	Minor chalk	Chalk badly

TABLE 4—*Tensile strength tests results during QUV exposure.*

Sample	Tensile Strength Data at Different QUV Exposure Hours (psi)					
ID	0 h	1000 h	2000 h	5000 h	10 000 h	17 000 h
1	424	427	611	463	470	554
2	406	474	556	445	460	441
3	428	534	590	447	470	364
4	405	504	621	462	490	506
5	356	407	518	415	420	433
6	386	461	554	424	470	N/A
7	417	472	589	445	500	451
8	418	468	614	437	440	461

TABLE 5—*Elongation tests results during QUV exposure.*

Sample ID	Elongation Data at Different QUV Exposure Hours (%)					
	0 h	1000 h	2000 h	5000 h	10 000 h	17 000 h
1	200	140	167	168	150	87
2	196	153	148	153	145	87
3	176	142	131	130	66	34
4	249	202	197	193	176	128
5	237	197	191	196	165	118
6	186	151	141	145	140	N/A
7	196	164	158	155	156	96
8	194	126	125	109	105	59

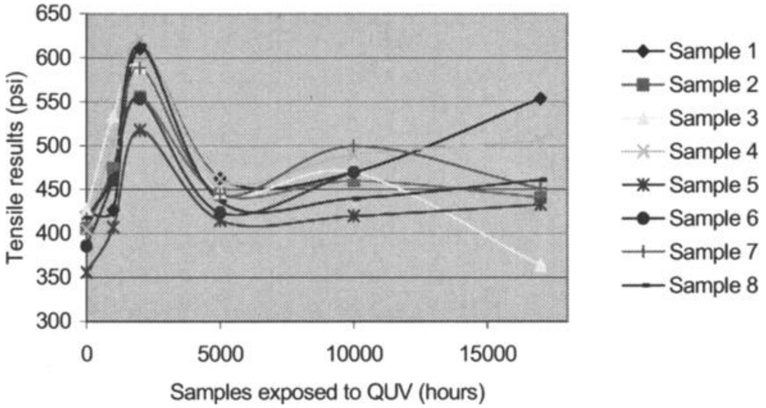

FIG. 1—*Tensile strength versus QUV exposure time.*

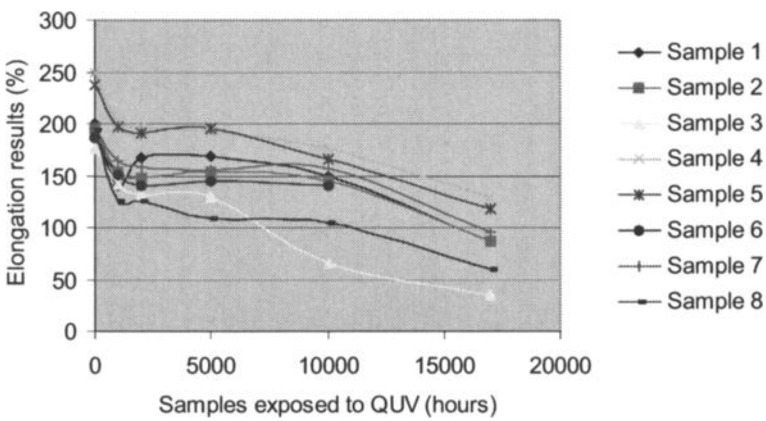

FIG. 2—*Elongation versus QUV exposure time.*

Discussions and Summary

Sample #3 started to show sign of chalking around 3000 h in the QUV chamber; its elongation value also decreased sharply between 5000 and 10 000 h in the QUV chamber. Samples 1, 2, 6, and 7, which had 33 % lower concentration of tin and aminosilane, started to show signs of chalking around 10 000 h during QUV; their elongation value decreased sharply between 10 000 and 17 000 h exposure in QUV.

It is unclear why all the samples had a sharp increase on tensile strength at 2000 h in QUV and the tensile strength dropped back at 5000 h. However, the effect does not appear to be related to the tin or aminosilane concentrations.

Based on the observations of the material chalking phenomena, as well as the measurements of the materials' mechanical properties, it is quite obvious that the concentration of tin in the formulation has the most pronounced impact on the long-term durability. The higher the concentration of the tin in the material, the faster the chalking. When chalking occurs, the elongation is reduced significantly.

The concentration of aminosilane in the product also has some impacts on durability, but not as significant as tin does. Sample #5, having low tin level, did not chalk after 17 000 h in QUV, despite the fact that the aminosilane level was high (however, samples with low tin level did not cure properly). Sample #8, having high tin level, chalked slower than sample #3 because the aminosilane level was lower in sample #8. Therefore a reduction of the aminosilane level can also improve the durability.

A coating made with the same formulation as sample #1 and a regular coating sample (as sample #3) were applied on the field for adhesion evaluation. The feedback indicated there was no substantial difference on the adhesion; the adhesion performance of both coatings was acceptable.

This study suggested that it is feasible to reduce current tin and aminosilane amounts by about 33 % and to improve coating's durability by more than 50 %. The change does not significantly impact the material's properties. Because of similar formulation/chemistry, these conclusions may also apply to some silicone sealants and adhesives.

References

[1] Odian, G., *Principles of Polymerization*, 3rd ed, John Wiley and Sons, Inc., New York, 1991.

[2] Box, G. E. P., Hunter W. G., and Hunter, J. S., *Statistics for Experimenters*, John Wiley and Sons, New York, 1978.

[3] Q-PANEL Lab Products web homepage, http://www.q-panel.com/html/quv.html, May 31, 2003.

[4] Fried, J. R., *Polymer Science and Technology*, Prentice Hall, Englewood Cliffs, NJ, 1995.

Durability Studies of Sealants and Adhesives

Journal of ASTM International, Vol. 4, No. 1
Paper ID JAI100409
Available online at www.astm.org

Claus Urban,[1] Tsuyoshi Matsumoto,[1] Shogo Tomari,[1] and François Adeleu[2]

Formulating High Weatherability Sealants: Possibilities and Challenges

ABSTRACT: Customers challenge sealant formulators to develop high weatherability construction sealants with ever-higher performance. This paper will discuss some of the factors that influence weatherability and durability of sealants, such as binder, pigments, stabilizers, and catalysts. One-component polyurethane and modified silicone sealants will be evaluated. Raw material influences need to be carefully tested and optimized in order to develop high weatherability sealants. Taking these factors into consideration, it is possible to formulate high weatherability sealants that meet customers' demands. These demands are expected to increase in the future.

KEYWORDS: construction sealants, polyurethane, modified silicone, weatherability, raw material influences

Introduction

Customers demand construction sealants with constantly increasing durability and weathering performance. Formulators have to respond to requests for outdoor weathering performances of 20 years and more. The challenge in meeting these requirements lies not only in the actual development of such sealants but also in finding reliable test methods to evaluate the different formulas and to estimate service life.

Xenon arc, fluorescent UV, carbon arc, and metal halide sources are commonly used to determine the accelerated weathering performance of sealants, adhesives, and other materials [1,2]. However, the practical value of accelerated weathering data is often limited to relative comparisons because such data applies only to specific formulas and test conditions; therefore, it seems to be difficult to arrive at reliable correlations between accelerated weathering data and outdoor weathering results [1–3]. Formulators will therefore often have to find their own methods to gauge outdoor performance.

In this paper we will consider some of the influences that determine durability and weatherability, such as binders, pigments, plasticizers, catalysts, and additives. Examples based on polyurethane and modified silicone [4] sealants will be discussed from a formulator's point of view.

Raw Material Influences on Weatherability

In order to develop high weatherability sealants, a solid understanding of the factors influencing durability and weathering behavior is necessary. Foremost among these factors are the raw materials that comprise the formula of the sealant. In this chapter the raw material influences on sealant durability will be discussed using selected examples of one-component polyurethane (PU-1) and modified silicone [4] (MS-1) sealants. For the MS-1 model formulas discussed in the paper, two kinds of binders were used: a modified silicone polymer with a polypropylene oxide backbone (in the following, referred to as modified silicone) and an acrylic-containing modified silicone polymer (in the following, referred to as acrylic modified silicone or acrylic MS) [5].

The examples given in this paper are meant to illustrate some of the challenges that can arise when formulating weather-resistant materials. In each of these examples, all raw material amounts, except the

Manuscript received June 16. 2005; revised October 17, 2006; accepted for publication November 20, 2006; published online January 2007. Presented at ASTM Symposium on Durability of Building and Construction Sealants and Adhesives, Second Symposium on 15–16 June 2005 in Reno, NV; A. T. Wolf, Guest Editor.
[1] Sika Ltd., Japan, Nagatoro 1-1, Hiratsuka, Kanagawa 254-0021. Japan.
[2] Sika France SA, Zone Industrielle. BP 111, FR-76220 Gournay-en-Bray, France.

TABLE 1—*Influence of binder type on weathering behavior of an MS-1 sealant*[a].

Sealant film thickness, mm	Exposure time in carbon arc weathermeter, h	Modified silicone (polypropylene oxide backbone)		50 % modified silicone (polypropylene oxide)/50 % acrylic modified silicone (acrylate)		Acrylic modified silicone (acrylate backbone)	
		Cracking[b]	Chalking[c]	Cracking[b]	Chalking[c]	Cracking[b]	Chalking[c]
0.2	800	5	5	1	1	1	1
	1350	5	5	1	1	1	1
	1900	—	—	1	1	1	1
	2950	—	—	2	1	1	1
5.0	800	5	5	1	1	1	1
	1350	5	5	1	1	1	1
	1900	—	—	3	5	1	1
	2950	—	—	3	1	1	1

[a]54 % Prepolymer, 27 % plasticizer, no filler; samples exposed in an open flame carbon arc weathermeter[5].
[b]Cracking 1: no cracks; 2: very small cracks; 3: small cracks; 4: large cracks; 5: entire surface covered with large cracks.
[c]Chalking 1: no change; 2: slight change in gloss; 3: onset of chalking; 4: chalking; 5: severe chalking.

one being studied, were kept constant; the formulas vary, however, between the examples given in the different tables. Hence, the data only allows for a relative comparison within each group discussed (within each table).

The accelerated weathering data discussed in this paper was generated using two kinds of accelerated weathering sources: open flame carbon arc [6] and xenon arc testing [7]. The accelerated weathering data was used for a relative ranking within each example only. A comparison of the influences of these two irradiation sources for a given sealant formula, however, is beyond the scope of this paper.

Influence of the Binder

The influence of the binder (polymer) chemistry is illustrated for a modified silicone construction sealant. In Table 1, an unfilled sealant model formula based on a modified silicone binder (polypropylene oxide backbone) is compared with two sealants that use an acrylic modified silicone binder.

In the formula that is based on an acrylic modified silicone binder, the cracking and chalking resistance could be significantly improved over the conventional modified silicone prepolymer (polypropylene oxide backbone). No cracks were observed even in thin films. When a 50/50 mixture of modified silicone and acrylic modified silicone was used, improved weathering resistance was still observed; cracks and chalking were detected only after extended carbon arc weathering (approximately 2000 h).

Next a range of formulas with increasing amount of acrylic modified silicone was prepared to study the influence of the acrylic modified silicone polymer in more detail. Figure 1 illustrates how the crack formation changes with the acrylic modified silicone content after various exposure times in the carbon arc

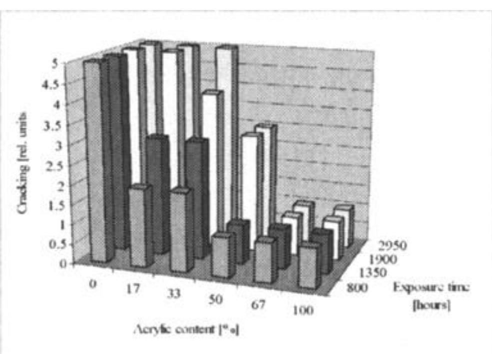

FIG. 1—*Cracking behavior of an MS-1 sealant versus acrylic modified silicone content and exposure time in carbon arc weathermeter [5] (5.0 mm film).*

TABLE 2—*Influence of titanium dioxide grade on weathering behavior of a PU-1 sealant*[a].

Titanium dioxide type (surface treatment)	Type A: Alumina	Type B: Alumina+Silica	Type C: Alumina+Silica +organic coating
Onset of polymer degradation[b], h	500	500	>500
Cracking[c]	3	5	2
Chalking[d]	4	4	3
Heat stability[e]	4	3	2
Total (sum of above)	11	12	7

[a]4.0 % Titanium dioxide; thickness of film tested 2.0 mm; samples exposed in a xenon arc weathermeter[6], exposure time: 500 h.

[b]Surface of the film starts to become pasty and soft.

[c]Cracking 1: no cracks; 2: very small cracks; 3: small cracks; 4: large cracks; 5: entire surface covered with large cracks.

[d]Chalking: 1: no chalking; 2: onset of chalking; 3: some chalking; 4: chalking; 5: severe chalking.

[e]Heat stability: change of Shore A hardness after 2 months at 80°C relative to the value before heat exposure; 1: 0–5 %; 2: 5–33 %; 3: 34–67 %; 4: 67–95 %; 5: 95–100 %.

weathermeter. No cracking was observed for an acrylic modified silicone content of 67 % or higher, even after approximately 3000 h of accelerated weathering. Crack formation was significantly reduced even when lower amounts of acrylic modified silicone binder were used: No cracking was observed in case of 50 % acrylic binder and 1350 h of exposure, at 2950 h crack formation was reduced by half. Only when 33 % or less of acrylic modified silicone binder was used, were cracks detected already in the early stages of weathering (800 h). However, already an addition of acrylic modified silicone binder in an amount as low as 17 % resulted in an improvement of the cracking performance compared to the reference sample.

This example illustrates that the binder chemistry is one of the main factors that determine the weathering performance of a sealant.

Influence of Titanium Dioxide

Titanium dioxide is a white pigment used in many sealant formulas. In this study, different grades of titanium dioxide, which differ with respect to the surface treatment applied by the manufacturer (inorganic metal oxide and/or organic), were compared. As base sealants, a one-component polyurethane (PU-1) and a one-component modified silicone (MS-1) sealant formula were selected.

In the PU-1 model formula (Table 2), three different grades of titanium dioxide, which have a surface treatment of alumina (type A), alumina and silica (type B), and alumina, silica, and an organic coating (type C) were used. In each case, 4 % of titanium dioxide was used. Titanium dioxide type A and type B gave comparable weathering results, whereas type C, which has an organic coating in addition to the inorganic coating, gave a significantly better result.

Table 3 shows the influence of three different grades of titanium dioxide on the weathering performance of an acrylic MS-1 sealant. In this series titanium dioxide type F (alumina, silica and zirconia surface treatment), a grade optimized for weatherability, gave the best weathering performance in the early stages of exposure. After 1200 h of exposure the three different grades showed a similar behavior: severe cracking was observed in all samples.

TABLE 3—*Influence of titanium dioxide grade on weathering behavior of an acrylic MS-1 sealant*[a].

Titanium dioxide type	Type D: Alumina		Type E: Alumina+ Silica		Type F: Alumina+ Silica+Zirconia	
(surface treatment)	Cracking[b]	Chalking[c]	Cracking[b]	Chalking[c]	Cracking[b]	Chalking[c]
Evaluation after 640 h carbon arc exposure	5	2	3	2	1	2
Evaluation after 1200 h carbon arc exposure	5	2	5	3	5	2

[a]3.3 % Titanium dioxide; thickness of film tested 0.2 mm; samples exposed in an open flame carbon arc weathermeter[5].

[b]Cracking 1: no cracks; 2: very small cracks; 3: small cracks; 4: large cracks; 5: entire surface covered with large cracks.

[c]Chalking: 1: no chalking; 2: onset of chalking; 3: some chalking; 4: chalking; 5: severe chalking.

TABLE 4—*Influence of various polypropylene oxide (PPO)-based plasticizers (acetate end-capped) on weathering behavior of an acrylic MS-1 sealant (cracking)*[a,b].

		0.2 mm sealant film		5.0 mm sealant film
Structure of basic polyol	Molecular weight (g/mol)	1150 h carbon arc exposure	2850 h carbon arc exposure	5000 h carbon arc exposure
Heptaol	5000	5	5	1
Heptaol	8000	1	3	1
Triol	5000	4	5	1
Diol	5000	5	5	1

[a]20 % Plasticizer, 25 % acrylic modified silicone polymer; samples exposed in an open flame carbon arc weathermeter[5].

[b]Cracking 1: no cracks; 2: very small cracks; 3: small cracks; 4: large cracks; 5: entire surface covered with large cracks.

The data presented here are too limited to allow drawing general conclusions as to the best type of titanium dioxide grade or best surface treatment. The results demonstrate, however, that the type of titanium dioxide has a significant influence on the weathering behavior of a sealant and that the grade has to be selected carefully when high weatherability is needed.

Influence of the Plasticizer

Plasticizers are used in many sealant formulas to control the flexibility. The influence that plasticizers exert on the weatherability was studied for a series of plasticizers that are based on polypropylene oxide type polyols end-capped with acetate groups (Table 4). As a model system an acrylic MS-1 sealant was selected. Sealant films of 0.2 and 5.0 mm thickness were exposed in a carbon arc weathermeter and evaluated after various exposure times. No difference between the plasticizers was observed in the case of the 5.0 mm film. However, for a 0.2 mm sealant film some differences were observed.

The results indicate that polypropylene oxide plasticizers of higher molecular weight improve the cracking performance slightly. However, data from thin films are not as reliable and need to be interpreted with caution.

Influence of Stabilizers

Stabilizers are common additives used in plastics, sealants and adhesives to improve durability and weatherability [8]. Several classes of stabilizers are commercially available, such as UV absorbers (UVAs), antioxidants, hindered amine light stabilizers (HALS) and others. Often combinations of stabilizers are used to increase the sealant performance and to utilize synergistic effects which sometimes exist between stabilizers.

In Table 5, a PU-1 formula without stabilizers (reference) is compared with a sealant formula stabilized with an antioxidant and HALS (formula A), and with a formula which had, in addition to antioxidant and HALS, an UV absorber added (formula B). The nonstabilized reference gave rather poor results, especially with respect to cracking, chalking, and yellowing. The performance could be significantly improved by using stabilizers (formulas A and B). The additional use of an UV absorber in formula B did not result in a further improvement of the sealant performance.

The series given in Table 5 illustrates that in many cases stabilizers or suitable combinations of stabilizers will improve sealant durability compared to a nonstabilized sample. However, there are instances where stabilizers do not improve the overall durability or even have a negative influence. Examples for such a behavior are given in Tables 6 and 7.

In Table 6, a PU-1 formula without stabilization (reference) is compared with two formulas which were stabilized with 0.2 % of a UVA each. In the total durability rating, no significant difference between the nonstabilized sealant and the formulas with added UVA could be seen. However, when comparing chalking performance, the formula stabilized with an oxalanilide gave a worse result than the nonstabilized reference; in addition, with respect to heat stability, the formula containing a benzotriazole derivate showed a performance slightly inferior to the nonstabilized sealant.

Another example for negative effects that stabilizers can give on occasion is shown in Table 7 for two antioxidants: Addition of antioxidants to the unstabilized reference resulted in an increase of the yellowing.

TABLE 5—*Influence of antioxidants on the performance of a PU-1 sealant*[a].

	Reference (without antioxidant)		Formula A: Antioxidant and HALS		Formula B: Antioxidant, UV absorber and HALS	
Film thickness	0.5 mm	2 mm	0.5 mm	2 mm	0.5 mm	2 mm
Cracking[b]	4	3	1	1	1	1
Chalking[c]	—	4	—	1	—	1
Yellowing[d]	5	1	1	2	1	2
Heat stability[e]	2	2	2	2	3	3
Total (sum of above)	11	10	4	6	5	7

[a]Formula A: 0.2 % antioxidant (trifunctional sterically hindered phenol) and 0.2 % HALS (dipiperidinyl sebacate derivative); formula B: 0.2 % UVA (benzotriazole derivative), 0.2 % antioxidant (same as formula A) and 0.2 % HALS (same as formula A); Film thickness: 2 mm; samples exposed in a xenon arc weathermeter[6], exposure time: 500 h.

[b]Cracking 1: no cracks; 2: very small cracks; 3: small cracks; 4: large cracks; 5: entire surface covered with large cracks.

[c]Chalking: 1: no chalking; 2: onset of chalking; 3: some chalking; 4: chalking; 5: severe chalking.

[d]Yellowing: relative rating based on visual comparison of the exposed with an unexposed sample; 1: no color change; 2: beginning of yellowing: 3: slight yellowing; 4: yellowing; 5: severe yellowing.

[e]Heat stability: change of Shore A hardness at 80°C after 2 months relative to the value before heat exposure; 1: 0–5 %; 2: 5–33 %; 3: 34–67 %; 4: 67–95 %; 5: 95–100 %.

In the case of the second antioxidant (2,4-bis(dodecylthiomethyl)-6-methylphenol) the chalking was also worse than for the reference. In this example, none of the properties studied were actually improved by addition of an antioxidant only.

In conclusion, it can be said that stabilizers often improve the weathering performance and durability of sealants (Table 5). However, there are also cases in which a stabilizer can have a negative impact on the total weatherability of a sealant, or on selected weathering properties (Tables 6 and 7). Thus, each stabi-

TABLE 6—*Influence of UV absorbers on the performance of a PU-1 sealant.*

	Reference[a] (without UVA)	0.2 % Oxalanilide	0.2 % Benzotriazole derivative
Cracking[b]	5	4	4
Chalking[c]	3	5	3
Yellowing[d]	5	4	3
Heat stability[e]	2	3	5
Total (sum of above)	15	16	15

[a]Film thickness: 2 mm; samples exposed in a xenon arc weathermeter[6], exposure time: 500 h.

[b]Cracking 1: no cracks; 2: very small cracks; 3: small cracks; 4: large cracks; 5: entire surface covered with large cracks.

[c]Chalking: 1: no chalking; 2: onset of chalking; 3: some chalking; 4: chalking; 5: severe chalking.

[d]Yellowing: relative rating based on visual comparison of the exposed with an unexposed sample; 1: no color change; 2: beginning of yellowing; 3: slight yellowing; 4: yellowing; 5: severe yellowing.

[e]Heat stability: change of Shore A hardness at 80°C after 2 months relative to the value before heat exposure; 1: 0–5 %; 2: 5–33 %; 3: 34–67 %; 4: 67–95 %; 5: 95–100 %.

TABLE 7—*Influence of antioxidants on the performance of a PU-1* sealant[a].

	Reference (no antioxidant)	0.2 % Di-*tert*-butyl-alkylphenol	0.2 % Bis(alkylthiomethyl)—phenol derivative
Cracking[b]	5	5	5
Chalking[c]	1	1	4
Yellowing[d]	2	4	4
Heat stability[e]	2	3	2
Total (sum of above)	10	13	15

[a]Film thickness: 2 mm; samples exposed in a xenon arc weathermeter[6], exposure time: 500 h.

[b]Cracking 1: no cracks; 2: very small cracks; 3: small cracks; 4: large cracks; 5: entire surface covered with large cracks.

[c]Chalking: 1: no chalking; 2: onset of chalking; 3: some chalking; 4: chalking; 5: severe chalking.

[d]Yellowing: relative rating based on visual comparison of the exposed with an unexposed sample; 1: no color change; 2: beginning of yellowing; 3: slight yellowing; 4: yellowing; 5: severe yellowing.

[e]Heat stability: change of Shore A hardness at 80°C after 2 months relative to the value before heat exposure; 1: 0–5 %; 2: 5–33 %; 3: 34–67 %; 4: 67–95 %, 5: 95–100 %.

TABLE 8—*Influence of the catalyst amount of a MS-1 sealant on the accelerated weathering performance (cracking)*[a,b].

Catalyst amount, phr[c]	Exposure time in carbon arc weathermeter, h				
	500	1000	1500	2000	2500
1.5	1	1	1	2	3
3.0	1	1	1	2–3	3–4
4.5	1	1	1	4[d]	5[d]
6.0	1	2	3[d]	5[d]	5[d]

[a]Film thickness: 3mm; samples exposed in an open flame carbon arc weathermeter[5].
[b]Cracking 1: no cracks: 2: very small cracks; 3: small cracks; 4: large cracks; 5: entire surface covered with large cracks.
[c]phr: Parts of catalyst (dibutyltin diacetate) per hundred parts of resin.
[d]Chalking was observed.

lizer or mixture of stabilizers needs to be carefully tested and optimized: The use of a standard stabilizer pack in all formulas might give good results in many cases, but may also result in a reduced weathering performance for others.

Influence of the Catalyst

The influence of the catalyst amount on weathering behavior was studied for a one-component modified silicone sealant; the results are summarized in Table 8. Cracking is seen at catalyst concentrations which are typically used in MS-1 sealants (around 1.5 phr) only after extended accelerated weathering (2000–3000 h). At higher catalyst loadings, however, the weathering performance becomes increasingly poorer.

From this data, it is obvious that the amount of catalyst has a strong influence on the weathering behavior (crack formation) of MS-1 sealants and will reduce the weathering performance after extended periods of exposure. On the other hand, the catalyst is necessary to control the curing properties of the sealant, such as skinning time and curing speed, and the amount cannot be chosen at random. In practice, the catalyst amount will be a compromise between the necessary curing properties and the weathering behavior needed.

Similar results have been reported in the literature, [9] where it was also pointed out that the nature of the catalyst plays an important role.

Conclusions

In our studies, the most notable influences on weathering resistance were binder and stabilizer, but also catalyst, titanium dioxide, and plasticizer were also found to affect the weathering behavior. For optimum weathering performance, all raw materials influences need to be carefully tested. Combinations of raw materials, especially in the case of stabilizers, can have synergistic effects but may also reduce the weathering resistance.

Weathering Requirements

Accelerated weathering testing is used during sealant development mainly to establish a relative ranking of the formulas under examination (as illustrated in the previous chapter).

In some cases, however, the actual performance in "hours of durability" will be needed: In order to ensure the necessary durability and weathering performance of a sealant, customers often require sealants to pass a certain time in an accelerated weathering test. For example, in the case of carbon arc accelerated weathering, often 1500–2000 h of exposure time is required for construction sealants. In more demanding cases, such as for industrial applications, 5000, 10 000, or more hours of carbon arc weathering may be requested.

Accelerated weathering requirements can be tested under defined conditions and the results are reproducible for a given piece of equipment. However, not all customers require accelerated weathering tests merely to ascertain the actual durability of a sealant; weathering data can also serve as basis for warranties for minimum service life. In these cases, the task of finding a correlation between the accelerated weathering data and the actual service life lies with the sealant producer.

Such service life requirements can range anywhere from 5 to 30 years (or more), however, 10 to 20 years are most frequently encountered. However, the actual outdoor conditions are often poorly defined and conditions can change during the service life of a sealant. Therefore, the actual service life is difficult to assess and predictions have a large degree of uncertainty [1,10].

Accelerated Weathering Tests and Their Correlation

In instances when an actual service life is specified by the customer, the predicted service life has to be estimated from accelerated weathering data. To arrive at such an estimate, a correlation between accelerated weathering results, which can be obtained in a reasonable span of time, and service life data are necessary.

Good and statistically reliable correlations between accelerated weathering data and outdoor service life are difficult to obtain and are hampered by the fact that this data are only valid for the particular sealant chemistry and exposure conditions used [1,2,9]. In other cases, the correlation cannot be verified, due to the very long actual outdoor exposure times needed for high weatherability sealants. Therefore, the practical value of these procedures is limited, and formulators will often have to find their own methods to estimate sealant service life.

Formulators often use rules of thumb to gauge outdoor performance, which equate a specific time of accelerated weathering with one year of service life, even though limitations and poor correlation of this approach are known [9]. These rules are not always based on systematic studies but rather on the formulator's practical experience. They are a practical compromise used in daily formulation work and can vary from formulator to formulator.

Accelerated weathering has its justification for relative ranking of a series of materials [2,9]. Accelerated weathering performance is also specified in many national and international standards for sealants, and as opposed to outdoor exposure, it can be performed under defined conditions and can be reproduced [1]. It has to be kept in mind, however, that no accelerated weathering test can be expected to give precisely the same results as an outdoor exposure test, nor can it be expected to predict the exact performance throughout the actual service life of a sealant.

Where is the Limit?

High performance sealants that fulfill the current demands for outdoor service life have been developed and are commercially available. In the market some of these high performance materials are currently replacing the standard grades, essentially becoming the new standard grades. The next generation of high weatherability sealants is expected to expand the limit of weatherability even further.

New high performance grades will be based on more expensive raw materials, such as high grade binders, which means that new high weatherability sealants will be at the higher end of the price scale. Along with this, further improvements of workability and ease of application are to be expected.

References

[1] Scott, K., and McGreer, M., "The Effect of Various Light Sources on the Degradation of Polymers—A Fundamental Approach," *Society of Plastics Engineering Olefins Conference*, Houston, TX, February 2001, pp. 471–481.

[2] Ramaraji, B., "An Understanding About Accelerated Weathering Properties," *CIPET Bulletin*, 2004, pp. 38–41.

[3] Wootton, A., "Sunlight Weathering Tests for Coatings," *Polymer Paint Color Journal*, 1995, pp. 16–22.

[4] Modified silicone (commonly abbreviated MS) refers to materials based on prepolymers (polymeric binders) derived from an organic polymer (typically polyether or acrylic-based) that are modified with reactive silyl groups. These silyl groups react with moisture to form a cross-linked material.

Such prepolymers are commercially available from Kaneka Corp. under the trade name Kaneka MS Polymer™.

[5] For the *modified silicone polymer* (polypropylene oxide backbone) Kaneka MS Polymer™-S203 and for the *acrylic modified silicone polymer* (partly acrylic backbone) Kaneka MS Polymer™-S903 was used.

[6] Open flame carbon arc weathering: SUGA WEL-300 Sunshine Weather Meter; WS type; bp.: 63°C, 550 W/m^2; cycle: 18 min water spray at 43°C and 50 % rel. humidity (rh), followed by 102 min at 43°C and 50 % rh, tested according to JIS A 1415:1999 "Methods of Exposure to Laboratory Light Sources for Polymeric Material of Buildings".

[7] Xenon arc weathering: ATLAS Suntest XLS, bp.: 65°C, tested according to ISO 4892-2:2006 "Plastics-Methods of Exposure to Laboratory Light Sources, Part 2: Xenon-arc lamps".

[8] *Plastics Additives Handbook*, R. Grächter and H. Müller, Eds., Hanser Publishers, Munich, 1984.

[9] Harper, M. D. and Cranley, P. E., "Effect of Catalysis on Construction Sealant Performance under Accelerated Weathering Conditions," *35th Annual Polyurethane Technical/Marketing Conference*, October 1994, pp. 52–61.

[10] Brennan, P. J., "Shedding Light on Laboratory Weathering," *Paint & Ink International*, 1996, pp. 2–5.

Journal of ASTM International, Vol. 3, No. 10
Paper ID JAI100450
Available online at www.astm.org

Yoshiteru Masaoka,[1] Yoshiki Nakagawa,[2] Takashi Hasegawa,[3] and Hiroshi Ando[4]

New Durable Sealant of Telechelic Polyacrylate

ABSTRACT: In this paper, we discuss the application possibilities of a novel telechelic acrylic polymer (NTP) which we have been developing as a versatile base polymer for sealants and adhesives. Due to its unique features, our NTP is expected to offer a variety of applications, including the one for sealants applied in contact with self-cleaning glass (SCG). Our discussion here focuses on the possibilities of this particular application. SCG possesses a photocatalyst layer which enables two reactions, i.e., lessening the contact angle of the glass surface and decomposing organic compounds on the glass surface, by reacting with sunlight. The reactions help wash off dust from the glass surface, mainly by rainwater, to maintain the clearness and beauty of the glass used for building windows in particular. Conventional sealants for this application often lack sufficient weatherability or risk, or a combination thereof contaminating the glass surface causing hydrophobicity. The NTP sealants, on the other hand, has no surface-polluting substances such as a low-molecular-weight silicone often contained in silicone sealants, while maintaining high weatherability. We have conducted our research to study the weatherability of the NTP sealants on SCG and the possible contamination of the SCG surface by the sealants. Our studies have found that the NTP sealants retain good adhesiveness after more than 10 000 h of exposure to UV irradiation (in a Super Xenon Weather Meter) at the interface between the sealant and the glass. We also have found almost no contamination on the SCG surface by the NTP sealants, demonstrated by the results of our tests conducted to measure the contact angles of sealant samples to the glass, through outdoor exposure for about two months.

KEYWORDS: telechelic polyacrylate, self-cleaning glass, contact angle, silyl-terminated polyacrylate

Introduction

Telechelic polymers with cross-linkable silane terminal groups are well-known as base polymers for elastic sealants and adhesives. Cross-linkable silane terminal groups such as alkoxy silane groups on the polymers react with moisture in the air, generating a silanol, and silanol groups then react with each other in a condensation reaction to form three-dimensional network structures. This cross linking and the design of polymer backbone form an elastic rubber with high elongation and strength.

Since 1978, Kaneka has launched several types of telechelic polymers. The first polymer was a silyl-terminated polyether which has been used for a wide range of applications in many parts of the world, such as construction sealants and industrial sealants and adhesives, because of the polymer's good workability, high weatherability, good adhesion to various substrates, high durability, and environmental friendliness [1,2]. Now silyl-terminated polyether-based sealants have a leading share in the Japanese elastic sealant market. As a second backbone type, a silyl-terminated polyisobutylene was launched in 1997. This polymer is in a liquid form at room temperature and is manufactured by means of living cationic polymerization technology. This polymer's features include such functions as low-gas permeability, excellent weatherability, high durability, and high-heat resistance. The silyl-terminated polyisobutylene is a base

Manuscript received May 20, 2005; accepted for publication July 31, 2006; published online October 2006. Presented at ASTM Symposium on Durability of Building and Construction Sealants and Adhesives, Second Symposium on 15–16 June 2005 in Reno, NV; A. T. Wolf, Guest Editor.

[1] Assistant Manager, Oligomers Group, Liquid Polymers Division, Kaneka Corporation. 1-8 Miyamae-machi, Takasago-cho, Takasago, Hyogo 676-8688, Japan.

[2] Manager, High Performance Materials Research Laboratories, Kaneka Corporation, 5-1-1, Torikai-Nishi, Settsu, Osaka 566-0072, Japan.

[3] Manager, Oligomers Group, Liquid Polymers Division, Kaneka Corporation, 1-8 Miyamae-machi, Takasago-cho, Takasago, Hyogo 676-8688, Japan.

[4] Manager, New Product & Market Development Group, Liquid Polymers Division, Kaneka Corporation, 3-2-4 Nakanoshima, Kita-ku, Osaka 530-8288, Japan.

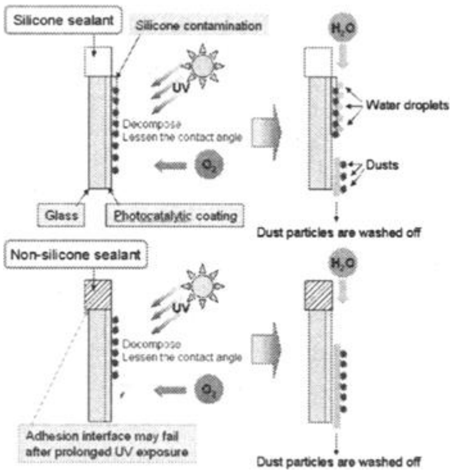

FIG. 1—*Cleaning mechanism of SCG.*

polymer for two-part sealants due to its low moisture permeability, and has been used for high-rise building sealants as its major applications.

Recently buildings and constructions with a large amount of glass have increased. To reduce the cleaning cost and to improve the visibility from the interior during rain, self-cleaning glass (SCG) has been introduced onto the world market. SCG is a titanium dioxide coated glass with photocatalytic and hydrophilic properties for easy cleaning of windows. As displayed in the mechanism shown in Fig. 1, the photocatalyst coated on SCG first decomposes the organic compounds, which promote the collection of dust, and decreases the contact angle of the SCG's surface at the same time. Running water over the SCG surface then flushes away dust and decomposed organic compounds, making the SCG surface clean. A silicone sealant is generally used as a glass glazing sealant, but is not suitable for self-cleaning glass, because low-molecular-weight silicone components can migrate onto the coating with the result that the glass surface becomes hydrophobic and that the self-cleaning effect is destroyed. Even a photocatalyst cannot decompose silicone contamination, thus the self-cleaning capability is lost.

The weatherability of a silyl-terminated polyether is sufficient as a construction joint sealant, but is not applicable for the window glazing application where the adhesion interface can be attacked by the UV irradiation from sunlight. For the above glazing situation, the silyl-terminated (telechelic) polyacrylate has been developed as the third backbone type. This paper discusses the abilities and application possibilities of our novel telechelic polyacrylate (NTP), as a sealant for SCG in particular, based on a variety of general and durability evaluations.

Basic Chemistry

Kaneka has been interested in acrylic polymers and their new polymerization methods, which can realize both high-moisture permeability and excellent weatherability of silylated telechelic polymers. The chemical structure of the novel telechelic polyacrylate (NTP) is shown in Fig. 2. The backbone is completely composed of carbon-carbon bonds, similar to a silyl-terminated polyisobutylene, which can give high weatherability to NTP sealants. Furthermore, NTP can be formulated as a one-part system which no

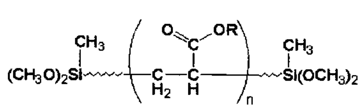

FIG. 2—*Chemical structure of NTP.*

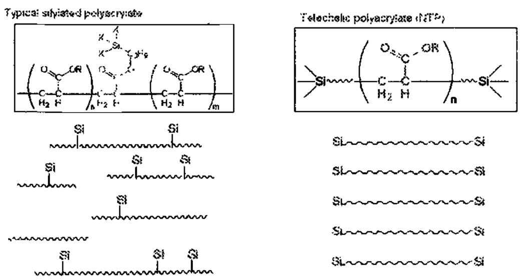

FIG. 3—*Structural differences between typical (pendant) silylated polyacrylate and telechelic polyacrylate.*

silyl-terminated polyisobutylene can provide, because of comparably high-water penetration resulting from the high polarity of the polyacrylate backbone.

Typical silylated polyacrylates have a chemical structure, as shown on the left side of Fig. 3, and are synthesized by well-known acrylic radical polymerization techniques. These silylated polyacrylate have the following drawbacks:

1. A wide molecular weight distribution (MWD, polydispersity), resulting in higher viscosity at a comparatively small number average molecular Weight (Mn).
2. Randomly placed silyl-functional groups in the molecule
3. Uncontrollable numbers of silyl-functional groups per molecule

Therefore, a new synthetic method has been investigated at Kaneka by which narrow MWD and the introduction of silyl-functional groups at the terminals has been obtained.

In recent years, many studies about living radical acrylic polymerization, useful for industrial companies, were conducted. Kaneka has found one of these studies, Atom Transfer Radical Polymerization (ATRP) [3,4], a quite promising polymerization method to synthesize a telechelic polyacrylate with silyl functional groups.

Methyl dimethoxy silyl groups at the polymer terminals are very stable under ambient conditions. However, in the presence of both water and a catalyst, as shown in Fig. 4, the silyl groups are first hydrolyzed and then condensation reaction occurs to create cross-linked structures.

Various types of polyacrylate backbone can be designed with the selection of acrylic monomers, and those polymers can be used to meet the requirements of various applications [5].

Advantages of Silyl-Terminated Polyacrylate (NTP) Sealant

A silyl-terminated polyacrylate was mixed with fillers, plasticizers, heat stabilizers, light stabilizers, UV absorbers, silane coupling agents, and hardening catalysts. This mixed material, referred to as NTP sealant, was used in all the tests reported in this paper.

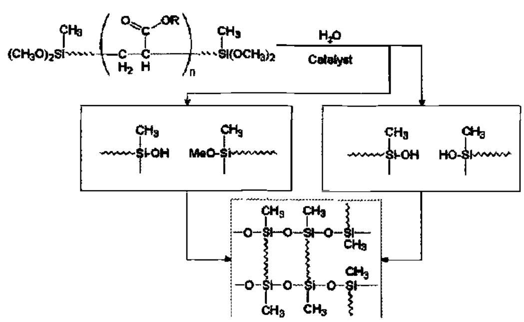

FIG. 4—*Curing mechanism of NTP.*

TABLE 1—*Properties of commercial sealants studied.*

			NTP[a]	ACR[b]	PU[c]	STPE[d]	SR[e]
Viscosity	1 rpm	Pa s	1960	1440	3010	2060	2820
	2 rpm		1100	1060	1960	1130	1690
	10 rpm		400	470	760	320	580
Skin formation time		min	85	8	>300	25	6
Tensile strength by dumbbell[f]	M50	MPa	0.16	-	0.35	0.48	0.33
	M100		0.32	-	0.59	0.73	0.48
	Tb		0.92	0.16	1.20	1.45	1.85
	Eb	%	600	40	300	380	480

[a]Telechelic polyacrylate sealant (silyl-terminated polyacrylate sealant).
[b]Commercial water-borne acrylic sealant.
[c]Commercial polyurethane sealant.
[d]Commercial silyl-terminated polyether sealant.
[e]Commercial silicone sealant.
[f]M50: Modulus at 50 % elongation, M100: Modulus at 100 % elongation, Tb: Tensile strength at break, Eb: Elongation at break.

Mechanical Properties—A Comparison of Commercial Sealant Properties

Tensile properties were measured using an appropriate tensile test machine with dumbbell No. 3 specimens at a pull speed of 200 mm/min in accordance with JIS K 6251 Tensile testing methods for vulcanized rubber. Although conventional water-borne acrylic sealants are widely known, and are often used for such benefits as workability and cost effectiveness as construction sealants, there are many usage limitations due to their drawbacks, including relatively large shrinkage, no cross linkage, low elongation, and poor adhesion properties to metals and plastics. On the other hand, NTP sealants have high flexibility, low modulus, and high elongation, as seen in high-performance sealants such as silicone sealants. See Table 1.

Surface Weatherability

Cured sheets of silicone and NTP sealants (3 mm thickness) were exposed to ultraviolet (UV) light in a Sunshine Weatherometer[1] with carbon arc light source (operation conditions: black panel temperature at 63°C, water spray of 18 min duration within a 120 min total cycle) according to JIS B7753: Light-exposure and light-and-water-exposure apparatus (open-flame sunshine carbon-arc type).

After exposure to UV irradiation for 10 000 h, no crack on the surfaces of both silicone and NTP sealants can be observed. The surface weatherability test still continues and further results will be reported in future.

Adhesion Properties—A Comparison of Commercial Sealant Properties

Sealants were applied on various substrates, and were tested by a 180° hand peeling method after cure at 23°C for seven days. The test results for commercial sealants and the NTP sealant are shown in Table 2. The good adhesion property of silyl-terminated polyethers to various substrates is generally known. The NTP sealant also shows good adhesion in this test as do silyl-terminated polyether sealant. It has been recognized that NTP's silyl-functional groups at the polymer terminals and the polar functional groups, e.g., ester groups, of side chain, can produce many interactions, enhancing their respective adhesiveness to metals, plastics, and glass. Therefore, a NTP can adhere to various substrates. It is expected that NTP sealants will be used for construction, industrial, and automotive applications because of their good adhesion to a wide range of substrates.

A Possible New Application—A Sealant for Self-Cleaning Glass

Self-cleaning glass (SCG) can provide a constant aesthetic appearance to the buildings, where the glass is used, and also to the clear vision area for the people living or working inside the building. To maintain these conditions, it is desirable and necessary to provide SCG with an efficient photocatalytic function. Gaskets and sealants are used as perimeter seals around the glass for the weather tightness and thermal

[1]Suga Test Instruments Co., Ltd, 5-4-14 Shinjuku, Shinjuku-ku, Tokyo, Japan 160-0022.

TABLE 2—*Adhesion properties measured by hand peeling.*

	NTP[a]	ACR[b]	PU[c]	STPE[d]	SR[e]
Float Glass	CF	AF	C2A8	CF	CF
SCG-1[f]	CF	AF	AF	CF	CF
SCG-2[f]	CF	AF	C1A9	CF	CF
Anodized aluminum	CF	AF	AF	CF	CF
Acryl coated aluminum	CF	TF	C3A7	CF	CF
Electrodeposited aluminum	CF	AF	AF	C9A1	CF
Stainless steel	CF	AF	AF	CF	CF
Polyvinylchloride	CF	TF	AF	C8A2	CF
Glass fiber reinforced plastic	CF	AF	C2A8	CF	C2A8
Polycarbonate	CF	TF	AF	C9A1	C3A7
Polymethylmethacrylate	C9A1	TF	AF	AF	AF
ABS	C4A6	TF	AF	AF	AF
Pine wood	CF	TF	AF	CF	CF

[a]Telechelic polyacrylate sealant (silyl-terminated polyacrylate sealant).
[b]Commercial water-borne acrylic sealant.
[c]Commercial polyurethane sealant.
[d]Commercial silyl-terminated polyether sealant.
[e]Commercial silicone sealant.
[f]SCG: self-cleaning glass, CF or C: cohesive failure, AF or A: adhesive failure, TF or T: thin layer cohesive failure. For example, C5T2A3: 50 % of CF, 20 % of TF and 30 % of AF.

insulation of buildings. Sealants are important, especially for high-rise or unconventionally designed buildings. Nowadays, silicone sealants are often used for this particular application, mainly due to their durability. Other conventional non-silicone sealants are not recommendable because of their insufficiently UV resistant adhesion to glass, especially to SCG which decomposes organic compounds. However, silicone sealants are not suitable for SCG because of hydrophobic contamination caused by these sealants [6]. Thus there has been no ideal sealant available on the SCG market, limiting the design of SCG buildings with gaskets. We conducted various evaluations to prove that NTP sealants are capable of providing answers to the various problems that sealants for SCG need to solve.

Resistance to UV Exposure Through Float Glass

The UV resistance of NTP sealants was confirmed as being adequate for conventional glass glazing. A test piece, as shown in Fig. 5, was prepared, and the adhesion interface was irradiated through the glass in a Xenon tester according to JIS K5600-7-7: Testing methods for paints—Part 7: Long-period performance of film—Section 7: Accelerated Weathering (Exposure to filtered xenon-arc radiation), Japanese Industrial Standards Committee, Tokyo, Japan. After the UV irradiation for a certain period, tensile properties and failure mode were obtained (See Fig. 6 and Table 3). All of the results showed cohesive failure mode after UV irradiation of up to 10 000 h, and this finding proves that NTP sealants can have a sufficiently UV resistant adhesion to float glass.

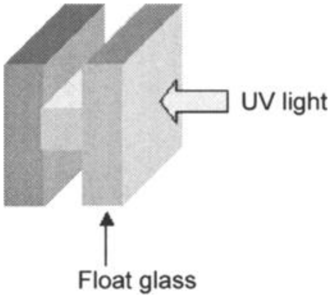

FIG. 5—*Test piece for glass adhesion test after UV irradiation.*

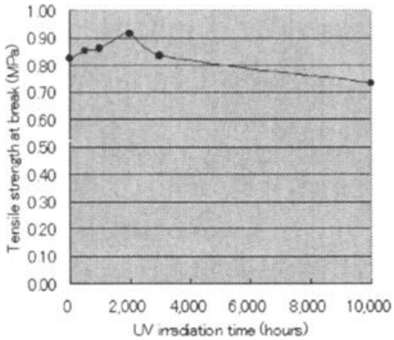

FIG. 6—*Change of tensile strength after UV irradiation.*

NTP is a polymer having both an organic backbone and terminal silyl groups, therefore we needed to assess the degree of possible degradation of the adhesion interface on a photocatalyst coating and the contamination adjacent to the sealant. Therefore, those two key issues were evaluated under the following headings.

UV Resistance of Adhesion Interface on SCG

Test specimens were prepared as shown in Fig. 7, and were cured at 23°C for four weeks. The specimens were set in a Xenon tester so that the adhesion interface could be directly irradiated through the SCG. After a certain irradiation period, the test pieces were evaluated by a 180° hand peeling method (Table 4).

It was confirmed that the NTP sealant maintained excellent adhesion to SCG under UV irradiation because it showed cohesive failure after UV irradiation of up to 10 000 h.

Hydrophobic Contamination

Test specimens were prepared shown in Fig. 8, were cured at 23°C for seven days, and were installed on an outdoor exposure rack facing south, (the inclination angle of the exposure rack was 45° to the horizontal, the location of the rack was in Hyogo prefecture in Japan) outdoors. The contact angle data were taken every four weeks and are shown in Fig. 9. The water shedding length from the sealant is also shown in Table 5.

TABLE 3—*Failure mode of UV resistant test pieces.*

	Initial	500 h	1000 h	2000 h	3000 h	10 000 h
Failure mode	TCF	CF	CF	CF	CF	CF

Note: TCF: thin layer cohesive failure; CF: cohesive failure.

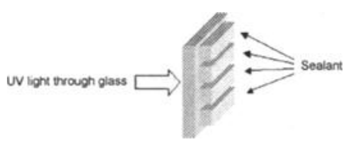

FIG. 7—*Test piece.*

TABLE 4—*Adhesion test results after UV irradiation.*

	1000 h	3000 h	5000 h	7000 h	10 000 h
SR	CF	CF	CF	CF	CF
NTP	CF	CF	CF	CF	CF

Note: CF: cohesive failure.

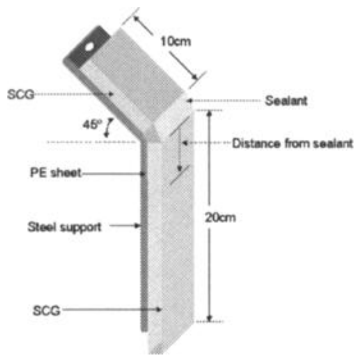

FIG. 8—*Test piece for SCG outdoor exposure.*

The contact angle close to the silicone sealant was very high, and the length of water shedding area also increased during exposure time. During the exposure period, the NTP sealant showed just 5 mm of water shedding without further increase.

Other Features

Paintability—Adhesion of water-borne paints on NTP sealants were measured by 5×5 cross-cutting test using 2 mm intervals between cuts (See Fig. 10 and Table 6). The sealant was applied as a sheet (3 mm thickness), and after curing for one day at 23 °C, a paint was applied on the sheet and allowed to dry for seven days at 23 °C.

In case of water-borne paints to silicone sealants, cross-cutting tests could not be performed due to paint shedding, since no paint adhesion to the silicone sealant was observed. Meanwhile, the NTP sealant showed good paint adhesion as well as good wetting ability.

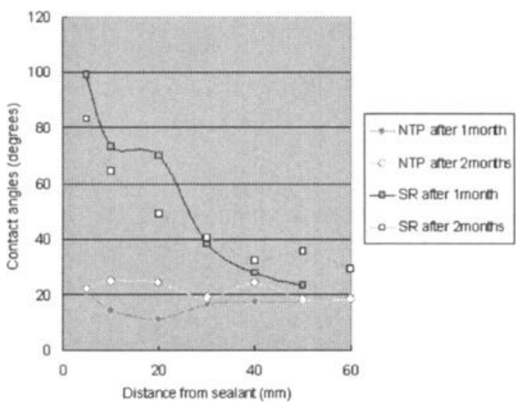

FIG. 9—*Contact angle after outdoor exposure.*

TABLE 5—*Water shedding distance after outdoor exposure.*

	Water shedding distance (mm)	
	After 1 month	After 2 months
NTP	5	5
SR	40	58

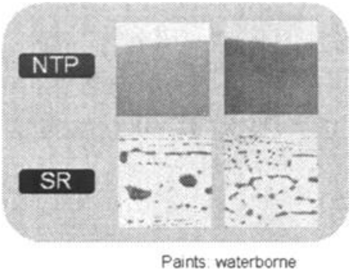

FIG. 10—*Wetting ability of water-borne paints on sealants.*

Nonstaining to the Adjacent Area

It is important for construction sealants not to stain the substrate adjacent to the sealing joints. Figure 11 shows silicone and NTP sealants applied on marble and exposed outdoors for four years. No staining was observed with the NTP sealant, while the silicone sealant showed staining.

TABLE 6—*Adhesion property of water-borne paints.*

	NTP	STPE
Paint-A	25/25	25/25
Paint-B	25/25	25/25

Note: Good adhesion: 25/25.........0/25: Poor adhesion.

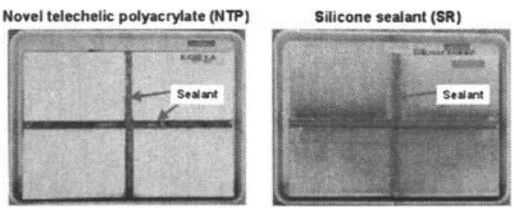

FIG. 11—*Staining around NTP and silicone sealants tested, after four-year outdoor exposure.*

Standardization

As a standard for glass glazing sealant, "AAMA" is well-known, and the NTP holds an official certificate for AAMA802. 3-92, Type II (Ductile Back-Bedding Compound).[2]. Furthermore, the durability of the NTP sealant was internally evaluated in accordance with International Standard ISO11600 [7] (Building construction - Jointing products - Classification and requirements for sealants), and the NTP sealant has been found to satisfy the requirements of ISO 11600 Class 25HM Type G.

Conclusion

Kaneka has been developing the novel telechelic polyacrylate (NTP) as a new-generation material consisting of acrylic polymer as main chain, and their cross-linkable silyl-functionalities at the polymer terminals. NTP sealants have unique features because of their chemical structures, and the new sealants are expected to be used for a wide range of new applications, including SCG.

[2]AAMA—American Architectural Windows Manufacturers Association, 1827 Walden Office Square, Suite 550, Schaumburg, IL 60173-4268.

References

[1] Furukawa, H., "Stability of MS Polymer based sealants and adhesives," *ASC International Convention 2002*, The Adhesive and Sealant Council, Inc., LA, USA, 2002.

[2] Kusakabe, M., Masaoka, Y., and Phanopoulos, C., "Review of innovative developments of silyl modified polymers for sealants, adhesives and coating applications," *STICK 2003 3rd European Congress on Adhesive and Sealant Raw Materials*, April 2003, Vincentz Network, Germany, pp. 117–127.

[3] Wang, J. S., and Matyjaszewski, K., "Controlled/"Living" Radical Polymerization. Atom Transfer Radical Polymerization in the Presence of Transition-Metal Complexes," *J. Am. Chem. Soc.*, Vol. 117, 1995, pp. 5614–5615.

[4] Matyjaszewski, K., and Xia, J., *Handbook of Radical Polymerization*, 2002, Wiley, Inc., Hoboken, NJ.

[5] Nakagawa, Y., "Commercialization of Telechelic Polyacrylates Prepared by ATRP, PMSE109," *American Chemical Society*, Wiley, Inc, Hoboken, NJ Spring 2005, PMSE preprint, 2005.

[6] Hautekeer, J. P., De Buyl, F., and Gallez, L., "Study and Recommendations on the Use of Sealants with Easy-to-Clean and Self-Cleaning Glasses," *Glass Processing Days 2003 - Session 15*, 2003, pp. 334–337.

[7] International Standard ISO 11600, "Building construction – Jointing products – Classification and requirements for sealants,".

Journal of ASTM International, Vol. 3, No. 10
Paper ID JAI100407
Available online at www.astm.org

Ali M. Memari,[1] Xuezhen Chen,[2] Paul A. Kremer,[3] and Richard A. Behr[4]

Seismic Performance of Two-Side Structural Silicone Glazing Systems

ABSTRACT: This paper presents the results of the first phase of an experimental research program on simulated seismic performance of structural silicone glazed (SSG) curtain wall systems. Full-scale, two-side SSG mockups made up of three side-by-side glass panels were tested under cyclic racking displacements to determine serviceability and ultimate behavior responses. Variables were glass type (annealed and fully tempered) and panel configuration (monolithic, laminated, and insulating glass). In the experiments carried out, damage states such as gasket deformation/pullout, sealant failure (e.g., adhesion/cohesion, etc.), glass cracking glass and fallout were identified and their corresponding drift levels were determined. The extent of damage to silicone sealant was determined through air leakage tests.

KEYWORDS: silicone sealant, structural glazing, architectural glass, seismic behavior, curtain wall, racking test, air leakage test

Introduction

Since its introduction nearly four decades ago, structural silicone glazing (SSG) has become a popular glazing method for curtain wall construction. Perhaps the most important reason for SSG popularity is the aesthetics associated with a mullionless curtain wall system [1,2]. The major difference between SSG systems and the more widely used "dry-glazed" systems is that glass lites or panels in SSG systems are adhered to the supporting glazing frame with structural silicone sealant along either two edges of the glass panel or all four edges. Common practice consists of attaching the two vertical glass panel edges to mullions located behind the glass with structural silicone sealant, while the two horizontal glass panel edges are held in aluminum framing pockets by gaskets (dry glazed). This glazing procedure, which is used to create a "strip window" system, is known as "two-side" SSG construction [3]. A similar procedure referred to as "four-side" SSG construction, uses structural silicone sealant on all four edges of the glass panel. The vertical edges of adjacent glass panels in two-side SSG systems and all edges of adjacent glass panels in four-side SSG systems are separated by silicone weatherseal joints.

Glass panel edges in dry-glazed curtain walls are mechanically captured; and thus, out-of-plane loads are transferred from the glass to glazing frame through confining gaskets. In contrast, SSG systems rely upon the silicone sealant to transfer such loads to the supporting frame. For this reason, the strength and modulus properties of the silicone sealant and the quality of the bond between the sealant and the substrates (glass edge and glazing frame) are of great importance in SSG systems design.

Structural sealant material properties and guidelines for its use are usually provided by sealant manufacturers using a number of standard test methods (e.g., [4]). However, most tests carried out by manufacturers are limited to coupon tests to determine tensile and shear strain capacities, modulus properties, adhesion, and material compatibilities. Data from tests on components such as glass panels attached with

Manuscript received June 2, 2006; accepted for publication July 31, 2006; published online September 2006. Presented at ASTM Symposium on Durability of Building and Construction Sealants and Adhesives, Second Symposium on 15–16 June 2005 in Reno, NV: A. T. Wolf, Guest Editor.

[1] Associate Professor, Department of Architectural Engineering, Penn State University, 104 Engineering Unit A, University Park, PA 16802

[2] Graduate Student, College of Architecture and Urban Planning, University of Michigan, Art and Architecture Building, Ann Arbor, MI 48109

[3] Research Associate, Department of Architectural Engineering, Penn State University, 104 Engineering Unit A, University Park, PA 16802

[4] Professor and Head, Department of Architectural Engineering, Penn State University, 104 Engineering Unit A, University Park, PA 16802

silicone to glazing frames are scarce. Although design guidelines for SSG systems under wind loading conditions are well developed, there is a lack of knowledge related to the behavior of SSG systems under in-plane displacements experienced by buildings during earthquakes. It is generally believed that SSG systems perform well in seismic regions due to the "resilient attachment" of glass to the glazing frame. In fact, it is noted in ASTM Standard C 1401 [5] that, "Since the lite or panel is not captured in a metal glazing pocket, the opportunity for it to impact the metal glazing pocket surfaces is minimized, eliminating a primary cause of breakage." This notion has merits in four-side SSG systems, but may need moderation for two-side systems, wherein the top and bottom edges are typically captured in metal glazing pockets. It is further noted in ASTM Standard C 1401 [5] that, "Depending on system design, however, adjacent glass lite or panel edges could contact each other and cause breakage or other effects." Despite these claims, there is only limited full-scale experimental test data from in-plane racking tests on SSG systems [6,7] to substantiate them.

Seismic design requirements based on building codes (e.g., [8]) require that nonstructural components including curtain walls accommodate building interstory drifts. For glazing design purposes, the code normally requires the drift capacity of the glazing system corresponding to glass fallout to be known. Currently, the only full-scale glass fallout data available in the literature was collected during the limited tests conducted by Behr [6].

In order to develop a better understanding of seismic behavior of SSG systems, an experimental program is underway at Penn State University. The objective of this paper is to present the results of cyclic racking tests on two-side SSG curtain walls. The serviceability and ultimate performance of conventional two-side SSG systems are evaluated for two different glass types and three different configurations.

Experimental Program

The research presented in this paper was aimed at characterizing the serviceability and ultimate behavior of conventional two-side SSG curtain walls under cyclic racking displacements. Serviceability drift capacities corresponding to damage states such as gasket distortion, weatherseal, and structural seal failure leading to air leakage and glass cracking were identified. Ultimate drift capacities associated with damage such as glass fallout [defined as a shard of at least 645 mm^2 (1 $in.^2$)] were also identified. Air leakage tests were included to provide an index for serviceability failure criterion following an earthquake.

It was necessary to test specimens made with more than one glass panel so that both the interaction of glass panel edges and mullions and the interaction of glass panels to one another could be studied. Of particular interest was the characterization of the behavior of structural silicone sealant between glass panel vertical edges and aluminum frame members and also the behavior of the silicone weatherseal between adjacent glass panels. For this reason, it was decided to construct specimens with three glass panels. Two configurations were devised depending on whether a structural sealant joint or dry-glazed joint was used at exterior edges of the end panels, as shown in Fig. 1. Configuration A was devised to investigate the effect of dry-glazed exterior end panel vertical edges on the performance of the interior panels. One specimen of Configuration A and seven specimens of Configuration B were tested. The glazing frames were conventional stick frame type using Kawneer 1600™ aluminum frame members. A one-part GE silicone with medium modulus normally recommended for field-assembled SSG systems was the structural silicone sealant used. The details shown in Fig. 1 include a 10.7 mm (0.42 in.) structural silicone bite and a 6.4 mm (0.25 in.) bead thickness. The weatherseal consisted of a 12.7 mm (0.5 in.) wide bead at the interior joints and either a 12.7 mm (0.5 in.) or 6.4 mm (0.25 in.) wide bead at the end panel exterior vertical joints. The two different widths at the exterior joints were used to investigate the effect of the exterior weatherseal width on the behavior of the interior panel.

The full test specimen matrix is shown in Table 1. Annealed glass (AN) and fully tempered glass (FT) were the glass type factor levels, and monolithic glass (Mono.), laminated glass (Lami.), and insulating glass units (IGU) were the configuration factor levels. Four combinations of glass type and glass panel configuration were selected for the study. Two repetitions for each combination proved to be sufficient because no significant difference in the results of the two repetitions of each combination was observed. For full-scale mock-up testing, if there is a significant difference in the results of the two repetitions, typically a third test of the same combination is conducted.

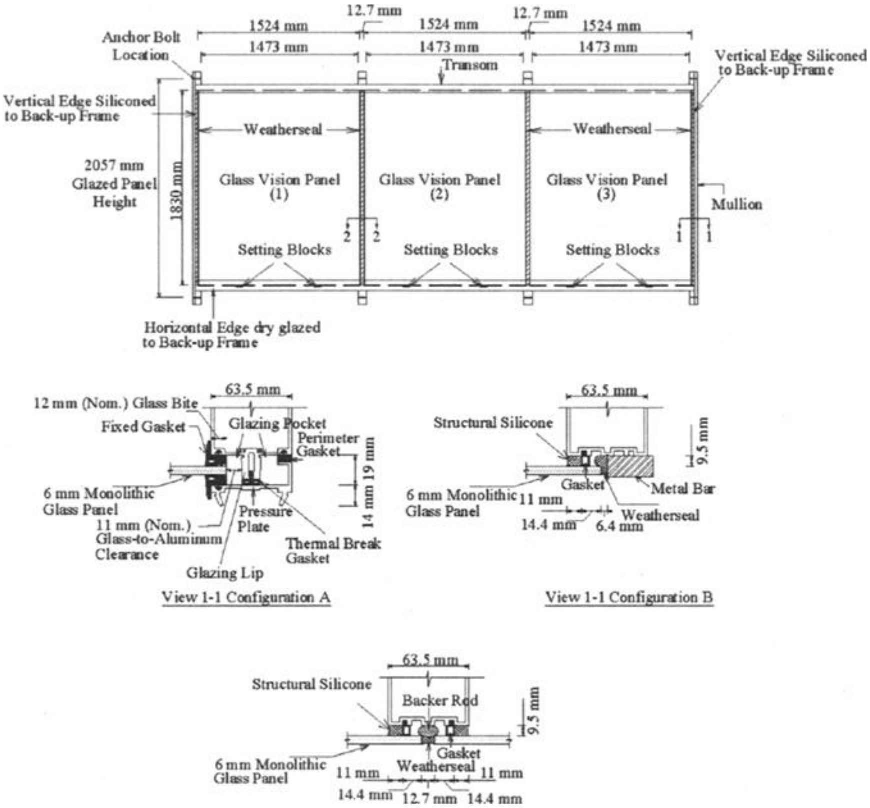

FIG. 1—*Glazing details of Configurations A and B (1 mm = 0.0394 in.)*

Test Procedures

The racking test facility for the experimental study is shown in Fig. 2. Specimens were subjected to the AAMA 501.6-01 [9] displacement-controlled racking protocol shown in Fig. 3. The protocol requires that

TABLE 1—*Two-side SSG mockups for dynamic racking crescendo tests and air leakage tests.*

Combination	Glass type and dimensions	Weatherseal width: Mid joint	Weatherseal width: Edge joint	Frame type and sealant
A-1,[a] B-1 (Mockups 1,2)	Clr AN Monolithic [6 mm(1/4 in.)] 1.52 m × 1.83 m (5 ft × 6 ft) panels	12.7 mm (1/2 in.)	6.4 mm (1/4 in.)	Kawneer 1600 two-side SSG curtain wall
B-2 (Mockup 3, 4)	Clr FT Monolithic [6 mm(1/4 in.)] 1.52 m × 1.83 m (5 ft × 6 ft) panels	12.7 mm (1/2 in.)	6.4 mm (1/4 in.)	GE one-part silicone (SCS2000)
B-3 (Mockups 5, 6)	AN Lami [2.7 mm (1/8 in. nom.) AN/ 0.03 in. Saflex interlayer/2.7 mm (1/8 in nom.)] 1.52 m × 1.83 m (5 ft × 6 ft) panels	12.7 mm (1/2 in.)	6.4 mm (1/4 in.)	
B-4 (Mockups 7, 8)	AN IGU [6 mm (1/4 in.) AN/0.5 in. air space/6 mm (1/4 in.)] 1.52 m × 1.83 m (5 ft × 6 ft) panels	12.7 mm (1/2 in.)	12.7 mm (1/2 in.)	

[a]A-1 refers to Combination 1 of Configuration A, and B-1 refers to Combination 1 of Configuration B. Configurations A and B are defined in Fig. 1. Similarly, B-2, B-3, and B-4 represent Combinations 2, 3, and 4, respectively, of Configuration B.

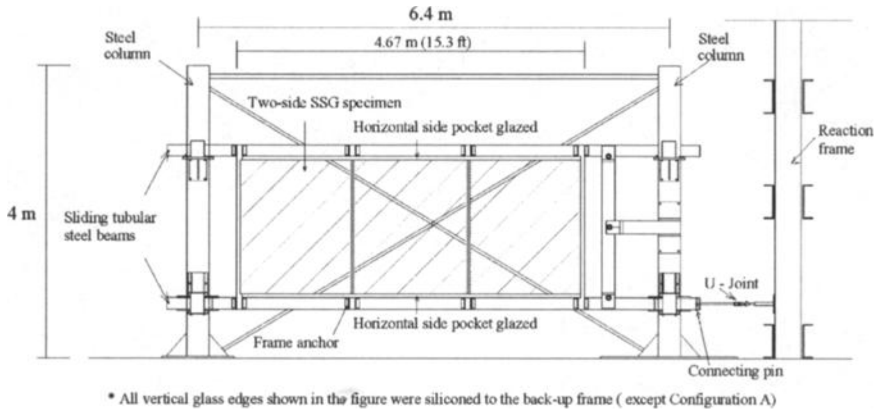

FIG. 2—*Schematic of dynamic racking test facility with curtain wall test specimen attached.*

the incrementally increasing racking step should continue until (a) glass fallout in the specimen occurs, (b) drift ratio over the height of the glass panel reaches 10 %, or (c) a racking displacement amplitude of ±150 mm (±6 in.) is applied to the specimen. In this study, the tests continued beyond glass fallout. Racking displacements were continued until the middle glass panel (the "test panel") shattered. Glass fallout/shattering did not always first occur in the middle panel. Load and displacement data corresponding to various damage or failure modes, which included serviceability and ultimate drift capacities, were recorded during the tests.

Air leakage tests were conducted in accordance with ASTM Standard E 283-91 [10] with some modification to the specimen size. ASTM Standard E 283-91 suggests that the specimen be at least a full building story high and include both vertical and horizontal joints. In this study, however, air leakage measurement was confined to vertical joints of the middle panel, referred to as Joints A and B in Fig. 4. Initially the air leakage chamber was constructed as shown in Fig. 4(*a*) using a plastic shroud taped over the middle panel for mockups 1 and 5. After these initial tests, it was decided that an independent evaluation of the air leakage in each middle panel joint would be more informative, and the smaller chambers covering individual vertical joints [Fig. 4(*b*)] were used in the other six mock-ups tests.

A baseline air leakage test was conducted on each specimen before the start of the cyclic racking test, and air leakage measurements were then taken about every other racking step when the racking was stopped for inspection of the specimen. The air supply pressure was maintained at 75 Pa (1.57 lb/ft^2).

Discussion of General Response of Tested Mockups

The common behavior of the test specimens during racking displacements consisted of deformation of the glazing frame as the top sliding steel tube of the racking facility (Fig. 2) moved in the opposite direction of the bottom sliding steel tube. This caused each glass panel to rotate in an effort to adjust to the deformed position of the glazing frame. All three glass panels would rotate in the same direction causing the

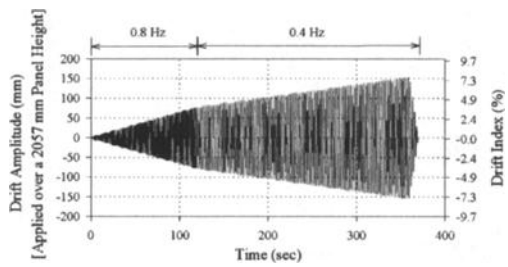

FIG. 3—*Drift time history for dynamic racking tests.*

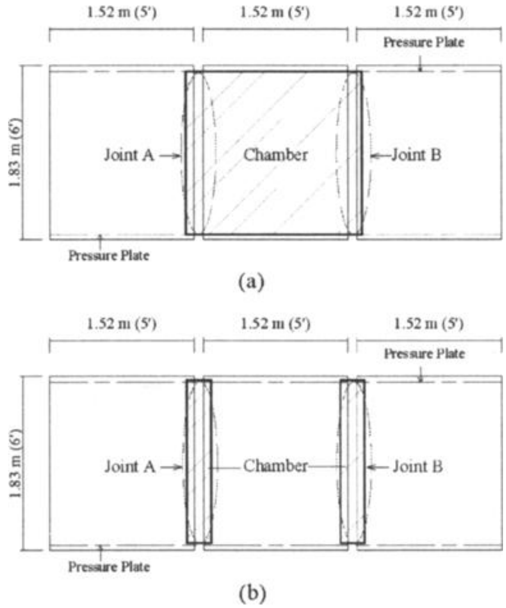

FIG. 4—*Plastic shrouds used to form chambers for air leakage tests: (a) shroud location for tests on mockups 1 and 5; (b) shroud location for tests on all other mockups.*

weatherseal between each pair to be stretched vertically as the edge of one panel moved up and the edge of the adjacent panel moved down. As racking displacement amplitude increased, glass panel horizontal edges near corners started to come in contact with the lip (Fig. 1) of the dry-glazed horizontal framing members. Glass-to-frame contact eventually led to cracking and fallout of glass. Figure 5 shows a typical specimen under test.

In all the tests performed, adjacent glass panels did not come in contact with each other, because the combination of the structural seals and weatherseals along the vertical edges of each panel kept the side-by-side panels close to parallel throughout the racking displacements. This was observed even as the structural seals and weatherseals began to exhibit extensive failure. Furthermore, end panel glass edges did not contact the boundary mullions (shown as Sec. 1-1 in Fig. 1) during any of the tests with the exception of mockup 5, whose bottom frame-to-facility anchor welds broke at large racking displacements.

Glass panel rotation relative to the deforming mullions during racking exerted longitudinal and transverse shear strain in both the weatherseals and structural seals. Longitudinal shear strain was dominant in

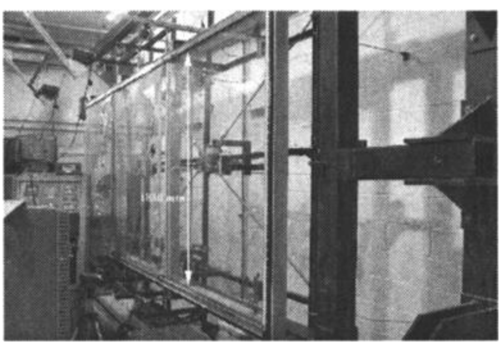

FIG. 5—*Mockup 8 (AN IGU) under test.*

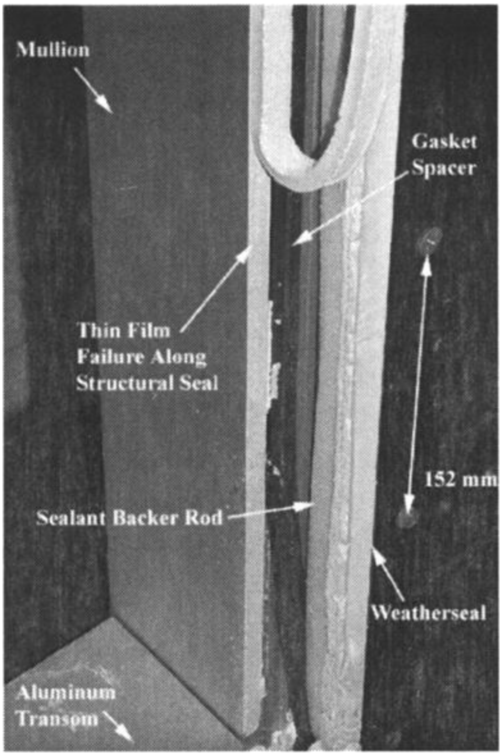

FIG. 6—*Inspection of two-side SSG silicone joint failures that occurred during in-plane dynamic racking tests.*

the weatherseals, and transverse shear strain was the cause of observed failures in the structural seals. Three primary silicone sealant failure modes were identified in the weatherseals and structural seals: cohesive failure, adhesive failure, and thin film failure. In racking tests cohesive failure occurs in the seals when their shear strain capacity is exceeded and is characterized by rupture within the sealant. Adhesive failure occurs in the seals due to loss of bond between the sealant and its substrate and is characterized by a complete peeling away of the sealant from the substrate in the areas where it is observed. Adhesive failure is typically the result of less than ideal substrate surface preparation and is not a desirable failure mode. Thin-film failure could easily be mistaken for adhesive failure and is characterized by a thin layer of sealant left behind on the substrate as the sealant ruptures as shown in Fig. 6. In the experiments carried out in the study, adhesive failure was only observed in one instance along less than a 25 mm (1 in.) length of seal in an end panel weatherseal joint and did not have any detrimental effect on the performance of the mock-up. Typical gasket seal degradation (e.g., distortion, pullout, shifting), noted in previous studies [e.g., 6] was observed in the horizontal dry-glazed joints. In general, gasket seal degradation occurred before silicone sealant failure and at a later stage than would be expected of a mockup using gaskets around its entire perimeter.

As previously noted, glass-to-frame contact near corners of transoms was the cause of glass failure. This was evidenced using view windows cut into some of the pressure plates and postmortem inspections of the glazing lip (Fig. 1) and pressure plates of the transoms that supported the glass panel bottom edges. Inspections revealed scraping and gouging marks along the glazing lip and the inside surface of the pressure plates at the corner regions of the framing for each glass panel. As observed in dry-glazed racking tests, scraping marks were more extensive for AN Lami. and IGU configurations.

TABLE 2—*Serviceability and ultimate drift capacities of glass panels in two-side structural silicone mockup tests.*

	Cracking			Fallout			Shattering		
	Panel 1 mm (in.)	Panel 2 mm (in.)	Panel 3 mm (in.)	Panel 1 mm (in.)	Panel 2 mm (in.)	Panel 3 mm (in.)	Panel 1 mm (in.)	Panel 2 mm (in.)	Panel 3 mm (in.)
Mockup 1	63.5 (2.50)	69.9 (2.75)	63.5 (2.50)	69.9 (2.75)	[a]	63.5 (2.50)	59.9 (2.75)	[a]	69.9 (2.75)
Mockup 2	69.9 (2.75)	82.6 (3.25)	82.6 (3.25)	76.2 (3.00)	82.6 (3.25)	82.6 (3.25)	76.2 (3.00)	82.6 (3.25)	[a]
Avg.	**66.7 (2.63)**	**76.3 (3.00)**	**73.1 (2.88)**	**73.1 (2.88)**	**82.6 (3.25)**	**73.1 (2.88)**	**73.1 (2.88)**	**82.6 (3.25)**	**69.9 (2.75)**
Mockup 3	114.3 (4.50)	114.3 (4.50)	82.6 (3.25)	114.3 (4.50)	114.3 (4.50)	82.6 (3.25)	114.3 (4.50)	114.3 (4.50)	82.6 (3.25)
Mockup 4	114.3 (4.50)	114.3 (4.50)	108.0 (4.25)	114.3 (4.50)	114.3 (4.50)	108.0 (4.25)	114.3 (4.50)	114.3 (4.50)	108.0 (4.25)
Avg.	**114.3 (4.5)**	**114.3 (4.5)**	**95.3 (3.75)**	**114.3 (4.5)**	**114.3 (4.5)**	**95.3 (3.75)**	**114.3 (4.5)**	**114.3 (4.5)**	**95.3 (3.75)**
Mockup 5	82.6 (3.25)	108.0 (4.25)	82.6 (3.25)	101.5 (4.00)	108.0 (4.25)	[a]	152.4 (6.00)	152.4 (6.00)	152.4 (6.00)
Mockup 6	88.9 (3.50)	88.9 (3.50)	95.3 (3.75)	108.0 (4.25)	108.0 (4.25)	108.0 (4.25)	152.4 (6.00)	152.4 (6.00)	152.4 (6.00)
Avg.	**85.8 (3.38)**	**98.5 (3.88)**	**89.0 (3.5)**	**104.8 (4.13)**	**108 (4.25)**	**108 (4.25)**	**152.4 (6)**	**152.4 (6)**	**152.4 (6)**
Mockup 7	120.7 (4.75)	127.0 (5.00)	127.0 (5.00)	133.4 (5.25)	133.4 (5.25)	133.4 (5.25)	139.7 (5.50)	139.7 (5.50)	139.7 (5.50)
Mockup 8	133.4 (5.25)	127.0 (5.00)	127.0 (5.00)	133.4 (5.25)	133.4 (5.25)	133.4 (5.25)	139.7 (5.50)	139.7 (5.50)	139.7 (5.50)
Avg.	**127.1 (5.00)**	**127.0 (5.00)**	**127.0 (5.00)**	**133.4 (5.25)**	**133.4 (5.25)**	**133.4 (5.25)**	**139.7 (5.5)**	**139.7 (5.5)**	**139.7 (5.5)**

[a]Data not available because of test stoppage prior to occurrence of the fallout or shattering event.

Discussion of Glass Performance at Various Drift Levels

The results of the cyclic racking tests carried out on four different configurations with the same boundary conditions are summarized in Table 2 and Fig. 7. The data for each configuration are the average of its two test repetitions. Drift amplitude (and drift index) corresponding to glass spalling, glass cracking, glass fallout, and glass shattering of only the middle panel (considered the test panel) are plotted in Fig. 7. The data show that FT Mono. glass in the two-side SSG configuration has an approximately 38 % higher drift capacity than AN Mono. before cracking occurs. Of course, for FT glass cracking/fallout/shattering occurs at the same drift value. The FT Mono. configuration also showed slightly higher cracking (15 %) and fallout (5 %) drift capacities than AN Lami. In contrast, the AN IGU configuration showed larger cracking (13 %) and fallout (16 %) drift capacities than FT Mono. It is obvious that panel configuration is an important parameter in the simulated seismic response of two-side SSG curtain walls.

For a comparison of the expected performance of a given two-side SSG curtain wall on an actual building with the test results shown in Fig. 7, one should note the differences in the boundary conditions between these laboratory mockups and the actual curtain wall installation. These mockups were constructed under controlled conditions and also had somewhat different boundary conditions than would

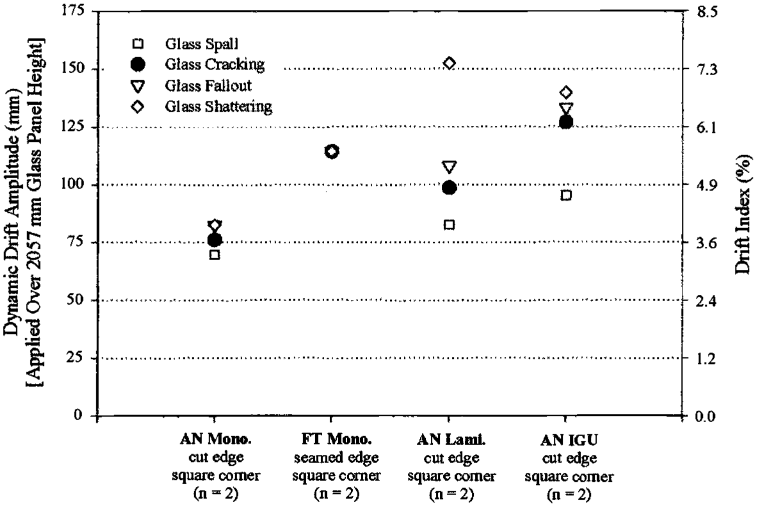

FIG. 7—*Drift capacities of middle test panels (Fig. 2) observed during two-side structural silicone mockup tests.*

curtain walls on actual buildings. Boundary conditions are influenced by a number of factors such as the type of glazing frame, end conditions, and restraints (end panel versus interior panel), and method of attachment of the glazing frame to the structural system. Thus, a quantitative comparison of the failure capacity of the lab mockups in this study to SSG curtain walls on actual buildings cannot be made. One should also note that the ASCE Standard 7-02 [11] design criteria for curtain walls, which is based on life safety, is that the drift causing glass fallout be at least 25 % larger than the building design drift multiplied by the building importance factor. Therefore, to determine the drift capacity of glass in curtain walls for life safety design, the satisfaction of ASCE criterion should be demonstrated. This can be done through mock-up testing that reflects the exact condition of the curtain wall on the real building (e.g., boundary conditions, glass panel aspect ratio, and size, among other parameters).

Previous dry-glazed racking tests on mockups constructed with the same curtain wall framing used for the dry-glazed portions of the mockups tested in this study have shown that the cracking drift capacity of dry-glazed FT Mono. is approximately 87 % higher than that of AN Mono. [12]. When compared to the 38 % difference observed between the FT and AN Mono. two side SSG mockups tested in this study, it is clear that the effect of glass type is reduced in SSG construction. It is also possible to make direct comparisons between the two-side SSG mock-ups test results in this study with the results from previous racking tests on dry-glazed mock-ups [6,12] that were constructed with the same glass configurations, the same curtain wall framing system, and anchored in a similar fashion to the racking facility. For example, Memari et al. [12] reported a cracking drift capacity of 39.1 mm (1.54 in.) for dry-glazed, 6 mm (0.24 in.) AN Mono. glass. As shown in Table 2 and Fig. 7, the SSG system with AN Mono. has a cracking drift capacity of 83 mm (3.25 in.) for the middle panel, which is approximately 112 % higher than its dry-glazed counterpart. Comparisons between the two-side SSG FT Mono., AN Lami., and AN IGU configurations and their dry-glazed counterparts also reveal sizable performance gains for two-side SSG systems. These comparisons confirm the widely held view that SSG systems perform favorably in earthquakes.

The test matrix employed in this study also provided some insight into how the boundary condition of adjacent panels and the weatherseal width can affect performance. Mock-up 1, which had dry-glazed exterior vertical edges at its end panels exhibited lower serviceability and ultimate drift capacities in the end panels when compared with mock-up 2, which was constructed with the same wet-glazed detail used for the other mockups in this study (Fig. 1). However, the end panel detail had only a small effect on the performance of the middle "test" panel.

Discussion of Air Leakage Performance

Air leakage tests were performed at selected racking displacement intervals in order to serve as an indicator of serviceability damage to the weatherseals and structural seals of the test panel. Air leakage test results are summarized in Fig. 8. As shown in the figure, a constant air leakage was measured up to a drift index of about 4 % for mock-ups 1 and 2 and about 5–6 % for the other mockups. Beyond about 4–5 %, a sharp increase in air leakage was generally observed, which was coincident with serviceability failure in the sealant joints.

Observations of sealant damage during these tests suggest that the onset of damage to the weatherseal and structural seals is repeatable and perhaps predictable. However, the mode of failure (in particular, cohesive versus thin film failure), its exact location, and the length over which the failure will occur is variable and somewhat uncertain after the onset of damage. Sealant failures were observed in both the weatherseals and structural seals. During air leakage tests, if there was no observable failure in the weatherseal, air leakage tests would not easily detect failure in the structural seal behind it. A plot of sealant damage length as a function of drift index is shown in Fig. 9, and appears to correlate well with the air leakage data plotted in Fig. 8. The two figures provide a basis for developing a correlation between air leakage rate and visible damage to seals. The AN Lami. and AN IGU configuration mockups had slightly thicker weatherseals than the AN and FT Mono. configurations, and as shown in Figs. 8 and 9, this led to improved air leakage resistance and sealant damage resistance in these configurations.

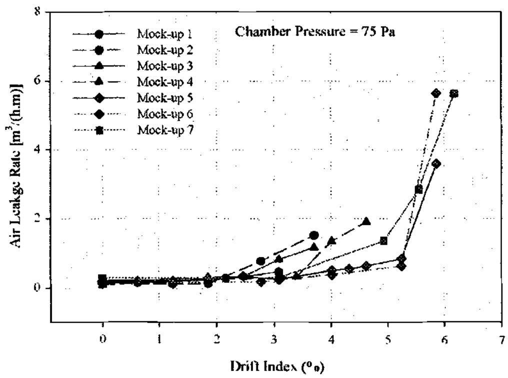

FIG. 8—*Air leakage rates through silicone sealant joints versus drift ratio imposed on the two-side structural silicone mockups.*

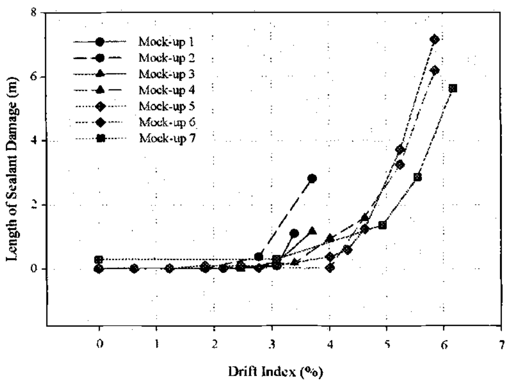

FIG. 9—*Length of sealant damage versus drift index imposed on the two side structural silicone mockups.*

Conclusions

Based on the results obtained in this study and comparisons with data collected during comparable studies on dry-glazed curtain walls, several conclusions can be drawn.

- Serviceability and ultimate drift capacities of two-side SSG systems are significantly higher than their dry-glazed counterparts. The magnitude of the increase depends on the glass configuration.
- Wet-glazed end panels within a two-side mockup lead to superior serviceability and ultimate drift capacity performance for all the panels in the mockup than do dry-glazed end panels.
- Glass-to-frame contact at the corner location of horizontal framing members is the cause of glass cracking in two-side SSG systems.
- When compared to comparable dry-glazed systems, the effect of glass type on serviceability and ultimate glass panel drift capacities is not as significant in two-side SSG systems.
- Air leakage tests showed that for the curtain wall mockups tested, beyond a drift index of 4–5 %, air leakage rate increases sharply.
- Air leakage tests and sealant damage observations suggest that there is a strong correlation between air leakage rate and sealant failure length.

References

[1] Stubbs, M. S., "Glued-on Glass—Examining Structural Silicone Sealant Glazing," *Arch. Technol.*, 1986, pp. 46–51.

[2] Parise, C. J., and Spindler, R. G., "Structural Sealant Glazing in the 1980s," *Exterior Wall Systems: Glass and Concrete Technology, Design, and Construction*, ASTM STP 1034, B. Donaldson, ed., American Society for Testing and Materials, Philadelphia, PA, 1991, pp. 94–117.

[3] AAMA, "Structural Sealant Glazing Systems—A Design Guide," AAMA Aluminum Curtain Wall Series No. 13, American Architectural Manufacturers Association (AAMA), 1985, Des Plaines, IL.

[4] Dow Corning, *Dow Corning Americas Technical Manual.*, 2005, Dow Corning, Midland, MI.

[5] ASTM Standard C 1401-02, "Standard Guide for Structural Sealant Glazing", *Annual Book of ASTM Standards*, Vol. 4(7), ASTM International, 2006, West Conshohocken, PA.

[6] Behr, R. A., "Seismic Performance of Architectural Glass in Mid-rise Curtain Wall," *J. Archit. Eng.*, Vol. 4, No. 3, 1998, pp. 94–98.

[7] Zarghamee, M. S., Schwatrz, T. A., and Gladstone, M., "Seismic Behavior of Structural Silicone Glazing," *Science and Technology of Building Seals, Sealants, Glazing and Waterproofing*, Vol. 6, ASTM STP 1286, James C. Myers, ed., American Society for Testing and Materials, Philadelphia, PA, 1996, pp. 46–59.

[8] (ICC), *International Building Code (IBC) 2003*, International Code Council, Falls Church, VA.

[9] AAMA, "Recommended Dynamic Test Method for Determining the Seismic Drift Causing Glass Fallout from a Wall System," Publication No. AAMA 501.6-01, 2001, American Architectural Manufacturers Association (AAMA), Des Plaines, IL.

[10] ASTM, Standard E 283-91, "Standard Test Method for Determining Rate of Air Leakage Through Exterior Windows, Curtain Wall, and Doors Under Specified Differences Across the Specimen," *Annual Book of ASTM Standards*, ASTM International, 2006, West Conshohocken, PA

[11] ASCE Standard 7-02, "Minimum Design Loads for Buildings and Other Structures," 2003, American Society of Civil Engineers, Reston, VA.

[12] Memari, A. M., Kremer, P. A., and Behr, R. A., "Architectural Glass Panels with Rounded Corners to Mitigate Earthquake Damage," *Earthquake Spectra*, Vol. 22, No. 1, 2006, pp. 129–150.

Development of New Test Methods and Performance-Based Specifications

Journal of ASTM International, Vol. 4, No. 1
Paper ID JAI100403
Available online at www.astm.org

Lawrence D. Carbary,[1] *Errol D. Bull,*[2] *and Steve S. Mishra*[3]

Development of a Practical Method to Evaluate the Fatigue Properties of Structural Silicone Glazing Adhesives

ABSTRACT: Structural silicone sealants have been used since the mid 1960s in the construction industry to attach glass to curtainwall framing systems. Design standards for these sealants have been in practice since the early 1970s and continue to be developed today. Most of these standards require tests that are based on a one-time destructive test of the joint material in tension. The industry established structural silicone design stress is intended to be reached only during the highest windload for the specified return wind period. The existing practice has had great success because the industry guidelines minimize stress on the silicone, and dictate quality assurance procedures that are instituted by curtainwall producers. In real life situations the sealant is additionally fatigued through a cyclic shear mechanism caused by daily thermal movement differences between the glass pane and the aluminum frame. This paper discusses a method for testing the effect of fatigue in sealants used in structural designs and comparing the data to control samples.

KEYWORDS: fatigue, structural silicone, durability, shear strain

Introduction

Design standards for structural silicone glazing (SSG) have been in practice since the early 1970s. [1] The existing practice has had great success because of the low design stress on the structural silicone (SS) along with the industry standard quality assurance procedures.

The success of SSG can be attributed to the fact that panels of glass and or metal are attached to a frame with a continuous silicone rubber adhesive. The weatherability, and durability of the silicone makes it an excellent product for the application, and the continuous adhesion keeps air and water out of the system. The resultant product is an architecturally pleasing facade that has a performance unmatched by panels captured by gaskets.

Figure 1 shows a typical SS design incorporated into a commercially available curtainwall system.

Although the SS design stress is designed for a certain return wind period, its use has been based on a tension test to destruction. The most popular methods of testing are based on the ASTM C1135 Standard Test Method for Determining Tensile Adhesion Properties of Structural Sealants and ISO 8339 Building Construction-Jointing Products-Sealants-Determination of Tensile Properties.

Sandberg performed fatigue testing of SS published data on the Creep Rupture and Fatigue of Structural Sealants. [2] The testing was performed to determine if the constant load designs of SS were appropriate for the applications based on Civil Engineering standards and logic. The conclusion was that the existing designs were conservative and appropriate.

Later on in 1990, the International Conference of Building Officials in Whittier California published the Acceptance Criteria for Type 1 Structural Silicone Glazing Sealants (Adhesive) [3]. This criteria required cyclic load tests between 0.5 and 1.0 times the design stress for 50 cycles. The condition of acceptance was the fatigued samples must show 95 % of the control sample strength and modulus. The spirit of this test was to show that the structural sealant would allow more than a once-in-50-years return windload at design stress without being affected.

The European Organization for Technical Approval developed the ETAG 002 Guideline for European

Manuscript received June 3, 2005; accepted for publication November 22, 2006; published online January 2007. Presented at ASTM Symposium on Durability of Building and Construction Sealants and Adhesives, Second Symposium on 15–16 June 2005 in Reno, NV; A. T. Wolf, Guest Editor.

[1] Associate Industry Scientist, Dow Corning Corporation, P.O. Box 994, Midland, MI 48686-0994, U.S.A.
[2] Technical Marketing Engineer, GE Advanced Materials-Silicones, 260 Hudson River Rd., Waterford, New York 12188 U.S.A.
[3] Vice President Technology, Tremco Inc, 3777 Green Rd., Beachwood, OH 44122 U.S.A.

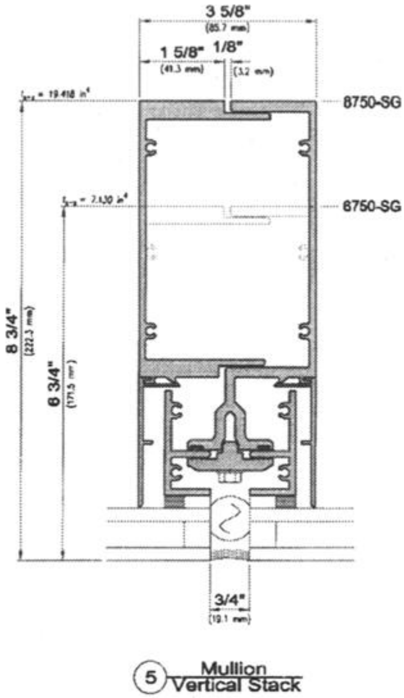

FIG. 1—*Vertical structural silicone detail on Wausau Window and Wall Systems 8750 SG Series curtainwall. (Wausau Window and Wall Systems, 1415 West St., Wausau WI, 54402, USA, www.wausauwindow.com)*

Technical Approval for Structural Sealant Glazing Systems [4], and it also contains a mechanical fatiguing requirement. It states that the test pieces are to be subjected to repetitive tensile loads with a cycle time of 6 s for 100 times from 0.1 to 1.0 times the design stress, then 250 times from 0.1 to 0.8 times the design stress, and then 5000 times from 0.1 to 0.6 times the design stress. The condition of acceptance is that after testing the fatigued sealant must have greater than 75 % of the strength compared to the control.

These two initial standards are performed by fatiguing the samples in tension based on an anticipated windload for the structure. However, daily thermal movement differences between glass and aluminum framing will cause the structural silicone sealants to experience shear. The logic of tension fatigue testing is easy to understand because the equipment used in these tests was developed for tension testing.

Members of ASTM Committee C24 on Building Seals established a task group to develop a logical method of shearing SS joints and comparing the strength and modulus after testing to control samples. The amount of shear should be based on the thermal cycles placed upon the system for the life of the system.

Large lites of monolithic glass that are adhered to aluminum curtainwall frames can be as large as 1800 mm wide by 3650 mm tall. These lites are typically fabricated in a shop at temperatures of 15–30°C. A thermal cycle in Minneapolis, Minnesota can cause the exterior wall to experience −40°C in the winter and can reach up to 80°C in the summer. Thus, thermal movement in Minnesota would be driven by a temperature difference of 65 C° (80−15). Phoenix, Arizona may not have the winter cold and the exterior skin may only experience 0°C in the winter, but may reach 100°C in the summer. The Phoenix thermal cycle could be as large as 85 C° (100−15).

When considering a worse case scenario of a silicone structurally glazed 3650 mm tall lite experiencing an 85 C° temperature change, the dimensional change of the glass will be absorbed by the thickness of the SS. It is assumed that the thermal movement of the glass is in one direction only, because the glass is supported with setting blocks to absorb gravity loads. This thermal movement of the glass would be equivalent to 2.79 mm at the top of the lite. If this 2.79 mm of movement is induced through a 6.0-mm SS

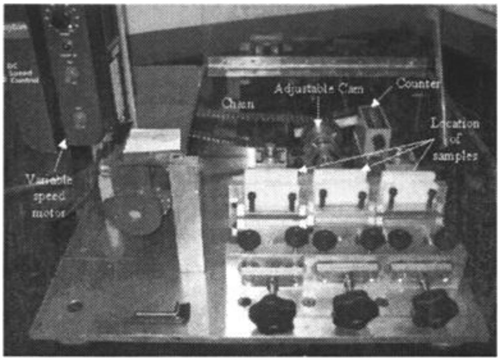

FIG. 2—*Fatigue testing device.*

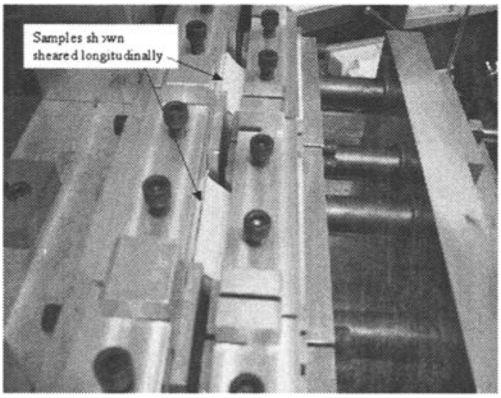

FIG. 3—*Samples in fatigue device, sheared longitudinally.*

adhesive thickness, the resultant strain on the sealant is 10.3 %. This is determined by comparing the thermally induced dimension to the original dimension using the Pythagorean relationship for a right triangle.

It is assumed that the thermal cycling on the curtainwall frame could happen twice per day. If the life span of a curtainwall is 50 years and the SSG system cycles twice per day, 36 512 cycles could occur. At one time per day, 36 525 cycles could occur in 100 years.

The task group chose to evaluate specimens for strength and modulus after 36 500 cycles of 15 % shear strain. A rate of five cycles per minute was selected to minimize any potential internal heat build-up in the specimens. The device that was used was a machine that operates on a cam to perform the cycling.

Test Method Intent

Since SS construction techniques can have life safety implications, such as falling glass, to pedestrians and building occupants, it is imperative to use only products that have a performance profile that can withstand the loads imposed on such a system and which can withstand such loads for the duration of the intended service life.

Development of this test method is intended to serve as an enhancement to current performance requirements for SS and to help the industry ascertain that current and new products are sufficiently resilient to withstand years of fatigue imposed on systems by thermal expansion and contraction, or other loads which impose shear.

TABLE 1—*Description of sealants tested.*

Sealant	Type	Movement capability, %	Cure chemistry
1	2 part	12.5	Alkoxy silicone
2	2 part	12.5	Alkoxy silicone
3	2 part	12.5	Alkoxy silicone
4	2 part	20	Alkoxy silicone
5	1 part	25	Alkoxy silicone
6	1 part	25	Oxime silicone
7	1 part	25	Oxime silicone
8	1 part	50	Alkoxy silicone
9	1 part	50	Alkoxy silicone

Test Method Description

The proposed method is designed to simulate shear forces of a magnitude that are typically seen in structurally glazed curtainwall designs including an additional safety factor. This test method uses cured ASTM C1135 specimens inserted into a device (shown in Fig. 2) that can impose shear either transversely (as would occur at a head or sill condition) or longitudinally (as would occur at jambs) across the long width of the specimen (see Fig. 3). The direction of shear is dependent upon how the specimens are affixed into the device. Once inserted, they are firmly secured such that when the shearing force is imposed the plates remain parallel.

The device (shown in Fig. 2) consists of a chain-driven adjustable cam powered by a variable speed electric motor. A mechanical counter is fitted on the device to count cycles. The cam in turn causes a floating head assembly to move relative to a fixed head assembly between which the sealant samples are inserted.

Results and Discussion

A variety of silicone sealants with different physical properties and chemistries were tested and are described in Table 1. Results reported are based upon ASTM C1135 testing with respect to maximum stress, maximum strain, and the secant modulus at a given strain. Standard deviations are reported, and each data point is the average of a minimum of three specimens. Sealants are listed in order of the manufacturers' stated movement capability.

Summary

Each sealant was tested for a minimum of at least 36 000 cycles that exerted a 15 % shear displacement to the samples. The results for each sealant are summarized in Figs. 4–13 and Tables 2–10. The shear strain imposed by this testing is conservative. Realistic thermal movement displacements for in-service curtainwalls will rarely approach movements of 15 %. Products capable of 12.5 % movement have been performing without failure for many years lending credence to this point.

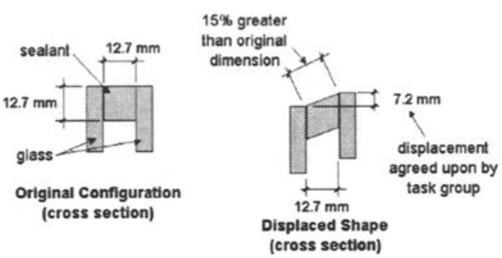

FIG. 4—*Depiction of shear displacement.*

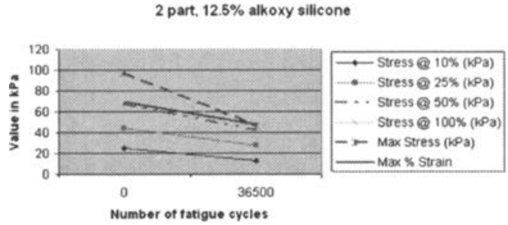

FIG. 5—*Behavior of Sealant 1.*

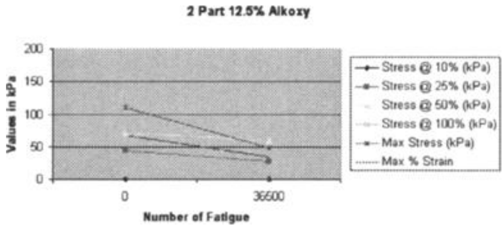

FIG. 6—*Behavior of Sealant 2.*

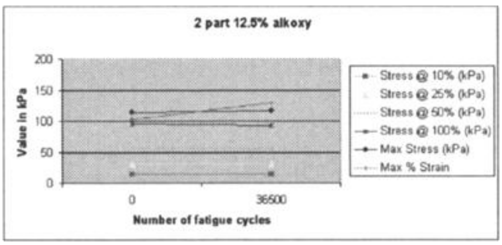

FIG. 7—*Behavior of Sealant 3.*

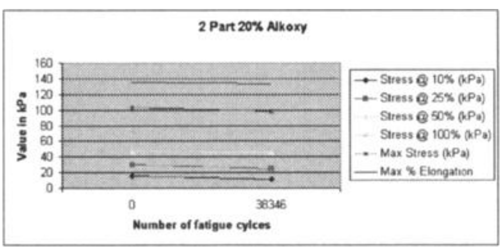

FIG. 8—*Behavior of Sealant 4.*

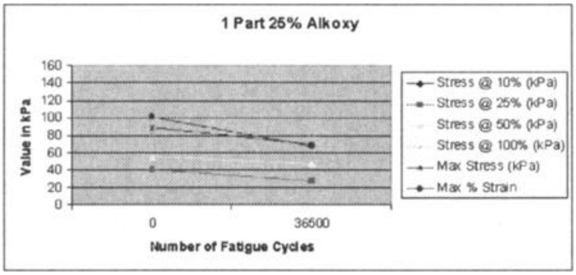

FIG. 9—*Behavior of Sealant 5.*

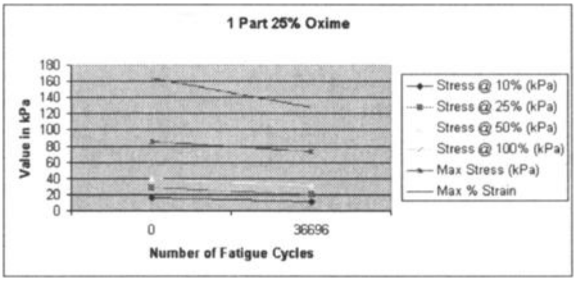

FIG. 10—*Behavior of Sealant 6.*

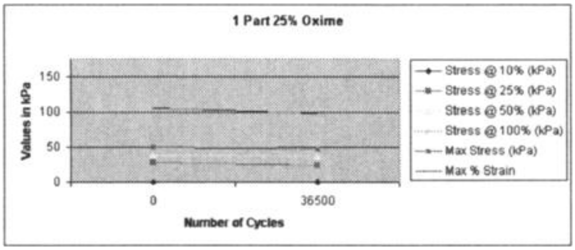

FIG. 11—*Behavior of Sealant 7.*

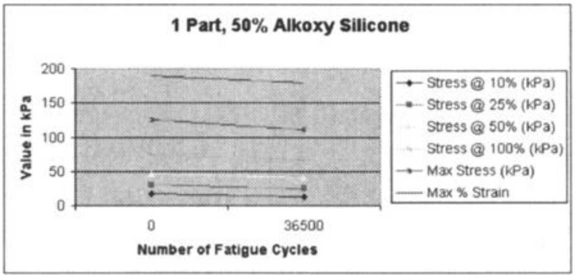

FIG. 12—*Plot of behavior of Sealant 8.*

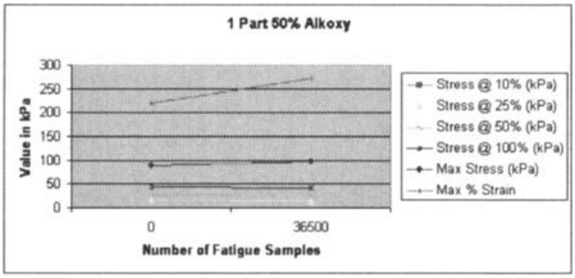

FIG. 13—*Behavior of Sealant 9.*

TABLE 2—*Details of Sealant 1.*

	15 % Elongation cycles			
2 Part 12.5 % Alkoxy	Average values		Standard deviations	
Fatigue cycles	0	36 5000	0	36 500
Stress @ 10 %, kPa	25.392	13.455	0.2691	2.1114
Stress @ 25 %, kPa	44.0289	27.393	0.5727	4.1814
Stress @ 50 %, kPa	68.241	42.504	1.3386	8.4249
Stress @ 100 %, kPa	97.29	34.6242	2.5323	0.6969
Max stress, kPa	97.635	46.713	2.9394	10.074
Max % strain	69.5244	47.679	3.9123	2.7807

TABLE 3—*Details of Sealant 2.*

	15 % Elongation cycles			
2 Part 12.5 % Alkoxy	Average values		Standard deviations	
Fatigue cycles	0	36 500	0	36 500
Stress @ 10 %, kPa	...	...	...	...
Stress @ 25 %, kPa	44.16	28.221	3.8847	13.7448
Stress @ 50 %, kPa	72.312	59.133	4.5678	16.0701
Stress @ 100 %, kPa	116.058	...	1.8768	...
Max stress, kPa	109.779	48.369	9.4116	30.4566
Max % strain	66.93	34.5	6.0168	13.3239

TABLE 4—*Details of Sealant 3.*

	15 % Elongation cycles, 1873-164			
2 Part 12.5 % Alkoxy	Average values		Standard deviations	
Fatigue cycles	0	36 500	0	36 500
Stress @ 10 %, kPa	13.8	13.8	0.2139	0.828
Stress @ 25 %, kPa	31.05	31.05	0.1725	1.794
Stress @ 50 %, kPa	55.752	55.752	0.5451	2.622
Stress @ 100 %, kPa	95.979	92.322	0.8418	4.071
Max stress, kPa	114.264	117.369	2.1459	11.454
Max % strain	103.224	130.272	5.9961	11.247

TABLE 5—*Details of Sealant 4.*

	15 % Elongation cycles			
2 Part 20 % Alkoxy	Average values		Standard deviations	
Fatigue cycles	0	38 346	0	38 346
Stress @ 10 %, kPa	15.7596	11.2608	1.0212	0.7383
Stress @ 25 %, kPa	30.1461	25.1367	1.4283	0.7452
Stress @ 50 %, kPa	47.4996	45.5193	1.6491	0.4899
Stress @ 100 %, kPa	74.3337	73.7334	1.6905	1.1661
Max stress, kPa	102.7272	98.3595	12.8271	8.832
Max % elongation	135.516	132.9009	34.7484	10.419

TABLE 6—*Details of Sealant 5.*

	15 % Elongation cycles			
1 Part 25 % Alkoxy	Average values		Standard deviations	
Fatigue cycles	0	36 500	0	36 500
Stress @ 10 %, kPa	...	...	...	...
Stress @ 25 %, kPa	39.951	27.531	2.0631	2.3391
Stress @ 50 %, kPa	55.821	47.334	2.1942	8.5974
Stress @ 100 %, kPa	81.765	81.213	4.3401	2.0424
Max stress, kPa	88.941	69.138	6.486	14.8833
Max % strain	100.74	68.31	13.5378	5.5269

TABLE 7—*Details of Sealant 6.*

	15 % Elongation cycles			
1 Part 25 % Oxime	Average values		Standard deviations	
Fatigue cycles	0	36 696	0	36 696
Stress @ 10 %, kPa	16.353	11.4954	0.2139	3.5811
Stress @ 25 %, kPa	28.0416	20.0721	0.2829	0.5037
Stress @ 50 %, kPa	39.2196	31.6503	0.2208	2.7117
Stress @ 100 %, kPa	56.856	54.2961	0.8901	1.8009
Max stress, kPa	85.2426	72.6363	6.6654	1.1109
Max % strain	163.9233	128.2227	15.1041	2.4426

TABLE 8—*Details of Sealant 7.*

	15 % Elongation cycles			
1 Part 25 % Oxime	Average values		Standard deviations	
Fatigue cycles	0	36 500	0	36 500
Stress @ 10 %, kPa	...	...	...	...
Stress @ 25 %, kPa	29.049	23.667	3.9744	3.8433
Stress @ 50 %, kPa	38.502	36.363	5.2785	6.4101
Stress @ 100 %, kPa	50.646	47.679	3.6225	5.4579
Max stress, kPa	49.404	47.61	12.8409	14.6073
Max % strain	105.57	97.98	50.2872	52.5504

TABLE 9—*Details of Sealant 8.*

	15 % Elongation cycles, 1873-164			
1 Part 50 % Alkoxy	Average values		Standard deviations	
Fatigue cycles	0	36 500	0	36 500
Stress @ 10 %, kPa	17.733	12.558	0.6003	0.05382
Stress @ 25 %, kPa	30.774	25.185	0.7866	0.18906
Stress @ 50 %, kPa	46.575	40.572	0.7383	0.33327
Stress @ 100 %, kPa	75.003	66.4746	0.4347	0.7038
Max stress, kPa	124.959	110.262	1.587	5.175
Max % strain	189.957	179.814	10.764	11.523

TABLE 10—*Details of Sealant 9.*

	15 % Elongation cycles			
1 Part 50 % Alkoxy	Average values		Standard deviations	
Fatigue cycles	0	36 500	0	36 500
Stress @ 10 %, kPa	...	...	...	...
Stress @ 25 %, kPa	17.388	14.421	1.1799	0.9039
Stress @ 50 %, kPa	26.979	25.116	1.6077	0.621
Stress @ 100 %, kPa	44.091	42.504	2.4357	1.3248
Max stress, kPa	89.079	97.014	8.2317	7.038
Max % strain	220.11	272.55	37.6188	37.6671

Conclusions

(1) The standard deviations of the fatigued samples are larger than the nonfatigued samples which is indicative of the degradation seen in the fatigued sample sets.

(2) The sealants with higher movement capability show less susceptibility to degradation than the lower movement sealants when strained to 15 %.

(3) The test method can differentiate between similar sealants. The test method is discriminatory enough to show significant degradation of the 12.5 % movement sealants when strained to a movement beyond which they are expected to endure.

(4) The tested SS (when not strained in shear beyond their movement capacity) experience degradation. The degradation is small enough that shear rupture of the sealant due to fatigue is not probable.

(5) A reduction in modulus of the sealant was observed in each case after undergoing fatigue.

Future Work

Given the numerous variables associated with any given SSG installation, this in development test method can never accurately mimic nor replicate the fatigue actually occurring for any specific installation. It can provide a basis and a model from which to further study fatigue and to provide some guidelines and understanding of how the SS reacts under repetitive loading. Further development of this method may result in its inclusion in the ASTM C1184 Specification for Structural Silicone Sealants.

References

[1] Hilliard, J. R., Parise, C. J., and Peterson, C. O. Jr., "Structural Sealant Glazing, Sealant Technology in Glazing Systems," *ASTM STP 638*, ASTM International, West Conshohocken, PA, 1977, pp. 67–99.

[2] Sandberg, L. B., and Rintala, A. E., "Resistance of Structural Silicones to Creep Rupture and Fatigue, Building Sealants: Materials, Properties, and Performance," *ASTM STP 1069*, T. F. O'Connor, Ed., American Society for Testing and Materials, West Conshohocken, PA, 1990, pp. 7–21.

[3] Acceptance Criteria for Type 1 Structural Silicone Glazing Sealants (Adhesive) International Conference of Building Officials, Whittier CA, 1990.

[4] ETAG 002 Guideline for European Technical Approval for Structural Sealant Glazing Systems, The European Organization for Technical Approval, Brussels, Belgium, November 1999, Amended October 2001.

Journal of ASTM International, Vol. 3, No. 2
Paper ID JAI13117
Available online at www.astm.org

James C. Strong,[1] *Jennifer R. Kovach,*[2] *and Virginia S. Eng*[3]

Standards Development for Impermeable, Constructible, and Durable Waterproofing

ABSTRACT: Building owners' expectations for waterproofing systems are simple. Waterproofing must prevent the passage of water (impermeability), must be capable of successful installation under typical construction conditions (constructability), and must continue to provide waterproofing for the life of the structure (durability). The realization of these expectations is thwarted, in part, by a lack of consensus on how these features are defined, tested, and compared to performance-based criteria. This investigation includes waterproofing materials commonly used on plazas and below-grade walls. The authors discuss important properties of waterproofing and review the requirements of standards for waterproofing systems. The results of testing bentonite and cold liquid-applied waterproofing are reported. In conclusion, the authors suggest improvements in standards.

KEYWORDS: waterproofing, impermeability, constructability, durability, bentonite, liquid-applied

Introduction

Buildings are often designed to utilize below-grade space beneath the building footprint and plazas. Occupied above-grade building spaces are sometimes topped with terraces and "green" roofs. Each of these areas must be protected from water intrusion by a waterproofing system.

When waterproofing systems fail, unsightly stains occur, building contents are damaged, mold can grow, occupied spaces may be unwillingly abandoned, and the structure deteriorates. Waterproofing systems may be completely inaccessible for repair, as with deep below-grade walls, or accessible at a high cost, as when plaza finishes and planters must be removed.

The authors are often called upon to investigate waterproofing system failures. We find that it is often challenging to restore waterproofing systems to the same level of reliability that should be provided by a new installation. The cost of repairing a widespread waterproofing failure is likely to far exceed the initial cost of materials and installation.

Setting increasingly well developed standards for waterproofing materials and installation methods contribute to improving the overall quality of these systems. With this paper, the authors seek to advance efforts to improve standards for waterproofing materials.

Application of Waterproofing in Building Construction

Two fundamental ways of categorizing waterproofing systems are in terms of their position relative to the structure and by the sequence of installation of waterproofing and structural elements.

Positive-Side Application—Positive-side applications are on the side of an assembly that is intended to be exposed to moisture. Positive-side applications include waterproofing installed at the top of the structural decks of plazas and as the lining of planters. Waterproofing may be installed on the positive-side of below-grade walls when an excavation on the exterior side of the wall allows access for safe waterproofing application.

Manuscript received May 23, 2005; accepted for publication August 29, 2005; published online February 2006. Presented at ASTM Symposium on Durability of Building and Construction Sealants and Adhesives, Second Symposium on 15–16 June 2005 in Reno, NV; A. T. Wolf, Guest Editor.
[1] Consultant, Wiss, Janney, Elstner Associates, Inc., 2200 Powell Street, Suite 925, Emeryville, CA 94608.
[2] Associate III, Wiss, Janney, Elstner Associates, Inc., 2200 Powell Street, Suite 925, Emeryville, CA 94608.
[3] Associate III, Wiss, Janney, Elstner Associates, Inc., 2200 Powell Street, Suite 925, Emeryville, CA 94608.

Positive-Side, Blind Application—This is waterproofing installed on the positive (wet) side prior to construction of the wall or slab. Examples are waterproofing that is installed before slabs-on-ground are poured over it and waterproofing that is attached to below-grade retaining walls before the concrete wall is placed. Methods of placing concrete walls against waterproofing include pneumatic placement (shotcrete) and cast-in-place with one-sided forms.

Negative-Side Application—Negative-side installation takes place on what is intended to be the dry side of a wall or slab. An example is the application of crystalline waterproofing slurry on the interior surface of the wall. Another approach to negative-side waterproofing is injection of waterproofing from the interior (dry) side of the wall. Holes are drilled into or through a concrete below-grade wall or slab and waterproofing grout is injected into cracks or through the concrete and into the soil.

Integral Waterproofing—Concrete is sometimes designed to retain water on its own, either without a waterproofing membrane or as a secondary line of protection against water intrusion. Water-stops are installed in concrete cold-joints. The concrete may be designed for minimal porosity and cracking. The integral waterproofing capacity of concrete may be augmented by including waterproofing admixtures in the concrete mix design.

Standards development is needed for all these types of waterproofing; however, the focus of this paper is materials used in building construction for positive-side applications and positive-side blind applications.

Types of Waterproofing Materials and Their Standards

This paper focuses on the development and improvement of standard specifications for waterproofing materials. As a first step, we identified some common types of waterproofing materials with specifications set by ASTM International or the Canadian General Standards Board (CGSB): cold liquid-applied, hot liquid-applied, and single ply. In addition, we consider a widely used waterproofing material, bentonite, which lacks ASTM or CGSB waterproofing standards.

Cold Liquid-Applied Membrane

This is a broad range of products with a diversity that is not fully reflected in current standards. The products are delivered in fluid state and they cure by various mechanisms after application to form a continuous membrane. Material types include one-component—moisture curing, one-component with accelerator, and two-component. They are applied with trowels, brushes, rollers, and spray. The base chemistry includes polymers, polymers modified with bitumen, and bitumen modified with a polymer. The materials may be reinforced with a fabric. This broad category of products is subject to the following ASTM standard and International Code Council (ICC) Evaluation Services (ES) Acceptance Criteria.

- ASTM Specification for High Solids Content, Cold Liquid-Applied Elastomeric Waterproofing for Use with Separate Wearing Course (ASTM C 836)
- ICC ES AC29 Acceptance Criteria for Cold, Liquid-Applied, Below-Grade, Exterior Dampproofing and Waterproofing Materials (AC29)

The following standards describe application considerations and installation methods for cold liquid-applied waterproofing.

- ASTM Guide for Use of High Solids Content, Cold Liquid-Applied Elastomeric Waterproofing Membrane with Separate Wearing Course (ASTM C 898)
- ASTM Guide for the Use of High Solids Content Cold Liquid-Applied Elastomeric Waterproofing Membrane on Vertical Surfaces (ASTM C 1471)

Hot Liquid-Applied Membrane

This product is asphalt with a polymeric modifier. It is delivered in solid kegs, heated to a fluid state on site, and applied as a hot liquid to form a continuous membrane. The material may be installed with a reinforcing scrim embedded in the hot fluid material. This product is subject to the following standard.

- CAN/CGSG-37.50-M89 Hot-Applied, Rubberized Asphalt for Roofing and Waterproofing (CAN/CGSG-37.50-M89)

The following standards describe application considerations and installation methods for hot liquid-applied waterproofing.

- CAN/CSB-37.51-M90 Application for Hot-Applied Rubberized Asphalt for Roofing and Waterproofing (CAN/CGSB-37.51-M90)
- ASTM Guide for Application of Fully Adhered Hot-Applied Reinforced Waterproofing Systems (ASTM D 6622), Type IV

Single-Ply Waterproofing Membranes

These waterproofing products include polyvinyl chloride (PVC), ethylene propylene diene terpolymer (EPDM), and isobutylene-isoprene rubber (butyl). The products are supplied as rolled sheets; sheet laps are sealed in the field by adhesive or heat welding. These materials are subject to the following waterproofing standards.

- ASTM Specification for Vulcanized Rubber Sheets Used in Waterproofing Systems (ASTM D 6134), Type I (EPDM); and Type II (Butyl)
- CAN/CGSB-37.54-95 Polyvinyl Chloride Roofing and Waterproofing Membrane, Reinforced with Embedded Fabric, Waterproofing (CAN/CSB-37.54-95) Type 4, Class C
- CAN/CGSB-37-GP-52M Roofing and Waterproofing Membrane, Sheet Applied, Elastomeric, Reinforced Membrane, for Non-Exposed Use (CAN/CGSB-37-GP-52M) Type 2, Class B

Bentonite

Sodium bentonite (bentonite) is a high-swelling form of weathered volcanic tuff. It takes its name from Fort Benton, Montana, where a deposit was discovered. Bentonite swells in the presence of water, and, when confined—for example, by an overlaying concrete slab—the hydrated bentonite forms a dense, flexible layer that stops the passage of liquid water. While there is a long history of use of the product as a waterproofing material, we are unaware of a material specification standard describing bentonite as a waterproofing material.

Additional Types of Waterproofing Not Addressed in this Paper

This paper does not address waterproofing that is intended to be exposed to traffic, such as the materials described in the following standard.

- ASTM Specification for High-Solids Content, Cold Liquid-Applied Elastomeric Waterproofing Membrane with Integral Wearing Surface (ASTM C957)

Additionally, several important types of waterproofing are not included in this review because of the lack of a material specification that covers the completed membrane as a waterproofing material. For example, there are material specifications for waterproofing asphalt and ply materials used in making a built-up bituminous waterproofing membrane—but none for the completed built-up membrane.

The installation of some of the materials we have omitted from this paper is described in the following standards.

- ASTM Guide for Design of Built-Up Bituminous Membrane Waterproofing Systems for Building Decks (ASTM C 981)
- ASTM Guide for Standard Details for Adhered Sheet Waterproofing (ASTM D 5898)
- ASTM Practice for Application of Self-Adhering Modified Bituminous Waterproofing (ASTM D 6135)
- ASTM Guide for Application of Fully Adhered Hot-Applied Reinforced Waterproofing Systems (ASTM D 6622)
- ASTM Guide for Application of Fully Adhered, Cold-Applied, Prefabricated Reinforced Modified Bituminous Membrane Waterproofing Systems (ASTM D 6769)
- ASTM Practice for Application of Heat Weldable Atactic Polypropylene (APP) Modified Bituminous Waterproofing Membranes Systems for New Building Decks (ASTM D 6950)

TABLE 1—*Impermeability—Requirements in standards regarding hydrostatic pressure resistance. Values and units are stated in the table as they are expressed in the standards.*

Standard	Value	Test Method
Cold Liquid-Applied		
ASTM C 836	...	...
ICC ES AC29	No leakage	Hydrostatic pressure over cracks, ASTM C 1306 or D 5385—with minimum 1.6 mm (1/16 in.) crack width, at twice the building's anticipated hydrostatic pressure
Hot Liquid-Applied		
CAN/CGSB-37.50-M89	...	...
Single Ply Membranes		
ASTM D 6134, Type I	...	...
ASTM D 6134, Type II	...	...
CAN/CGSB-37.54-95, Type 4, Class C	...	...
CAN/CGSB-37-GP-52M, Type 2, Class B	No leakage	Watertightness, CAN/CGSB -37-GP-52M. Following a dynamic impact test, 500 mm head of water for 16 h.

Essential Requirements for Waterproofing

Introduction

Waterproofing materials standards contain both requirements that are specific to the material described and requirements for properties that are essential to any waterproofing system. For example, nonvolatile content may be useful in distinguishing between cold liquid-applied waterproofing materials; but, it is a property that has little relevance to other kinds of waterproofing. On the other hand, the capacity to bridge cracks is important to any waterproofing. In the review that follows, we have attempted to identify requirements within existing material standards that indicate essential requirements for waterproofing. To set a manageable scope for this paper, we limited our review to two properties each in the three broad areas of impermeability, constructability, and durability.

Inpermeability—Hydrostatic Pressure Resistance

It may seem unnecessary to state, but waterproofing should be impermeable. Waterproofing should stop the passage of liquid water and it should provide that barrier at the hydrostatic pressure present at a particular project.[4] While resistance to hydrostatic pressure is a widely expected characteristic of waterproofing, four of the six material specifications have no requirement for hydrostatic pressure resistance. Refer to Table 1 for a review of standards.

AC29 and CAN/CGSB-37-GP-52M require hydrostatic testing after stressing the membrane test specimen. AC29 requires that the membrane specimen be stretched by the introduction of a gap in the substrate, which simulates a substrate crack. The CGSB test uses a dynamic impact test, which simulates abuse during construction, followed by a mild hydrostatic test.

The hydrostatic test method in CAN/CGSB SB-37-GP-52M is simple and probably reproducible. The impact test and the water test are conducted in separate operations, which contribute to the simplicity of the test. CAN/CGSB SB-37-GP-52M requires hydrostatic testing with a 500 mm (1.6 ft) column of water, which is the equivalent of the hydrostatic pressure in a shallow planter.

The hydrostatic testing required in AC29 is more demanding, but the standards it references provide little assurance of consistent results when conducted in different laboratories. AC29 allows either of two test methods to be used to measure hydrostatic pressure: ASTM Test Method for Hydrostatic Pressure Resistance of a Liquid-Applied Waterproofing Membrane (ASTM C 1306) and ASTM Test Method for

[4]Hydrostatic pressure on a below-grade structure increases with the depth below the groundwater level. The hydrostatic pressure of freshwater increases at 9.79 MPa $\times$ 10^{-3}/m (0.433 psi/ft).

TABLE 2—*Impermeability—Requirements in standards regarding moisture vapor resistance. Values and units are stated in the table as they are expressed in the standards.*

Standard	Requirement	Test Method
Cold Liquid-Applied		
ASTM C 836	...	...
ICC ES AC29	1 perm. max.	Permeance, ASTM E 96, Water Method
Hot Liquid-Applied		
CAN/CGSB-37.50-M89	1.7 ng/Pa.s.m^2, max.	Permeance, ASTM E 96, Procedure E (Desiccant Method at 37.8°C (100°F))
Single Ply Membranes		
ASTM D 6134, Type I	3.5 mg/pasm^2 (0.06 perms), max.	Permeance, ASTM E 96, "Procedure B. W. Relative Humidity at 45 % at 73°F±4°F" (Inverted Water Method)
ASTM D 6134, Type II	0.14 mg/pasm^2 (0.0025 perms), max.	Permeance, ASTM E 96, "Procedure B. W. Relative Humidity at 45 % at 73°F±4°F" (Inverted Water Method)
CAN/CGSB-37.54-95, Type 4, Class C	1.0 g/m^2, max.	Water Vapor Transmission, ASTM E 96, Procedure A (Desiccant Method)
CAN/CGSB-37-GP-52M, Type 2, Class B	...	...

Hydrostatic Pressure Resistance of Waterproofing Membranes (ASTM D 5385.) These standards are modified by AC29; instead of a normal 3.2 mm (1/8 in.) crack opening, a minimum 1.6 mm (1/16 in.) crack opening is allowed. AC29 requires that the materials do not leak when tested at twice the hydrostatic pressure anticipated for a specific building.

In the "Precision and Bias" sections of both standards referenced in AC29, there is an indication that the tests offer less reliability than the writers of AC29 may have desired. ASTM D 5385 makes no statement "concerning either the precision or bias of this test method since the result states merely that the system tested passes this test at a specific pressure and does not leak water for 1 h."

The subcommittee responsible for ASTM C 1306 organized a round-robin process to evaluate the test method in terms of repeatability (within a laboratory) and reproducibility (between laboratories); however, the results are not encouraging. Regarding reproducibility, ASTM C 1306 concludes that, "In future use of this test method, the difference between two test results obtained in different laboratories on the same material will be expected to exceed 21.082 psi only about 5 % of the time." A difference of 0.145 MPa (21.082 psi) is a very large variation in test results, considering that the variation is approximately equal to the total hydrostatic pressure on a structure 15 m (49.2 ft) below the water table.

Impermeability—Water Vapor Resistance

All but two standards reviewed have a requirement that addresses the passage of water vapor. The standards that address water vapor resistance all refer to ASTM Test Methods for Water Vapor Transmission of Materials (ASTM E 96). ASTM E 96 describes three basic test methods: the water method, the inverted water method, and the desiccant method. ASTM E 96 also includes six sets of test conditions, referred to as "Procedures." The test method allows for calculating results as water vapor transmission, permeance, or permeability. The waterproofing material standards reviewed here utilize most of the variations allowed in ASTM E 96, which makes comparison of materials challenging. Refer to Table 2 for a review of standards.

As seen in Table 2, there is agreement among many standards writers that water vapor resistance is a significant issue; however, none of the standards require the same combination of ASTM E 96 test procedures and methodology for expressing results. This diversity in test methods (water, inverted water, and desiccant) is surprising considering that ASTM E 96 states that the inverted water method should be used, "Where water is expected to be in contact with the barrier in service..." Waterproofing is clearly a barrier that by definition is intended to be in contact with water.

In this context, bentonite waterproofing deserves particular attention. Bentonite transforms from a dry

TABLE 3—*Constructability—Requirements in standards regarding penetration resistance and toughness. Values and units are stated in the table as they are expressed in the standards.*

Standard	Requirement	Test Method
Cold Liquid-Applied		
ASTM C 836	50, min	Hardness, ASTM D 2240, Type 00
ICC ES AC29	...	...
Hot Liquid-Applied		
CAN/CGSB-37.50-M89	5.5 J, min	Toughness test, CAN/CGSB-37.50-M89
Single Ply Membranes		
ASTM D 6134, Type I	32 Kg (70 lb)	Puncture Resistance, ASTM E 154
	60±10	Hardness, Durometer A, ASTM D 2240
ASTM D 6134, Type II	43 Kg (95 lb)	Puncture Resistance, ASTM E 154
	60±10	Hardness, Durometer A, ASTM D 2240
CAN/CGSB-37.54-95, Type 4, Class C	30 *N*, min	Cone penetration, CAN/CGSB-37.54-95
CAN/CGSB-37-GP-52M, Type 2, Class B	No leakage after impact test and hydrostatic test	Dynamic Impact, CAN/CGSB-37-GP-52M—Following impact test, 500 mm head of water for 16 h

granular material to a dense layer capable of stopping the flow of liquid water by absorbing water (hydrating). This widely used product is designed, quite unlike other waterproofing, to hold moisture against the structure. The wide acceptance of bentonite raises a question regarding whether waterproofing materials must be vapor resistant.

Nonetheless, there is wide support for permeance requirements, perhaps in part because permeance is an indicator of a products resistance to long-term water absorption. By convention in the U.S. construction industry, a material is considered a vapor barrier if it has a permeance of less than 8.7 $ng/Pa.s.m^2$ (1 Perm (inch-pound)). While some materials may have much lower permeance, this value may have broad support as a basic requirement for waterproofing.

Constructability—Penetration Resistance and Toughness

Building construction sites are not hospitable environments for easily damaged materials. While it is common to specify protection boards over waterproofing, these protection materials do not render the waterproofing invulnerable to impact from dropped tools and steel reinforcing bars. Pneumatic placement of concrete propels concrete aggregate with considerable velocity at typically unprotected waterproofing membranes. Refer to Table 3 for a review of standards.

ASTM Test Method for Rubber Property—Durometer Hardness (ASTM D 2240) is commonly used to measure hardness of materials. ASTM D 2240 testing uses a durometer to press a pin (indentor) into a specimen. ASTM D 2240 defines twelve different shapes and diameters of durometer indentors, which are selected based upon the relative hardness of the material. For example, a Type OO is referenced in the ASTM standard for cold liquid-applied materials, and a Type A is referenced in the ASTM standards for single-ply waterproofing. Note that several manufacturers of cold liquid-applied materials provide hardness information using the Type A durometer, perhaps because it is a more readily available device. Because it excludes use with coated fabrics, such as PVC, ASTM D 2240 does not appear to be useful for setting standards across material types.

The usefulness of the CAN/CGSB-37.50-M89 toughness test appears to be limited to comparing hot liquid-applied materials.

The dynamic impact testing in CAN/CGSB-37.54-95 and the puncture resistance testing in ASTM Test Methods for Water Vapor Retarders Used in Contact with Earth Under Concrete Slabs, on Walls, or as Ground Cover (ASTM E 154) appear to be more suitable methods of evaluating resistance to construction site damage. In the ASTM E 154 test, a steel rod 25 mm (1 in.) in diameter moves at rate of 6 mm (0.25 in.)/min against an unsupported membrane until visible failure occurs. In the CAN/CGSB-37.54-95 dynamic impact test, a falling weight strikes a steel rod 11.3 mm (0.4 in.) in diameter, which is placed on

TABLE 4—*Constructability—Requirements related to weather requirements during installation. Values and units are stated in the table as they are expressed in the standards.*

Standard	Requirement	Test Method
Cold Liquid-Applied		
ASTM C 836	Condition fluid materials for 24 h at standard conditions prior to forming specimens. Condition specimens for 14 days at standard conditions. Some tests require oven curing. Testing is typically done at standard conditions. For low temperature testing, specimens are then held for 24 h at −26°C (−15°F)	ASTM C 836 and referenced standards
ICC ES AC29	Same as above	
Hot Liquid-Applied		
CAN/CGSB-37.50-M89	Depending on the test, allow the specimen to condition at room temperature for 16 to 72 h	CAN/CGSB-37.50-M89
Single Ply Membranes		
ASTM D 6134, Type I	−45°C (−49°F), max.	Brittleness temperature, ASTM D 6134
ASTM D 6134, Type II	−40°C (−40°F), max.	Brittleness temperature, ASTM D 6134
CAN/CGSB-37.54-95, Type 4, Class C	No cracking at −40±1°C	Low temperature flexibility, ASTM D 2136
CAN/CGSB-37-GP-52M, Type 2, Class B	No cracking at −40°C(−40°F)	Low temperature flexibility. CAN/CGSB-37-GP-52M

a membrane specimen, which is supported by a rubber stopper. A specimen passes the CGSG test if it does not leak after being impacted and then placed under a 500 mm (19.7 in.) column of water.

Constructability—Resistance to the Effects of Weather During Construction

Waterproofing construction takes place outside in a wide range of environmental conditions. Temperature and humidity vary considerably from one location to another. While work should be scheduled for periods of dry weather, unexpected precipitation may occur not long after waterproofing installation.

Variations in temperature and humidity during installation affect the cure and application characteristics of some cold liquid-applied membranes. Cold temperatures will reduce the workability of hot liquid-applied materials and may make some single ply materials less flexible and more difficult to install. Hot temperatures may make waterproofing slide on some vertical substrates. Resistance to weather effects during installation is often not directly addressed in material specifications. Refer to Table 4 for a review of standards.

Meeting the requirements of the low temperature flexibility and impact (brittleness) tests for single ply membranes provide a reasonable assurance that these products can be handled without damage in less than arctic conditions.

Apart from a test that measures crack bridging of an installed membrane at low temperatures, standards for liquid-applied materials lack tests that relate to the installation characteristics of products at extremes of temperature or humidity.

The conditioning for cold liquid-applied materials typically includes an initial period at standard conditions or at room temperature for a duration of 7, 14, or 21 days, depending on the test method. Following this initial conditioning at moderate conditions, there is a period of one, two, or three weeks of oven curing at 23°C (73°F) or 70°C (158°F) depending on the test method.

Durability—Resistance to Damage from Substrate Cracking/Movement

Cracking of substrates is a common challenge for all waterproofing materials. Materials provide a solution to this issue in various ways. Liquid-applied materials bond to the substrate so that when a crack occurs the membrane must elongate the complete width of the crack. Single ply membranes that do not bond to the

TABLE 5—*Durability—Requirements related to crack bridging. Values and units are stated in the table as they are expressed in the standards.*

Standard	Requirement	Test Method
Cold Liquid-Applied		
ASTM C 836	No cracking	Low temperature crack bridging. C 1305. Dynamic test at −26°C (−15°F) with 3.2 mm (1/8 in.) opening
ICC ES AC29	No leakage	ASTM C 1306 or D 5385. Hydrostatic test after extension over fixed crack at standard conditions with min. 1.6 mm (1/16 in.) opening
Hot Liquid-Applied		
CAN/CGSB-37.50-M89	No cracking, splitting, or loss of adhesion over 3 mm crack	Crack Bridging Capability, CAN/CGSB-37.50-M89. Dynamic test at −25° ±2°C with 3 mm opening
Single Ply Membranes		
ASTM D 6134, Type I	300 %, min	Elongation, Ultimate, ASTM D 412, Die C
	9 MPa (1300 psi), min	Tensile strength, D412, Die C
ASTM D 6134, Type II	300 %, min	Elongation, Ultimate, ASTM D 412, Die C
	8.3 MPa (1200 psi), min	Tensile strength, D 412, Die C
CAN/CGSB-37.54-95, Type 4, Class C	15 %	Elongation at break ASTM D 751, Procedure A
	35 kN/m	Breaking Strength, ASTM D 751, Procedure A
CAN/CGSB-37-GP-52M, Type 2, Class B	200 %, min	Ultimate Elongation, ASTM D 412, Die C
	500 *N*, min.	Breaking Strength, ASTM D 751, Method A

substrate accommodate substrate cracking and movement by a combination of elongation (capacity to stretch) and tensile strength (resistance to breaking). Refer to Table 5 for a review of standards.

Liquid-applied materials have very similar test methods and acceptance criteria for low temperature crack bridging. The principle difference between the ASTM C 1305 and CAN/CGSB-37.50-M89 crack bridging tests is in the thickness of membrane test specimens; cold liquid-applied specimens are 1.52 mm (60 mils) thick and hot liquid-applied specimens are 3 mm (118 mils) thick.

A principle difference between the tests used for single ply membranes is the speed of extension. Test machines operate much slower for PVC (5 mm/min (0.2 in./min)) compared with the other single ply standards (500 mm/min (20 in./min)). Considering the intended use of the material, the slower speed of extension used for PVC seems appropriate.

Durability—Resistance to Water Absorption

This requirement is closely related to the requirement that waterproofing resist hydrostatic pressure as well as water vapor. Because waterproofing may be immersed in water for the life of the building, the membrane's important properties must not diminish as a result of water immersion. Customarily, materials are tested for water absorption at elevated temperatures with the intent of accelerating the effects of water immersion. Refer to Table 6 for a review of standards.

Cold liquid-applied materials test methods in Table 6 are appealing because they test the effect of water immersion on an important property, adhesion. However, the authors have observed excessive water absorption in cold liquid-applied waterproofing materials that meet the requirements of ASTM C 836. Because of this field experience, we believe that a water absorption test such as is specified for hot liquid-applied and for single-ply waterproofing would be an appropriate addition to ASTM C 836.

While single-ply materials are tested at 70°C (158°F), testing liquid-applied materials at a lower temperature, 50°C (122°F), may be suitable. It should be noted that plaza membranes in hot climates may reach a temperature in the range of 50°C (122°F). Testing at 50°C (122°F) should not be regarded as excessive, especially for products that may be installed in hot climates.

At the time when bentonite standards are developed, water absorption must be considered in an

TABLE 6—*Durability—Requirements related to resistance to water absorption. Values and units are stated in the table as they are expressed in the standards.*

Standard	Requirement	Test Method
Cold Liquid-Applied		
ASTM C 836	175 N/m (1 lbf/in.), min	Adhesion-in-Peel after water immersion, ASTM C 794. Water exposure is 7 d at standard conditions
ICC ES AC29	No blistering or reemulsification	Resistance to water, ASTM C 2939. Water exposure is 24 h at 24±3°C (75±5°F)
	1 foot lbf./in.	Adhesion strength after water immersion, ASTM C 836. Water exposure is 7 d at standard conditions
Hot Liquid-Applied		
CAN/CGSB-37.50-M89	0.18 *g* max loss mass; 0.35 *g* max gain mass	CAN/CGSB-37.50-M89CGSB. Dimensions of sample are defined. Water exposure is 96 h at 50°C
Single Ply Membranes		
ASTM D 6134, Type I	4 %, max mass	Water Absorption, ASTM D 471. Water exposure is 166 h at 70°C± 2°C (158°F±4°F)
ASTM D 6134, Type II	2 %, max mass	Water Absorption, ASTM D 471. Water exposure is 166 h at 70°C± 2°C (158°F±4°F)
CAN/CGSB-37.54-95, Type 4, Class C	3.0 % max mass increase	Effect of water absorption, ASTM D 570. Water exposure is 7d at 70 ±1°C
	90 % of original tensile breaking strength	Effect of water absorption, ASTM D 570. Water exposure is 7 d at 70 ±1°C
	90 % of original elongation	Effect of water absorption, ASTM D 570. Water exposure is 7 d at 70 ±1°C
CAN/CGSB-37-GP-52M, Type 2, Class B	5 % change in mass, max; strength no less than test minimum	Water absorption, D 570. Water exposure is 7 d at 70°C

entirely different way. Water absorption is essential to the proper functioning of bentonite. Bentonite should hydrate quickly enough to prevent leakage, but it is preferable if the product does not prematurely hydrate due to exposure to rain or ground water during construction. Manufacturers offer special formulations that promote water absorption in certain conditions, such as saltwater.

Testing Initial Leakage Resistance of Bentonite Waterproofing: An Exploratory Study

Background

Bentonite is a naturally occurring material with a well established property—expansion in the presence of water. When the expansion is sufficiently confined, hydrated bentonite forms a dense layer that stops the passage of liquid water.

Traditionally, bentonite waterproofing panels have consisted of granular bentonite laminated between layers of kraft paper, in a product with the appearance of corrugated cardboard. In newer products, bentonite is incorporated in a composite sheet that is shipped in rolls and can be cut as required and fastened in place. These composite sheets are often faced with a layer of impermeable plastic sheeting such as high-density polyethylene (HDPE) or a geomembrane. In some products there is a protective layer added for materials that are intended to have concrete placed against them.

The laps of bentonite sheets are typically not sealed during construction; they are intended to be self-sealing. The confined bentonite is presumed to expand and seal against the impermeable plastic sheet facing at the lap. Depending on the product and its application, manufacturers required lap widths that vary from 38 mm (1-1/2 in.) to 15 mm (6 in.). One of the aspects of bentonite that this study explores is the effect of varying the lap dimension.

If bentonite is not confined, leakage can occur. This study explores the degree to which variations in the confinement of hydrating bentonite affects its performance. For example, it is reasonable to expect excellent confinement when bentonite is placed over a relatively smooth structural slab and is then covered with a concrete topping slab, which is typically at least 76 mm (3 in.) or 102 mm (4 in.) thick. The placement and finishing of the topping slab, in addition to its weight, assures that the bentonite is uniformly confined where it is covered by the topping slab.

Applications on walls present more of a challenge to achieving uniform and lasting confinement. In positive side applications, bentonite is fastened to a below-grade wall and then back-fill is installed. Bentonite manufacturers specify a minimum degree of compaction for backfill, but possible future settlement of soil may alter the bentonite confinement resulting in possible leakage.

Even more challenging is the use of bentonite in positive-side, blind applications. The bentonite is attached to a retaining wall, which may have an irregular surface. For example, with walls consisting of steel piers and wood lagging boards, there is an offset in the plane of the wall between piers and boards, and there may be an offset between boards depending on the presence of cupping or bowing of the lumber. During the life of a building, wood lagging boards may decay and allow some change from the original confinement of the bentonite. In some cases, retaining walls are covered with drainage composite boards which ought to be interlocked at edges but are sometimes installed overlapped at the edges. The practice of overlapping drainage boards results in an offset equal to the thickness of the drainage composite board, which may be in the range of 6.4 mm (1/4 in.) to 25 mm (1 in.) thick. The concrete wall is expected to provide confinement on its side of the bentonite waterproofing; however, placement of concrete can result in undetected rock-pockets or voids that result in localized lack of confinement.

Procedures

This testing was intended to explore two factors in the application of bentonite composite sheets: lap width and the degree of confinement. A total of three types of bentonite composite sheets were generously provided for testing by several manufacturers. The materials are designated A, B, and C.

The test apparatus consists of a clear plastic box that is 600 mm (23.6 in.) deep, by 400 mm (15.7 in.), by 400 mm (15.7 in.). There is a 1.6 mm (1/16 in.) hole in the center of the bottom of the box. For testing, the box was filled with water to a depth of 500 mm (19.7 in.) and the amount of water flowing out of the hole was measured.[5]

Test specimens of the bentonite materials were prepared by cutting out circular pieces with diameters of 25 mm (1 in.), 51 mm (2 in.), 102 mm (4 in.), and 152 mm (6 in.). The specimens were placed in the bottom of the box, directly over the 1.6 mm (1/16 in.) hole.

Metal shims were placed in the bottom of the box, to support concrete pavers described below. The base shim was equal to the thickness of the dry bentonite specimen; each material was a different thickness. This condition is somewhat analogous to the installation of bentonite in a wall application: confining surfaces are present on both sides of the bentonite but spaced apart by the thickness of the bentonite sheet. This initial test condition is referred to as Plus 0.

To simulate the effect of unintentional but possible gaps or irregularities in confinement, three test conditions in addition to Plus 0 were created by adding shims. In separate tests additional shims were stacked on top of the base shim before installation of the concrete pavers. These test conditions have the following designations, Plus 1/16 (shims equal to the thickness of the bentonite sheet plus 1.6 mm (1/16 in.)), Plus 1/8 (shims equal to the thickness of the bentonite plus 3.2 mm (1/8 in.)), and Plus 3/16 (shims equal to the thickness of the bentonite plus 4.8 mm (3/16 in.)).

To resist the expansive pressure of the bentonite in our test apparatus, five concrete patio pavers, each 51 mm (2 in.) by 305 mm (12 in.) by 305 mm (12 in.), were stacked on shims over the specimen.

This test method is not meant to duplicate any actual construction condition; however, it is analogous to a lap in a bentonite waterproofing system. For example, in a test with a 152 mm (6 in.) diameter

[5]With the test box filled with water to 500 mm (19.7 in.) and no barrier over the hole in the bottom of the box, water flowed out at a rate of 1407 mL/min (47 oz/min).

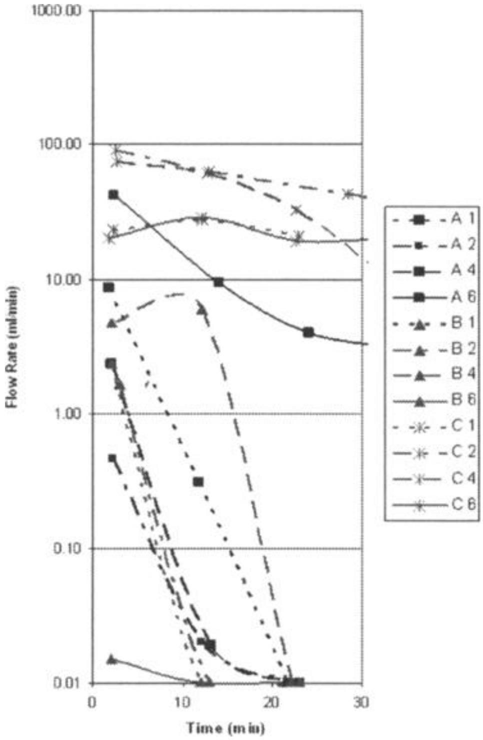

FIG. 1—*Plus 0 confinement.*

specimen, water must pass between the plastic box bottom and a 76 mm (3 in.) width (half the diameter of the specimen) of the overlying bentonite composite to reach the hole and cause a simulated leak. In the roughly analogous condition in actual construction, water must pass between the plastic facer of the lower composite sheet and a 76 mm (3 in.) width of the overlying bentonite composite panel to reach the wall and potentially cause a leak.

Specimens were designated by the material type and the diameter, in inches. For example, a specimen of material type B, with a diameter of 51 mm (2 in.), is designated B2. In this exploratory study one fresh unhydrated specimen was used in each combination of test conditions.

Water flowing out of the hole in the bottom of the test box was captured in a container placed below the test box at the start of a measurement interval. There were three measurement intervals, each approximately ten minutes in length. The test results are expressed as mL/min for approximately the first ten minutes after filling the test box with water, the next approximate ten minute interval, and the third approximate ten minute interval. In most test conditions, this period of approximately 30 minutes was not long enough for leakage to stop. It was, however, a long enough period to create results that distinguished between test conditions and materials.

Findings

Figures 1–4 illustrate the flow of water that occurred in the various test conditions. Figure 1 presents the flow rate when measured for all material types and specimen diameters in a condition of Plus 0 confinement (with shims equal to the thickness of the dry bentonite composite). Figures 2–4 show the same data with confinement at Plus 1/16, Plus 1/8, and Plus 3/16, respectively. A review of these figures indicates a significant difference in the performance of materials A, B, and C during the first half hour after exposure

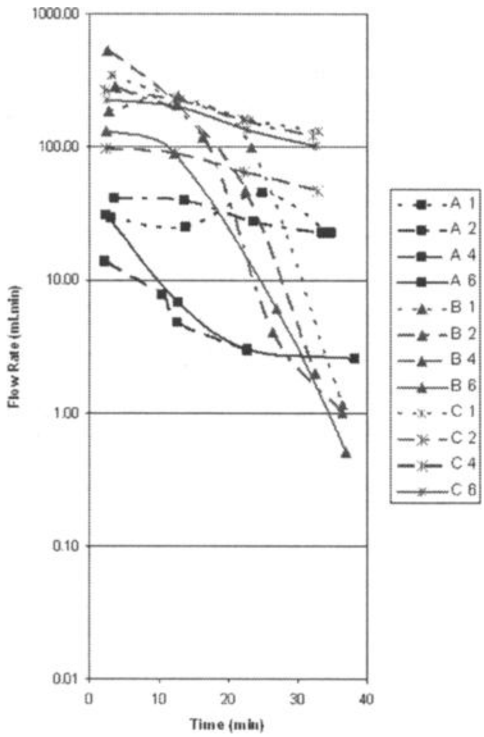

FIG. 2—*Plus 1/16 confinement.*

to a hydrostatic head of 500 mm (19.7 in.). Also evident from review of the figures is that as the confinement is reduced (going from Plus 0 to Plus 3/16) there are fewer instances of bentonite stopping leakage during the test period.

For the tests reported in Fig. 1, concrete confinement is supported on shims equal to the dry thickness of the bentonite. Specimen numbers represent material type (A, B, or C) and diameter in inches (1, 2, 4, and 6.)

For the tests reported in Fig. 2, concrete confinement is supported on shims equal to the dry thickness of the bentonite plus 1.6 mm (1/16 in.). Specimen numbers represent material type (A, B, or C) and diameter in inches (1, 2, 4, and 6).

For the tests reported in Fig. 3, concrete confinement is supported on shims equal to the dry thickness of the bentonite plus 3.2 mm (1/8 in.). Specimen numbers represent material type (A, B, or C) and diameter in inches (1, 2, 4, and 6).

For the tests reported in Fig. 4, concrete confinement is supported on shims equal to the dry thickness of the bentonite plus 4.8 mm (3/16 in.). Specimen numbers represent material type (A, B, or C) and diameter in inches (1, 2, 4, and 6).

To illustrate how the flow rate changes as the diameter of the specimen changes, Fig. 5 shows combined data for all three material types. The results do not show a strong association between specimen size and the corresponding flow of water from the hole covered by the specimen.

Figure 6 shows how the flow rate changes as the confinement is reduced by increasing the thickness of shims that separate the bottom of the test box from the concrete pavers. The shim space dimension is the thickness of shims added to the base shim, which is the thickness of the bentonite. Material specimens of all sizes increased flow rate as the thickness of shims was increased.

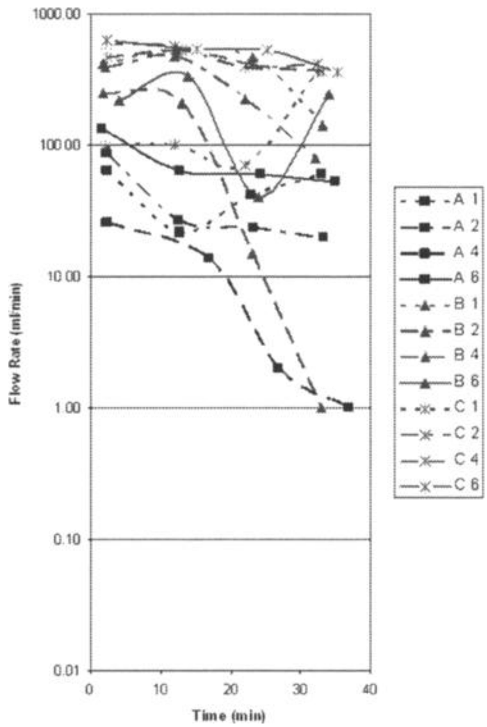

FIG. 3—*Plus 1/8 confinement.*

Conclusions

Future efforts to develop standards for these bentonite composite sheets should anticipate the differences between materials. For example, specimens should be allowed to hydrate and stop leaking before hydrostatic pressure is applied. The test report should include the time required to stop leakage with no additional hydrostatic pressure.

The tightness of confinement is important to the sealing of bentonite composite sheet laps. Standards developed for application of bentonite composite sheets should set high standards for the flatness and smoothness of substrates. Material specifications may include tests to show the capacity of materials to overcome the challenge of irregular confinement.

In our test apparatus, with flat and parallel confining surfaces, the width of a specimen covering the test box hole was relatively unimportant to determining the rate at which bentonite stopped or slowed leakage. In this test apparatus even very small specimens were capable of stopping water flow. We caution against applying this to actual construction. It would be prudent to assume imperfect confinement—good in one spot but poor in another. Wider laps appear to offer a better likelihood of having a continuous line of effective confinement occur within the area of the lap.

Testing Water Absorption in Cold Liquid-Applied Waterproofing: An Exploratory Study

Background

The wrinkled appearance of cold liquid-applied membranes that have absorbed water, termed "braining," is familiar to those who investigate waterproofing failures. Deterioration of cold liquid-applied membranes due to water absorption has been described by Laaly and Serenda [1], and by the authors [2]. Water absorption in similar materials, cold liquid-applied deck coatings, is described by Mailvaganam et al. [3].

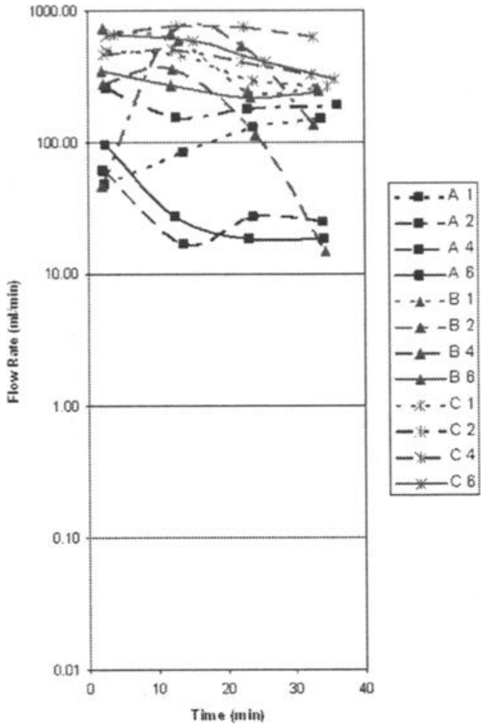

FIG. 4—*Plus 3/16 confinement.*

This study explores water absorption by subjecting specimens to a cycle of water immersion and drying over an extended period. The testing is not a duplication of actual construction conditions; however, it may be more similar to real conditions than is typical in laboratory water absorption testing. The accelerated oven curing used in tests cited in ASTM C 836 was not used. Oven curing is likely significant

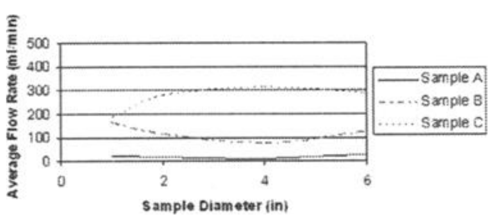

FIG. 5—*Average flow rate vs. sample diameter.*

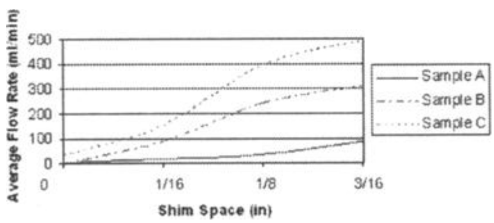

FIG. 6—*Average flow rate vs. shim space.*

TABLE 7—*Test cycle.*

Week #	Condition	Temperature
1	Water Immersion	50°C (122°F)
2	Air Drying	Room Temperature—Office Environment
3	Water Immersion	Room Temperature—Office Environment
4	Air Drying	Room Temperature—Office Environment

in the test performance of some materials because ASTM C 836 allows as low as 80 % non-volatile content. As required in referenced test methods, oven curing at 37.8°C (100°F) to 70°C (158°F) is likely effective in driving off volatiles and completing the cure of materials. Our decision to omit oven curing had the advantage of more closely replicating construction conditions. Omitting oven curing had the disadvantage that for some products, the weight changes measured would include both weight loss due to loss of volatile components and possible weight gain due to water absorption.

Procedures

Three brands of cold liquid-applied waterproofing were generously provided by local suppliers. Two materials were one-component bitumen modified urethanes; these were designated 1UM-#1 and 1UM-#2. The third material was a two-component unmodified urethane, designated 2U-#1A.

Experienced waterproofing installers prepared samples in the unconditioned environment of a waterproofing contractor's warehouse. Samples were cast as recommended by the manufacturer, in an application intended to produce a dry film thickness of 1.5 mm (60 mils). Specimens were prepared on release paper and remained in the warehouse for three days until they could be transported. The exterior conditions at the time samples were prepared and initially cured ranged from 8° to 16°C (46° to 61°F).

After conditioning, specimens 160 by 250 mm (6.3 by 9.9 in.) were cut from the sample material, weighed, and measured. Samples were subject to a four-week cycle of wetting and drying; as described in Table 7. The cycle was then repeated during the test period of 84 days. Weight was measured at the end of each week of water immersion or drying. Dimensions were measured through the first cycle only.

For the first set of specimens, the test cycle began with no additional conditioning after the three-day initial curing period. Following the initial three-day cure and prior to beginning their first test cycle, the second set of specimens was conditioned at standard conditions (23°C (73.4°F)) at 50 % RH) for seven days. The third set of specimens began their first test cycle after 14 days of conditioning at standard conditions and testing of the fourth set began after 21 days of conditioning at standard conditions.

Findings

Change in Dimension—All three material types decreased in dimension after the first four-week cycle of testing, as shown in Table 8.

Change in Weight—The following charts show two responses to the cycles of wetting and drying: the percentage gain and loss in each period of water immersion or drying, and the general trend of samples' weight loss or gain over an extended period. For materials with a relatively high solvent content, the general trend of losing weight is likely due to solvents being released from the specimen.

Material Type 1UM-#1—1-Component, Modified Urethane #1—Setting aside one anomalous data point, the greatest gain in weight in a seven-day period of water immersion was 8.8 %. The specimens exhibited a general trend to lose weight during the test period, with the average weight stabilizing after approximately 56 days. Refer to Fig. 7.

TABLE 8—*Average dimensional change during a four-week test cycle.*

	% Change	
Material	Height	Width
1UM-#1	1.4	1.1
1UM-#2	3.4	2.1
2U-#1	0.8	0.6

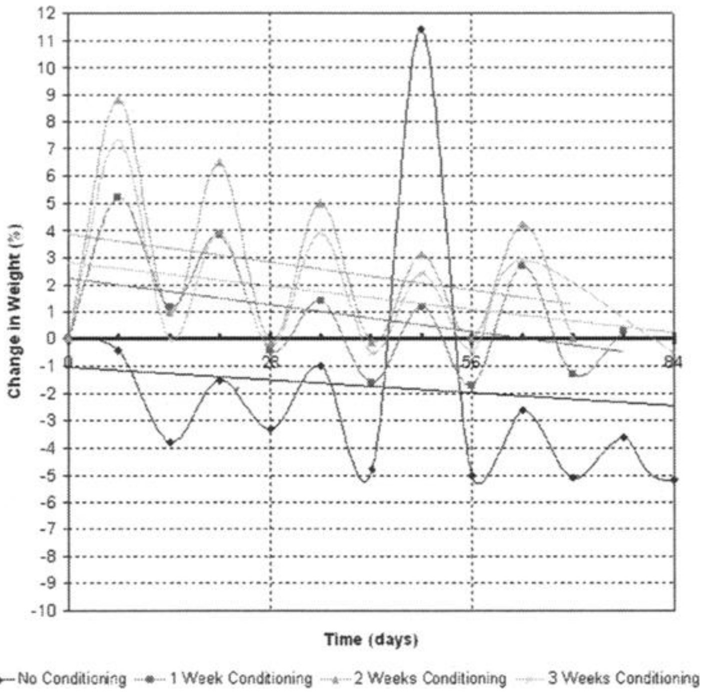

FIG. 7—*Specimens of material type 1UM-#1. Weight change through three test cycles.*

Material Type 1UM-#2—1-Component, Modified Urethane #2—The greatest change in weight in a seven-day period of water immersion was a loss of 3.6 %. The specimens exhibited a general trend to lose weight during the test period, with the average weight stabilizing after approximately 56 days. Refer to Fig. 8. The material did not complete curing during the test period. Throughout the 84-day test period an oily film was noted on the surface of water that held specimens of this material. In the field, the authors have observed a tacky condition in this material several years after installation.

Material Type 2U-#1—2-Component, Unmodified Urethane #1—Apart from two anomalous high values, the greatest gain in weight in a seven-day period of water immersion was 4.8 %. The specimens exhibited little change in weight during the test period, with the average weight stabilizing after approximately 28 days. Refer to Fig. 9.

Conditioning Environment—It is reasonable to expect some differences in the performance of cold liquid-applied materials when they are installed in different conditions of temperature and humidity. Liquid materials do not spread as easily when cold; single component materials depend upon moisture for curing.

Research by Mailvaganam et al. [4] studied the effects of curing temperature and humidity on the properties of cold liquid-applied deck coatings, which are similar to the products addressed in this paper. The CMHC researchers cured specimens in temperature and humidity controlled conditions: 30, 50, and 85 % RH and 5, 22, and 38°C (41, 72, and 100°F). They found that membrane properties, including permeability, were significantly affected by varying the temperature and humidity of installation and curing.

We conducted a set of tests in addition to the one described above. Samples for both sets of tests were prepared and cured for the first three days in a contractor's unconditioned warehouse during a time when the exterior temperature ranged from 8 to 16°C (46 to 61°F). Following the initial cure, samples were

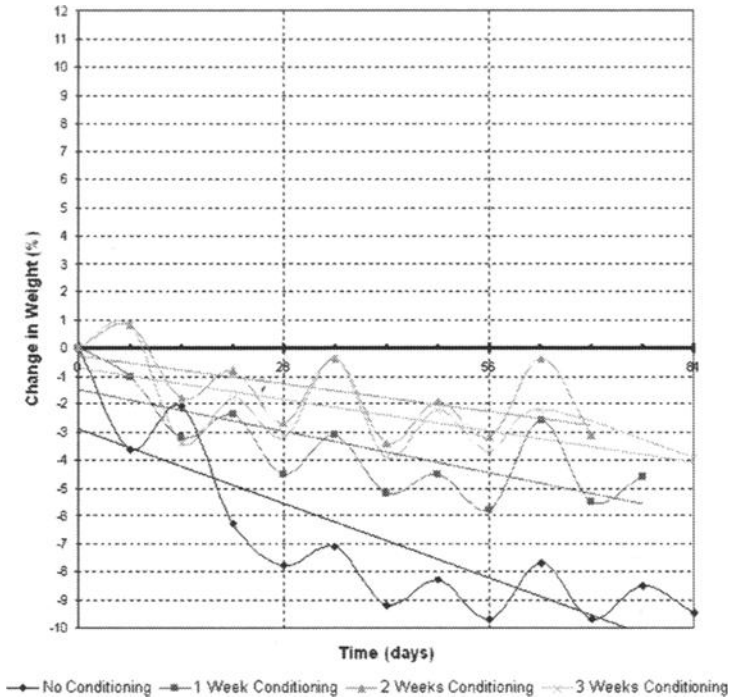

FIG. 8—*Specimens of material type 1UM-#2. Weight change through three cycles.*

conditioned for periods of one, two, and three weeks. Half of the samples (described in the Figs. 7–9 were held at standard conditions, while the other half were conditioned in an un-insulated and unconditioned garage at a time when exterior temperatures ranged from 5 to 21°C (41 to 70°F).

As shown in Fig. 10, the results of this testing did not reveal consistent differences between specimens cured in standard conditions versus those cured in an unconditioned garage. These samples shared a common environment for initial cure, which may be the time when cold liquid-applied materials are most sensitive to weather fluctuations.

Conclusions

While it is reasonable to expect that immersion of specimens in heated water would result in weight gain, the opposite occurred. Two of the samples had marked weight loss during the course of the test period, presumably because volatile materials were emitted from the specimens as a part of a prolonged curing process.

Specimens of all three materials responded to the test cycle by typically gaining weight when immersed in water and losing weight when dried. There is, however, a significant difference in the amplitude of changes in different samples.

Specimens of all three materials lost dimension during the course of a test cycle. The amount of loss paralleled the loss of weight in the specimens.

We did not find a significant difference between the performance of specimens conditioned in a laboratory versus those conditioned in variable cool conditions. Both sets of samples had the same environment during the first three days of curing, which may be a critical period.

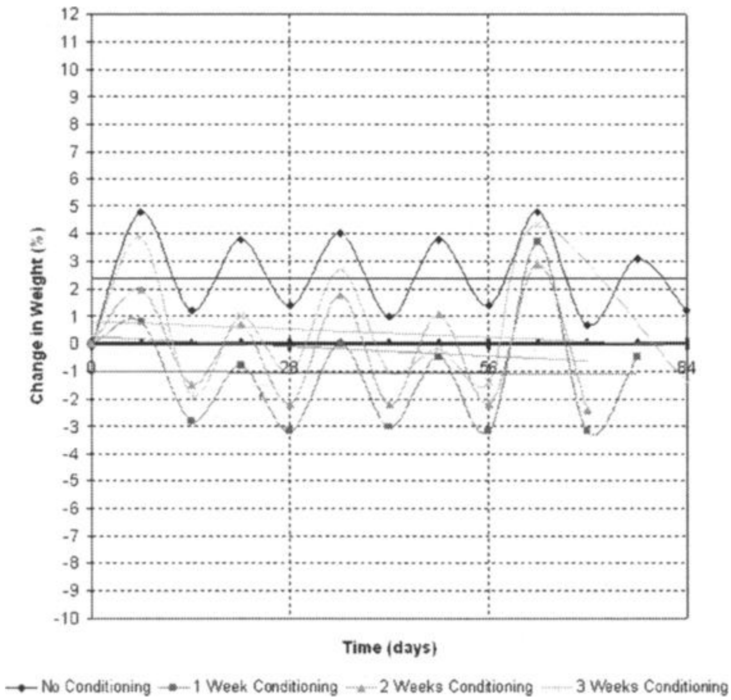

FIG. 9—*Specimens of material type 2U-#1. Weight change through three cycles.*

Recommendations for Standards Improvement

General

Open a dialogue between groups responsible for waterproofing materials specifications in ASTM, CGSB, and the ICC ES. Development of standards that allow comparison of essential properties of waterproofing will require communication and coordination. A logical starting place is coordination within ASTM, between Subcommittee C24.80 Building Deck Waterproofing Systems and the subcommittees responsible for materials standards in the D08 Committee.

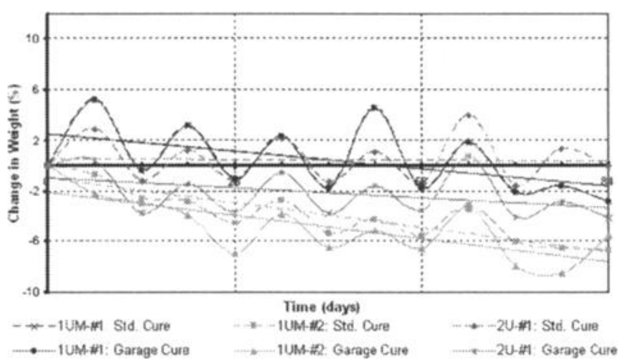

FIG. 10—*Average weight change through three cycles at varied conditioning.*

Impermeability

Develop a hydrostatic resistance test that is highly repeatable and reproducible, as well as suitable for a wide range of waterproofing products. A reasonable first step is the adoption of impact and hydrostatic tests similar to CAN/CGSB-37-GP-52M, with modifications as required to be used with a wide variety of materials. The existing ASTM standards for hydrostatic testing should undergo additional development to achieve a high level of repeatability and reproducibility.

Standardize the options available in ASTM E 96 for testing for permeance in waterproofing membranes. Add permeance testing requirements to specifications that currently lack them.

Constructability

In ASTM C 836, change the hardness measurement test from an ASTM D 2240 type OO durometer to a type A durometer.

In ASTM C 836, standardize the period and temperature of conditioning prior to all tests. Create classes of products in ASTM C 836; consider allowing the multi-component class of materials to be tested without oven curing.

Durability

Current requirements for crack bridging related properties should be reviewed; however, it does not appear that changes are required.

Develop a water absorption test suitable for both cold and hot liquid-applied materials standards.

Bentonite

Develop needed test methods, then a material specification. Needed test methods include hydrostatic pressure resistance, compatibility with saltwater or other contaminants, resistance to premature hydration, and resistance to damage from concrete placement.

Acknowledgments

The authors wish to thank their colleagues at Wiss, Janney, Elstner Associates, Inc. for their advice and encouragement. We are grateful to Rainbow Restoration (San Francisco, California) for preparing test samples, and to Testing Engineers, Inc., (San Leandro, California) for providing facilities for some of the testing. We also wish to acknowledge the inspiration provided by Carl Cash, the former chair of ASTM Committee D08, who challenged the waterproofing subcommittee (D08.22) to write a standard that defined the essential properties of waterproofing.

References

[1] Laaly, H. O. and Serenda, P. J., "Limitations of Present Test Methods for Roofing Materials," *Durability of Building Materials and Components, ASTM STP 691*, P. J. Serenda and G. C. Litvan, Eds., ASTM International, West Conshohocken, PA, 1980, pp. 755–756.

[2] Strong, J. C. and Kovach, J. R., "Water Absorption in Cold Liquid-Applied Waterproofing," *Durability of Building and Construction Sealants and Adhesives, ASTM STP 1453*, A. T. Wolf, Ed., ASTM International, West Conshohocken, PA, 2004.

[3] Mailvaganam, N. P., Lacasse, M. A., Collins, P. G., Paroli, R. M., and Henrie, J. P., "Evaluation of Elastomeric Membrane Systems Used in Parking Garage Protection,"National Research Council Canada, February 1992.

[4] Mailvaganam, N. P., Collins, P. G., Lacasse, M. A., and Henrie, J. P., "Influence of Application Factors on the Performance of Elastomeric Waterproofing Membranes," National Research Council Canada, 1993.

Journal of ASTM International, Vol. 4, No. 2
Paper ID JAI13127
Available online at www.astm.org

Noriyoshi Enomoto,[1] Akihiko Ito,[1] Ichirou Shimizu,[2] Takashi Matsumura,[3] Yoshimitsu Takane,[4] and Kyoji Tanaka[5]

Study of Weatherability of Construction Sealants with Novel Testing Method

ABSTRACT: Although construction sealants are used for all kinds of construction joints such as static joints with little movement, dynamic joints with thermal or seismically induced movement, and so on, the general test methods employed in the evaluation of the weatherability of construction joint are based on weathering test without movement. In November of 2000, AIJ (Architectural Institute of Japan) established a subcommittee chartered with developing an accelerated weathering test method, which enables the determination of the durability of waterproofing materials and sealants. In this activity, we evaluated the weatherability of sealants with a new test method using newly developed test specimens, which enable exposing the cured sealants to compression and extension at the same time in a single test specimen. In this paper, we report the interim test results, which cover twelve months of natural weathering and 3500 hours artificial weathering with xenon lamp and carbon flame weathering device. In this evaluation, we confirm that the surface degradation of sealants is accelerated by the additional movement cycles, and the differences in the degradation among the sealants are becoming observable.

KEYWORDS: sealant, weatherability, joint movement, out-door exposure, accelerated exposure

Introduction

In November of 2000, AIJ (Architectural Institute of Japan) established a subcommittee chartered with developing an accelerated weathering test method, which enables the determination of the durability of waterproofing materials and sealants. Sealants are used in a variety of applications. While some sealants are used in static joints with little movement, the majority of sealants are applied in dynamic joints, which are exposed to thermally, seismically, psychrometrically, or otherwise induced movement. Despite this fact, the majority of weatherability tests on sealants are carried out without exposing them to any movement [,2]. In this study on the durability of sealants, initiated by AIJ, newly developed test specimens have been employed, which enable exposing the cured sealant to compression and extension at the same time within a single test specimen. The magnitude of the movement can be adjusted to allow for the simulation of actual sealed joint conditions. This is the first interim report about this study.

Experimental Procedures

Test Specimen

A newly developed test specimen as shown in Figs. 1 and 2 was used in this study. By expanding one end of this joint test specimen, the other end gets compressed; thus, the test specimen can be exposed simultaneously to various degrees of extension and compression in a single movement.

Manuscript received June 13, 2005; accepted for publication October 20, 2005. Presented at ASTM Symposium on Durability of Building and Construction Sealants and Adhesives, Second Symposium on 15–16 June 2005 in Reno, NV; A. T. Wolf, Guest Editor.

[1] Member of Technical Committee, Japan Sealant Industry Association (JSIA), 1–5, Kanda-sudacho Showa Suda-cho Bldg., Chiyoda-ku, Tokyo, 101-0041, Japan, email:noriyoshi.enomoto@sunstar.com

[2] Team leader, Japan Testing Center for Construction Materials, 5-21-20 Inari, Souka-shi, Saitama, 340-0063, Japan

[3] Staff of Research Section, Hokkaido Northern Building Research Institute, 3-1-20 Midorigaoka Higashi 3-zyou, Asahikawa-shi, Hokkaido, 078-8801, Japan.

[4] Manager of Research Section, Japan Weathering Test Center, 1034-1 Shinmachi, Choushi-si, Chiba, 288-0825, Japan

[5] Professor, Tokyo Institute of Technology, 4259 Nagatsuta, Midori, Yokohama, 226-8503, Japan.

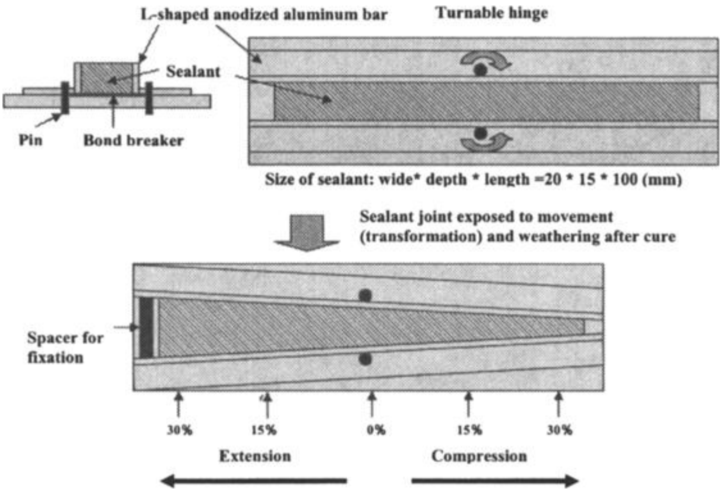

FIG. 1—*Outline of test specimen.*

Evaluation of Degradation for Tested Sealants

Ratings of surface crazing according to ISO 4628 Paints and Varnishes—Evaluation of degradation of coatings—Designation of quantity and size of defects, and of intensity of uniform changes in appearance—Part 4: Assessment of degree of cracking as shown in Tables 1 and 2 were used for the numerical evaluation of surface cracking of sealants caused by natural or accelerated weathering [3].

Based on the quantification of generated surface cracks, we used the product of quantity (Q) and size (S) of surface cracks, termed "degree of degradation" (DoD), as the indicator of degradation induced by weathering, as shown in Eq. 1 below.

$$\text{Degree of degradation (DoD)} = \text{Quantity } (Q) \times \text{Size } (S) \tag{1}$$

In Table 3, the approximate relationship between the degree of degradation indicator (DoD) and the state of degradation (crazing) is shown.

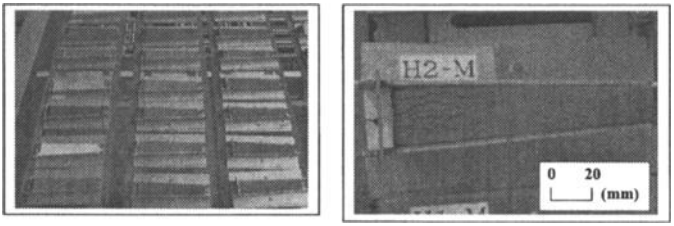

FIG. 2—*Test specimen.*

TABLE 1—*Rating scheme for designating the quantity of cracks.*

Rating	Quantity of cracks, Q
0	None, i.e., no detectable cracks
1	Very few, i.e., some just significant cracks
2	Few, i.e., small but significant amount of cracks
3	Moderate, i.e., medium amount of cracks
4	Considerable, i.e., serious amount of cracks
5	Dense, i.e., dense pattern of cracks

TABLE 2—*Rating scheme for designating the size of cracks.*

Rating	Size of cracks, S
0	Not visible under ×10 magnification
1	Only visible under magnification up to ×10
2	Just visible with normal corrected vision
3	Clearly visible with normal corrected vision
4	Large cracks generally up to 1 mm wide
5	Very large cracks generally more than 1 mm wide

Preliminary Outdoor Exposure Experiment

In order to determine the effect of the switching frequency of the extension/compression position on the degree of degradation, a preliminary natural outdoor weathering experiment was carried out with two sealants being exposed for 12 months. Sealant specimens according to Figs. 1 and 2 were prepared and cured for one week at 23°C and 55 % relative humidity (r.h.), followed by one-week storage at 50°C without humidity control. Afterward, one specimen of each sealant was installed on an outdoor exposure rack located in Yamanashi Prefecture in Japan facing south at an inclination angle of 45°. The sealant specimens were exposed to cyclic movements using three different switching frequencies (once/month, once/week, and twice/week), and, as a reference, no movement at all (fixed position without switching) as shown in Table 4. The switching of the compression and the extension positions was accomplished manually with the help of pliers and suitable spacers. The sealed joints were exposed to 0 %, ±15 %, and ±30 % movement.

Test results are shown in Fig. 3. As can be seen, exposing the specimens to movement had a strong effect on the degree of degradation (DoD) when compared to static exposure (no movement). However, no significant difference was observed between the specimens exposed to movements with different switching frequencies. With this result, we chose the switching frequency of the compression/expansion positions in the outdoor test procedure as once/month, giving consideration to work efficiency.

Sealants Tested

Twenty-four sealants of seven chemical types commercially available in Japan were selected for the study as shown in Table 5 [4]. The one-part silicone sealant was excluded due to cohesive failure early-on during the study. One sealant specimen according to Figs. 1 and 2 was prepared for each product. One-part sealants were allowed to cure for two weeks at 23°C and 55 % r.h., followed by two weeks storage at 30°C without humidity control. Two-part sealants were cured for one week at 23°C and 55 % r.h., followed by one week storage at 50°C without humidity control.

TABLE 3—*Relationship between the degree of degradation (DoD) and the state of degradation (crazing).*

Degree of degradation	State of degradation (Crazing)
25	Serious degradation
20	
15	Medium degradation
10	Minor degradation
5	Slight degradation
0	No or very little degradation

TABLE 4—*Experimental conditions for preliminary outdoor exposure experiment.*

Switching frequency	Sealants[a]	Movement amplitude, %
• None (fixed position)	• MS-2	• ±0 (static)
• Once / month	• PU-2	• ±15
• Once / week		• ±30
• Twice / week		

[a]MS-2: 2 part silicone-modified polyether. PU-2: 2 part polyurethane.

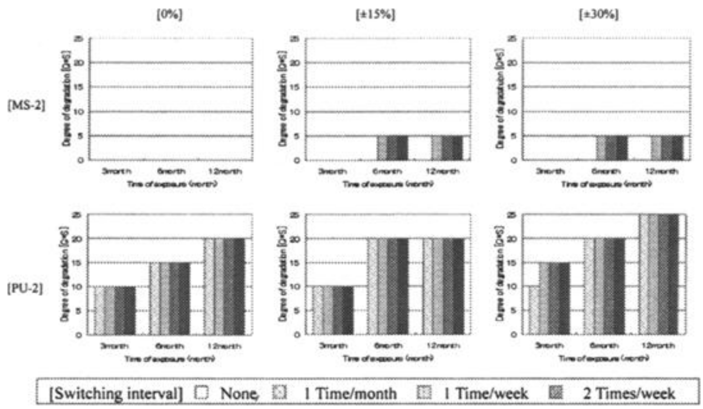

FIG. 3—*Dependency of degree of degradation on switching interval for different exposure times.*

Exposure Conditions

The current status of the weathering tests is described in Table 6. The outdoor exposure test is being carried out at three different sites (north: Hokkaido, central: Chiba and south: Okinawa) in Japan. Testing conditions of outdoor and accelerated weathering exposures are also shown in Table 6, while the geographic features of the different outdoor exposure locations are shown in Table 7. The conditions of the

TABLE 5—*Sealants tested.*

Sealants	Mark	Number of products
Silicone (two-part)	SR-2	2
Silicone-modified polyether (general purpose) (one- part)	MS-1 (GP)	3
Silicone-modified polyether (high weatherability) (one-part)	MS-1 (HW)	3
Silicone-modified polyether (general purpose) (two- part)	MS-2 (GP)	2
Silicone-modified polyether (stress relaxation type) (two-part)	MS-2 (SR)	2
Polysulfide (one-part)	PS-1	1
Polysulfide (two-part)	PS-2	2
Silicone-curable polyisobutylene (two-part)	IB-2	3
Polyurethane (one-part)	PU-1	2
Polyurethane (two-part)	PU-2	1
Acrylic urethane (two-part)	UA-2	1
Acrylic (water borne, one-part)	AC-1	2

TABLE 6—*Experimental conditions and current status of exposure tests.*

			Accelerated exposure		
		Outdoor exposure	Xenon arc lamp (XWM)	Open flame carbon arc (SWM)	Fluorescent UV lamp (UV)
Term	Plan	20 years	10 000 h	5000 h	5000 h
	Current status	12 month	3500 h	3500 h	- (started)
Interval of transformation		1 month	500 h		
Conditions		[Location within Japan] • North • Central • South • [Angle] • 45°	[Irradiation] • 550 W/m2 • 290–800 nm • b.p.:63°C • r.h.:50% • 102 min.irrad. + 18 min. spray	[Irradiation] • 255 W/m2 • 300–700 nm • b.p.:63°C • r.h.:50% • 102 min.irrad. + 18 min. spray	[Irradiation] • 25 W/m2 • 300–400 nm • b.p.:63°C (on) • 50°C (off) • 4 h on +4 h off

TABLE 7—*Geographic features of outdoor test locations.*

	North	Central	South
Latitude	43°46'N	35°43'N	24°44'N
Average maximum temperature (°C)	11.8	18.8	26.2
Average minimum temperature (°C)	2.2	10.6	21.0
Precipitation (mm/year)	1150	1481	2058
Amount of UV radiation[a] (0°, MJ/m2 in year)	240	313	367

[a]Wave length: 315–400 nm.

accelerated exposure were based on ISO 4892 (Plastics–Methods of exposure to laboratory light sources) [5]. The switching interval of the extension/compression position in the accelerated weathering exposure was chosen as 500 h.

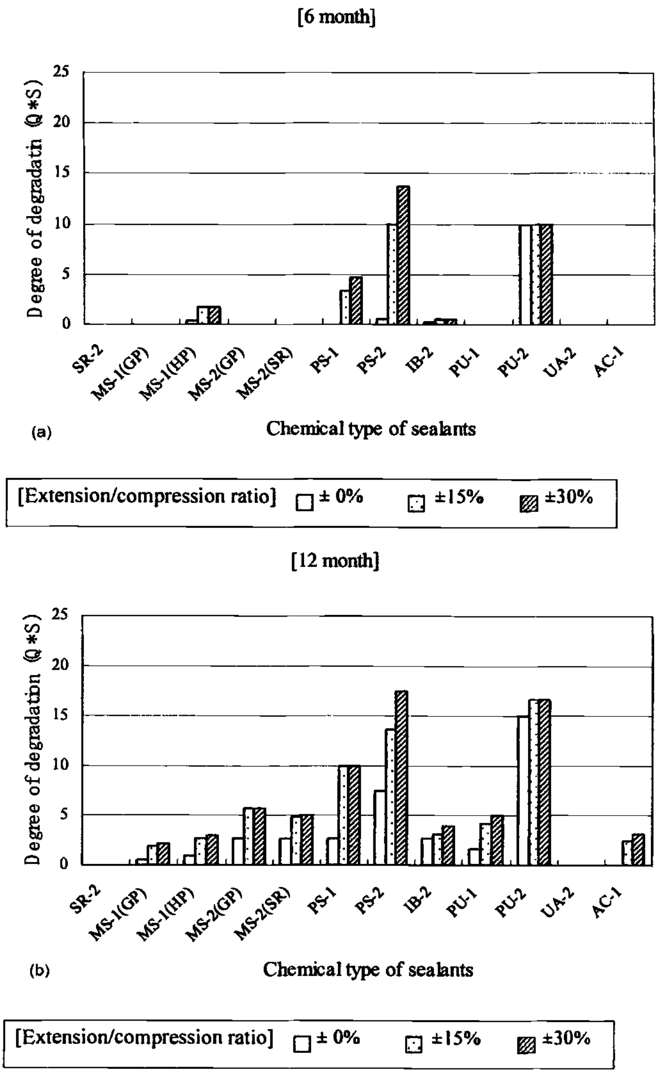

FIG. 4—*(a) Degree of degradation in outdoor weathering exposure (6 months). (b) Degree of degradation in outdoor weathering exposure (12 months).*

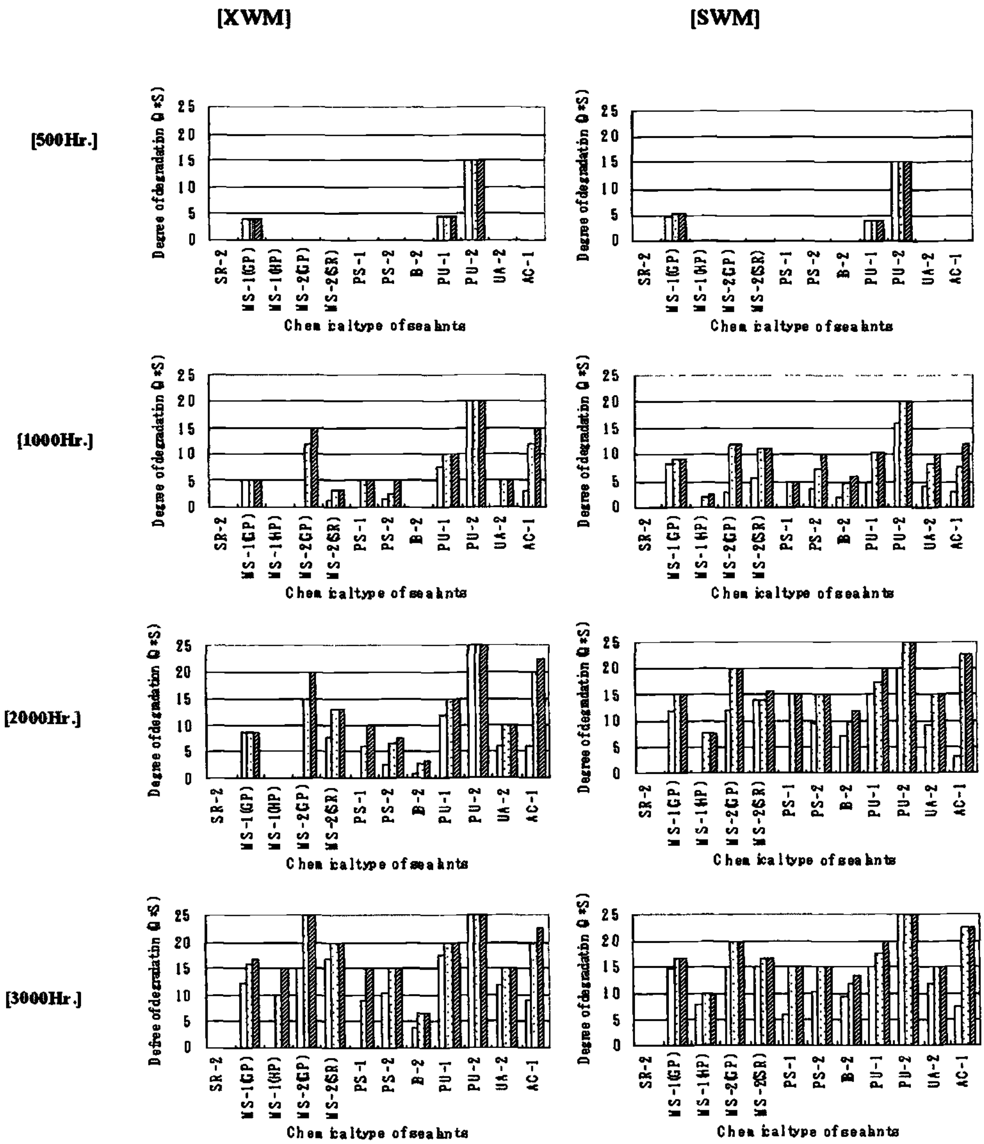

FIG. 5—*Degree of degradation in accelerated weathering exposure (Same legend as in Fig. 4).*

Intermediate Results

Outdoor Exposure

The degree of degradation of the sealants after 6 and 12 months outdoor exposure is shown in Figs. 4(*a*) and 4(*b*) as the average over the three outdoor exposure sites and the different sealant products for each chemical type of sealant.

Accelerated Exposure

The degree of degradation of sealants after 3500 h of exposure in a xenon-arc source weathering device and open-flame carbon-arc lamp weathering device is shown in Fig. 5 as the average of each chemical type of sealants. Accelerated weathering using the fluorescent UV lamp exposure has been started recently and no data are available to report at this stage.

Comparison between Outdoor and Accelerated Exposure

Figures 6(*a*)–6(*d*) show the degree of degradation for each extension/compression ratio as the average for each chemical type of sealant and as an average over all sealants.

Conclusions and Future Activities

The comparative evaluation of outdoor and accelerated weathering with newly developed flexible joint test specimen has started. After 12 months of natural weathering and 3500 h of accelerated weathering in xenon and carbon-arc weathering device, the following conclusions, as summarized below, can be drawn.

- Influences by chemical type of sealant: Although there are differences in the extent of damages, some degradation was observed in all chemical types of sealants except silicone.
- Influences of expansion/compression amplitude: A strong acceleration of degradation induced by the mechanical cycling was observed. However, the expansion/compression amplitude (±15 % versus ±30 %) showed only very little influence.
- Influence of light source in accelerated weathering: Although stronger surface degradation was observed in the open-flame carbon-arc weathering device than in the xenon-arc lamp weathering device until 2000 h of irradiation, a similar level of degradation was observed in both weathering devices after 3000 h of irradiation.
- Correlation between outdoor and accelerated exposures: Similar degradation features were observed in outdoor and accelerated weathering, however the natural weathering period (12 months) is too short to discuss a correlation between natural and accelerated weathering at present.

The efficiency of the new test method for weatherability of sealant simulating the in-service condition of seal joints by using a newly developed flex-joint test specimen has been confirmed. This new test

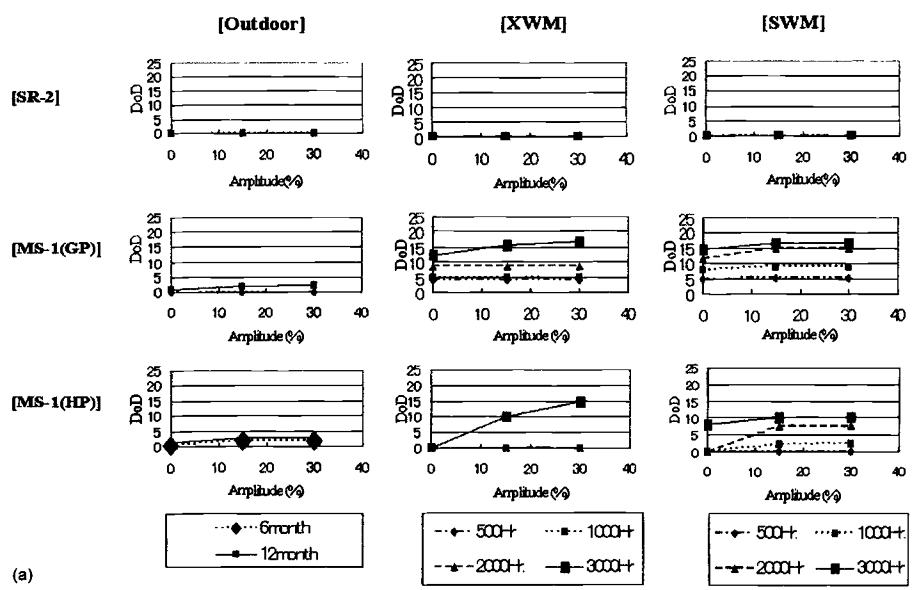

FIG. 6—

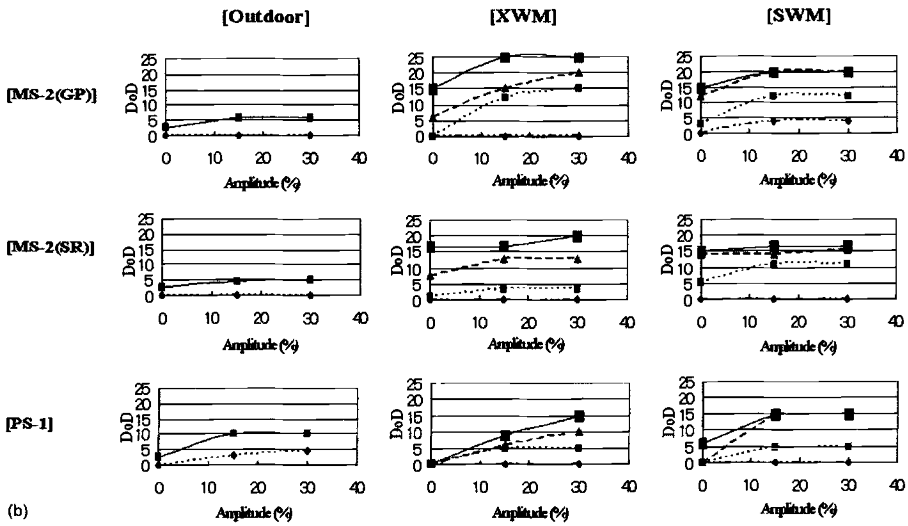

FIG. 6— *(Continued).*

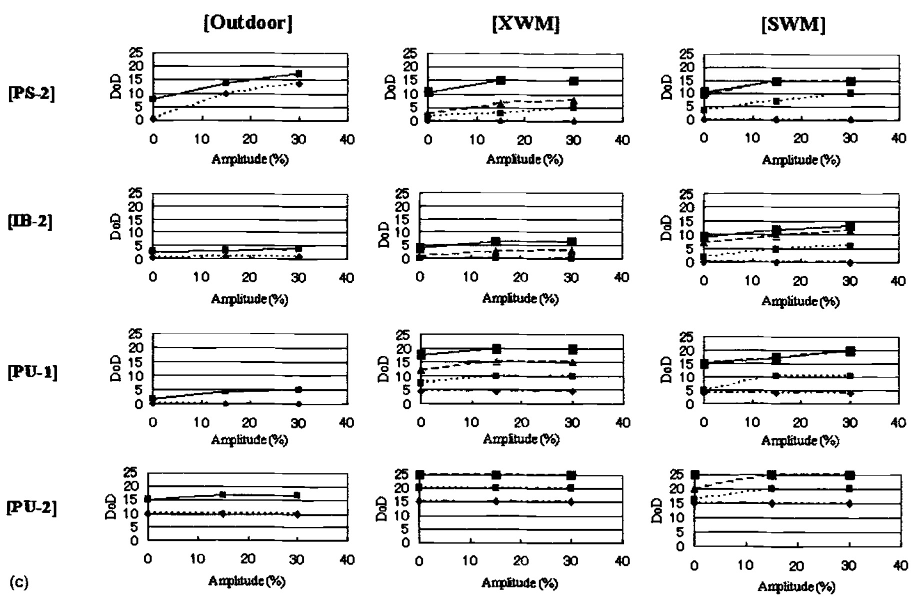

FIG. 6— *(Continued).*

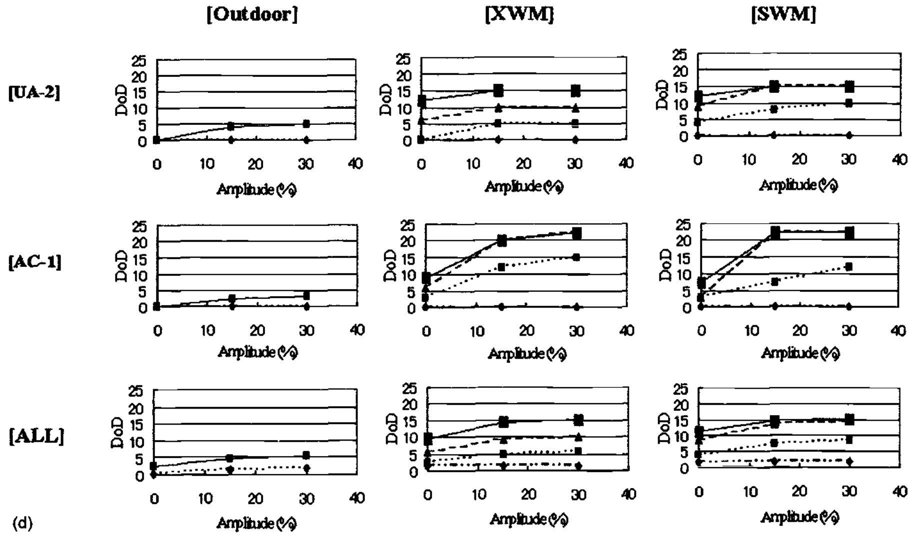

FIG. 6— (*Continued*).

(*a*) Degree of degradation (DoD) for different extension/compression amplitudes. *b* Degree of degradation (DoD) for different extension/compression amplitudes [Same legends as in Fig. 6(a)]. (*c*) Degree of degradation (DoD) for different extension/compression amplitudes [Same legends as in Fig. 6(a)]. (*d*) Degree of degradation (DoD) for different extension/compression amplitudes [Same legends as in Fig. 6(a)].

specimen is not expensive and allows a reduction in the total number of specimens employed by exposing the sealants simultaneously in a single specimen to compression and extension movements up to ±30 % of the joint width. The data obtained with this flex-joint test specimen will be used to design sealed joints in the future.

While the degradation of sealants has been evaluated by the quantification of surface crazing in this report, a more complete quantification of degradation is being planned for the future, including the evaluation of the depth of cracks.

References

[1] Tsurata, Y., "Outdoor Exposure Test of Membrane and Sealant (part 9)—Deterioration of Sealant Exposed for Seven Years," *Architectural Institute of Japan*, Tokyo, Japan, 1990, pp. 411–412.

[2] Miyauchi, H., "Artificial Weathering and Cyclic Movement Test Results Based on RILEM 139-DBS Durability Test Method for Construction," *Durability of Building and Construction Sealants and Adhesives, ASTM STP 1453*, ASTM International, edited by A. T. Wolf, West Conshohocken, Pennsylvania, 2004, pp. 206–212.

[3] Anonymous, *ISO 4628-4 Paints and Varnishes - Evaluation of Degradation of Coatings - Designation of Quantity and Size of Defects, and of Intensity of Uniform Changes in Appearance. Part 4: Assessment of Degree of Cracking*, International Standardization Organization, Geneva, Switzerland, 2003.

[4] Anonymous, *JIS (Japan Industry Standard) A 5758 - Sealants for sealing and glazing in buildings*, Japan Industry Standard Organization, Tokyo, Japan, 2004.

[5] Anonymous, *ISO 4892 (Plastics-Methods of exposure to laboratory light source).*

Journal of ASTM International, Vol. 4, No. 2
Paper ID JAI13378
Available online at www.astm.org

Hiroyuki Miyauchi[1] *and Kyoji Tanaka*[1]

Proposed Design and Method for Providing Sealed Joint Performance under Relative Story Displacement

ABSTRACT: The fatigue resistance of sealed joints to relative story displacement movements caused by earthquakes was studied experimentally and analytically, and the new joint design method was proposed, providing adequate sealed joint performance over the joint's service life. First, the story drift *R* of a curtain wall panel and the number of movement cycles of relative story displacement at a sealed joint over its service life were investigated using earthquake data of the Japan Meteorological Agency. The results indicate that the number of cyclic movements at a sealed joint over its service life is inversely proportional to the story drift of the adjacent curtain wall panels. In regions where earthquakes are numerous, R=1/300 cyclic movements of the total length of the curtain wall panel occur several thousand times over a period of 75 years, while R=1/100 cyclic movements occur only several tens of times. Second, the three criteria required to create a joint design method were investigated, i.e., type of sealant, effect of cross-sectional size and shape of the sealed joint, and fatigue resistance of the sealant at intersectional zones of sealed joints to the sliding and rocking motions of curtain wall panels. It was obvious that the fatigue resistance of sealed joints was lower in the intersectional area than in the linear sections of the joints, and was lowest in the event of the same movement occurring in both vertical and horizontal joints. The fatigue resistance of a sealant at the intersection of sealed joints is not sufficient to attain the targeted service life and the fatigue resistance of this area of the sealed joint must be improved by applying larger curvature radii at the corner of the curtain wall panel. Finally, the new joint design process for the linear section and the intersection of the sealed joints to relative story displacement movements was developed based on the experimental data. Further, we proposed the methodology to estimate the expected service life of a sealed joint.

KEYWORDS: sealant, performance, design method, relative story displacement, movement, fatigue resistance

Introduction

In sealed joint design [1], fatigue resistance against both extension-contraction movements and shear movements (relative story displacement) needs to be considered. In Japan, where there are many earthquakes, it is especially important to evaluate the fatigue resistance of sealed joints to relative story displacement. In the aftermath of the 1995 earthquake in the southern area of Hyougo prefecture in Japan, the design method used specified a performance standard for a seismic-proof structure, introducing requirements for steel structures or curtain wall panel systems, and, consequently, building service life began to be defined [2–5].

The fatigue resistance of sealant to relative story displacement is affected by the story drift (R), which defined as the relative displacement of a curtain wall panel over the panel beneath it and is calculated as $R=\delta/H$ (δ: story drift movement, H: curtain wall panel height).

The sealed joint design method considers only R=1/300 relative story displacement of a curtain wall panel and only allows the use of sealants in sound conditions, after testing for R=1/300. However, when considering the targeted service life of a sealed joint, there is the possibility for displacements of the curtain wall panels to be larger than R=1/300. Thus, it is important to evaluate the fatigue resistance of sealants to relative story displacement when story drift is greater than R=1/300. In the current study, the fatigue resistance of sealed joints to relative story displacement movements caused by earthquakes was evaluated using a fatigue test, and a new joint design method was proposed, providing adequate sealed joint performance over the targeted service life.

Manuscript received November 21, 2004; accepted for publication October 27, 2005; published online February 2007. Presented at ASTM Symposium on Durability of Building and Construction Sealants and Adhesives, Second Symposium on 15–16 June 2005 in Reno, NV; A. T. Wolf, Guest Editor.

[1] Research Associate and Professor, respectively, Structural Engineering Research Center, Tokyo Institute of Technology, 4259 Nagatsuta, Midori, Yokohama, 226-8503, Japan.

TABLE 1—*Factors evaluated in this study.*

Factors influencing performance	Evaluated Factor
Sealants	Two-part building sealants
Cross-section type of sealants	Cross-sectional size of sealants (joint width and depth of sealants)
	Cross-sectional shape of sealants
Type of sealed joints in building	Linear sectional area of the sealed joints
	Intersectional area of the sealed joints
	Sliding motion type
	Rocking motion type

Concept of Design Method Providing Adequate Sealed Joint Performance Over Service Life

Factors Considered in Joint Design Method

Table 1 shows the factors evaluated in this study in order to propose the design method providing adequate sealed joint performance. These factors affect the fatigue resistance of sealed joints when relative story displacement occurs at sealed joints. First, the previously utilized types of sealants were evaluated. Second, the effects of the cross-sectional size and shape of sealants were evaluated [6–8]. Third, the members of building sealed joints were evaluated. The present sealed joint method has mainly focused on the fatigue resistance of the linear sections of sealed joints. However, there are intersections of sealed joints that occur in actual buildings. Therefore, it is necessary to study the fatigue resistance of both sealed joint types (linear sections and intersections). Moreover, movements in the intersections of sealed joints are affected by the behavior of the adjacent curtain wall panels. The typical attachment methods for curtain wall panels are of the sliding motion and rocking motion types [9,10].

Performance Evaluation Factors

Table 2 shows the relationship between categories of damage level for precast concrete curtain wall panels specified in the Japanese Architectural Standard Specifications (JASS 14) [11] and the seismic intensity scale of the Japanese Meteorological Agency [12]. The story drift of curtain wall panels evaluated in our study was selected based on this table. The fatigue test was carried out for three levels, i.e., a large earthquake, with the story drift of the curtain wall set at R=1/100; a moderate earthquake, set at R =1/200; and, a small earthquake, set at R=1/300.

Number of Cyclic Movements at Sealed Joints Relative to Story Displacement

The number of cyclic movements at sealed joints depends on the story drift size of the curtain wall panel. Table 3 shows the frequency of seismic occurrence in Japan during the past 75 years. Figure 1 shows the relationship between the seismic intensity scale and the frequency of seismic occurrence. The frequency of seismic occurrence remarkably varies according to locality in Japan. For intensities of 4 and lower 5, the

TABLE 2—*Damage pattern and level of precast concrete curtain wall panel for estimated seismic intensities.*

Degree of seismic intensity (Seismic intensity scale)	Story drift (R)	Damage pattern and level	Story drift to be carried out in this study (R)
Large earthquake (intensity 6)	$R \geqq \frac{1}{75}$	Fastener is broken. Curtain wall panel is damaged or fallen down.	$R = \frac{1}{100}$
	$\frac{1}{120} \leqq R < \frac{1}{75}$	Fastener is damaged. Precast concrete is damaged.	
Moderate earthquake (intensity 5)	$\frac{1}{200} \leqq R < \frac{1}{120}$	Sealant is damaged.	$R = \frac{1}{200}$
	$\frac{1}{300} \leqq R < \frac{1}{200}$	Part of sealant is damaged.	
Small earthquake (intensity 4)	$R < \frac{1}{300}$	No damage.	$R = \frac{1}{300}$

TABLE 3—*Frequency of seismic occurrence in Japan in the past* 75 years.

	JMA seismic intensity scale[b]						JMA seismic intensity scale[b]				
		5		6				5		6	
Prefecture[a]	4	lower	upper	lower	upper	Prefecture	4	lower	upper	lower	upper
Hokkaido	175	23	0	3	0	Shiga	14	3	0	0	0
Aomori	53	7	1	1	0	Kyoto	21	3	0	0	0
Iwate	88	8	0	2	0	Osaka	13	1	0	0	0
Miyagi	54	14	0	3	1	Hyogo	29	3	0	1	0
Akita	16	4	1	0	0	Nara	14	4	0	0	0
Yamagata	19	3	1	0	0	Wakayama	31	2	0	0	0
Fukushima	64	13	0	0	0	Tottori	37	5	0	1	1
Ibaraki	105	8	0	0	0	Shimane	10	1	2	0	0
Tochigi	74	8	0	0	0	Okayama	8	2	1	0	0
Gumma	15	2	0	0	0	Hiroshima	13	3	1	1	0
Saitama	44	1	0	0	0	Yamaguchi	12	3	0	0	0
Chiba	89	6	0	0	0	Tokushima	13	1	1	0	0
Tokyo	44	3	0	0	0	Kagawa	20	1	1	0	0
Kanagawa	56	4	0	0	0	Ehime	15	3	0	0	0
Niigata	20	3	0	0	0	Kochi	16	5	1	0	0
Toyama	6	1	0	0	0	Fukuoka	5	0	0	0	0
Ishikawa	9	2	0	0	0	Saga	3	0	0	0	0
Fukui	19	3	0	1	0	Nagasaki	31	1	0	0	0
Yamanashi	32	3	0	0	0	Kumamoto	41	14	0	0	0
Nagano	94	11	0	1	0	Oita	25	4	0	0	0
Gifu	11	2	0	0	0	Miyazaki	42	9	0	0	0
Shiznoka	86	12	1	3	0	Kagoshima	84	8	4	1	0
Aichi	19	2	1	0	0	Okinawa	80	11	0	0	0
Mie	30	4	0	1	0						

[a]The number of earthquakes is shown for the entire prefecture in Japan.

[b]The JMA seismic intensity scale, which provides a measure of the strength of seismic motion, is measured with a seismic intensity meter. Because "intensity 5" or "intensity 6" did not necessarily correspond to the same degree of damage, "intensity 5" and "intensity 6" have been divided into two scales: "intensity 5 Lower (4.5–4.9)" and "intensity 5 Upper (5.0–5.4)" and "intensity 6 Lower (5.5–5.9)" and "intensity 6 Upper (6.0–6.4)" respectively, since 1996.

longer the service life of a building structure is, the higher the frequency of seismic occurrence. In contrast, for intensities of upper 5 and above, the frequency of seismic occurrence is nearly the same, regardless of service life duration.

It is difficult to calculate exactly the number of cyclic movements of relative story displacement within the service life for each earthquake. Therefore, the number of cyclic movements at sealed joints within their service life is calculated under the following assumption. Generally, the relationship between range of movement at sealed joints and the number of cycles at sealed joints were evaluated by applying a logarithmic scale. It is expected that the number of cyclic movements of relative story displacement for one earthquake falls between 1 and 100 times. In our study, the relationship between one earthquake and the

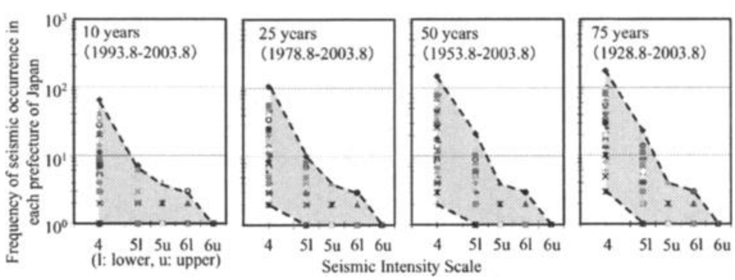

FIG. 1—*Relationship between seismic intensity scale and the frequency of seismic occurrence in each prefecture of Japan.*

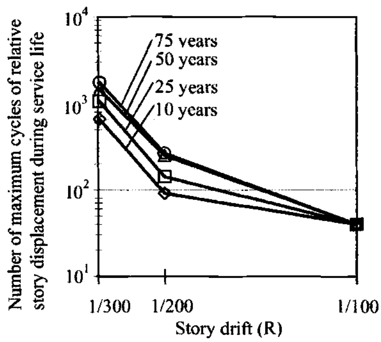

FIG. 2—*Relationship of story drift and the number of maximum cycles of relative story displacement for sealed joints during service life in Japan.*

number of cyclic movements of relative story displacement at sealed joints led to numerical formula—Eq 1—and the number of cyclic movements at sealed joints was assumed to be ten times for one earthquake.

$$n_i = A \times n_i' \quad (i = 1/300,\ 1/200,\ 1/100) \tag{1}$$

where:

n_i = number of cyclic movements of relative story displacement in service life,
n_i' = frequency of seismic occurrences in service life,
A = constant.

Figure 2 shows the relationship between the story drift of curtain wall panels and the number of maximum cycles of relative story displacement at a sealed joint during its service life in Japan. The larger the story drift, the smaller the number of cyclic movements occurring during the service life. Cyclic movements at sealed joints at R=1/300 occurred several thousand times; at R=1/200, occurred several hundred times; and, at R=1/100, occurred several tens of times during the last 75 years.

Fatigue Resistance of Sealed Joints to Relative Story Displacement

In our previous study, nine types of rectangular sections of different size were deformed by shear movement to evaluate the effect of the cross-sectional size of the sealed joint. The finding was that section size did not clearly affect fatigue resistance when the ratio of depth (D) to width (W) at the sealed joint was the same [6]. In the evaluation of the cross-sectional shape of sealed joints, rectangular and slightly concave shapes of sealed joints were recommended to enhance durability of sealed joints under relative story displacement [7,8].

Fatigue Resistance of Sealant at the Linear Section of Sealed Joints

Test Specimen—The test specimen simulating the linear sections of sealed joints in actual buildings is shown in Fig. 3. Table 4 shows the three types of two-part building sealants—two-part polysulfide PS-2,

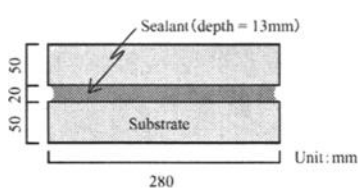

FIG. 3—*Test specimen.*

TABLE 4—*Sealants studied.*

Contents	SR-2	MS-2	PS-2
Tensile strength at 50 % elongation (N/mm^2)	0.13	0.13	0.11
Tensile strength at 100 % elongation (N/mm^2)	0.20	0.17	0.14
Maximum tensile strength (N/mm^2)	0.47	0.45	0.39
Elongation at the failure (%)	775	560	685
Color	gray	gray	gray

two-part silicon-modified polyether MS-2, and two-part silicone SR-2, and their evaluation and performance. Sealants were injected into the space between two aluminum bars, which were fixed to provide a joint with a cross section of 20 mm width and 13 mm depth. A polyethylene film was installed at the bottom of the test joint as a bond breaker; the film was removed just prior to fatigue testing. The specimens were cured for two weeks at room temperature, and then stored for two weeks more in a chamber controlled at a temperature of 50±2°C and relative humidity of 50±5 %.

Fatigue Test—The specimens were attached to the fatigue test equipment as shown in Fig. 4. In the sealed joint design method, when the story drift (R) is 1/300, a relative story displacement (shear movement) with amplitude of ±60 % of the joint width is allowed according to JASS 8 [1]. By the relationship between the story drift of the curtain wall panel and the size of the movement occurring in the sealed joint in this study, a story drift of R=1/200 can be calculated to an amplitude of ±90 % and a story drift of R=1/100 to ±180 %. By placing the joints at two locations in the apparatus, they were subjected to repeated relative story displacement in the form of a sine curve with amplitudes of ±60 % = ±12 mm, ±90 % = ±18 mm, and ±180 % = ±36 mm of 20 mm width and a period of 10 s. The surfaces of the specimens were periodically inspected, by visual examination of the top surface, and by using a glass-fiber scope for the bottom surface. The number of movement repetitions to crack initiation and the patterns of cracking were recorded. The fatigue tests were carried out at a temperature of 20±2°C and were stopped at one million cycles unless any defects were observed in the sealant beads.

Test Results and Discussion—Cracking pattern due to shear movement was observed, and the crack at the sealed joint started near the substrate bars. The number of cycles to crack initiation for the linear section of the sealed joint and the range between minimum and maximum values of the number of cyclic movements on sealed joints for the last 75 years in Japan are shown in Fig. 5. The larger the story drift (relative story displacement), the earlier the crack initiation of the sealed joint. Then, the number of cycles to crack initiation obtained through the fatigue test is higher than the number of maximum cycles to relative story displacement that occurred at the sealed joint during the last 75 years.

Fatigue Resistance at the Intersection of Sealed Joints

Test Specimen—The test specimen simulating the intersection of sealed joints is shown in Fig. 6. The cross section of the sealed joints, types of sealants, and curing method is the same as for the linear section of the sealed joint.

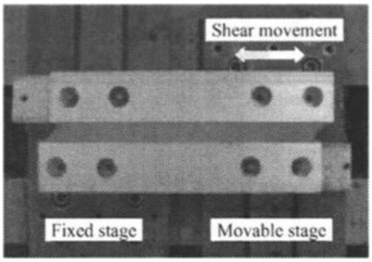

FIG. 4—*Conditions of shear fatigue test.*

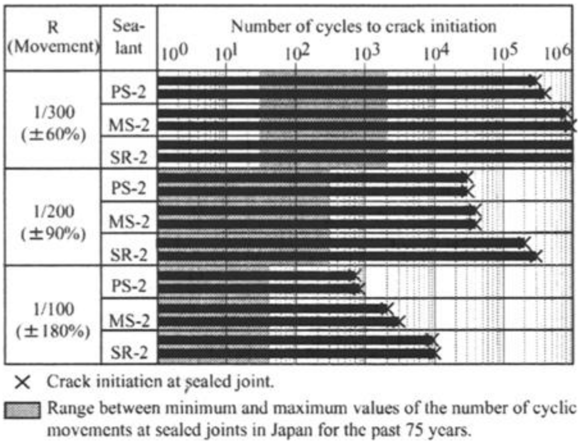

FIG. 5—*Number of cycles before crack initiation at linear section of sealed joint.*

Fatigue Test—For the sliding type of curtain wall panel fixing system, the specimen is deformed by repeated shear movement, as shown in Fig. 7. For the rocking type of curtain wall panel system, the movement occurs not only in the vertical direction, but also in the horizontal direction, as shown in Fig. 8. The movement in vertical direction is affected by the width (W_p) of the curtain wall panel. In contrast, movement in the horizontal direction is affected by the fixing position (F) of the curtain wall panel and is calculated by the following Eq 2.

$$\delta_h = R \times F \tag{2}$$

where:

δ_h = movement in the horizontal direction (mm),

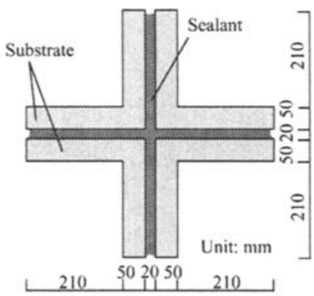

FIG. 6—*Test specimen.*

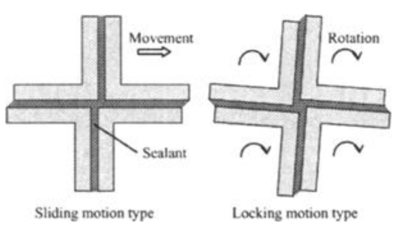

FIG. 7—*Condition of fatigue test specimens.*

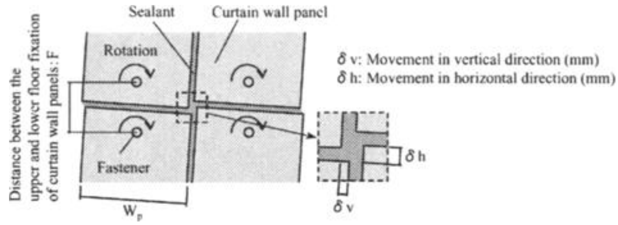

FIG. 8—*Behavior of the intersection of the sealed joints to rocking motion in actual building.*

R = story drift,
F = distance between the upper and lower floor fixation of curtain wall panels (mm).

For sealed joints, under the condition of $F/W_p=0$, movement occurs only in the vertical direction, with $F/W_p=1$, the movement occurs in both vertical and horizontal directions. In our study, the fatigue test was carried out under the condition of $F/W_p=1$, which is the most severe condition for sealants.

The fatigue test was carried out with the same conditions as for the linear section of sealed joint test. Namely, the fatigue test used the fatigue apparatus [10] to perform the same movements in the vertical and horizontal directions, as shown in Fig. 7. The fatigue tests were carried out at three amplitudes, i.e., ±60 %; ±90 %; and, ±180 %. A 10 s (6 cycle/min.) period was adopted for the fatigue test. All tests were carried out at a temperature of 20±2°C and were continued up to one million cycles, unless any defects were observed in the sealed joint.

Test Results and Discussion of Sliding-Type Curtain Wall Panel Fixing System—The comparison of the number of cycles to crack initiation at the intersection of sealed joints under sliding motion with the range between minimum and maximum values of the number of cyclic movements at sealed joints in Japan for the last 75 years is shown in Fig. 9. The cracks at the intersection of sealed joints occurred at an earlier stage when compared with the linear section of joints on the surface of all specimens. For R = 1/300, R = 1/200, and R = 1/100 with SR-2 and MS-2, the number of cycles to crack initiation obtained by the fatigue test is higher than the maximum values of the number of cyclic movements at sealed joints for the last 75 years. However, for R = 1/100 with PS-2, the number of cycles to crack initiation is lower than the maximum value.

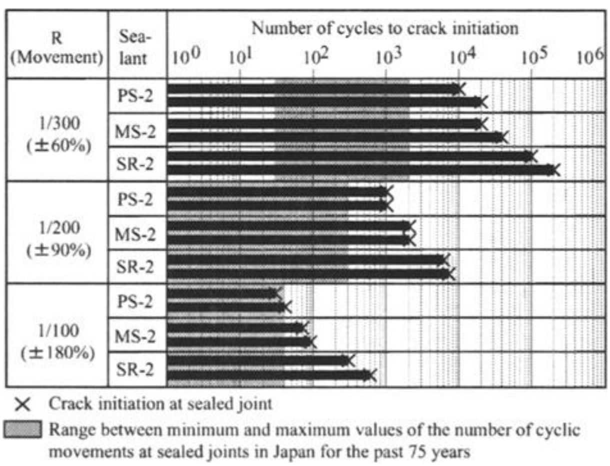

FIG. 9—*Number of cycles to crack initiation under sliding motion at intersection of sealed joints.*

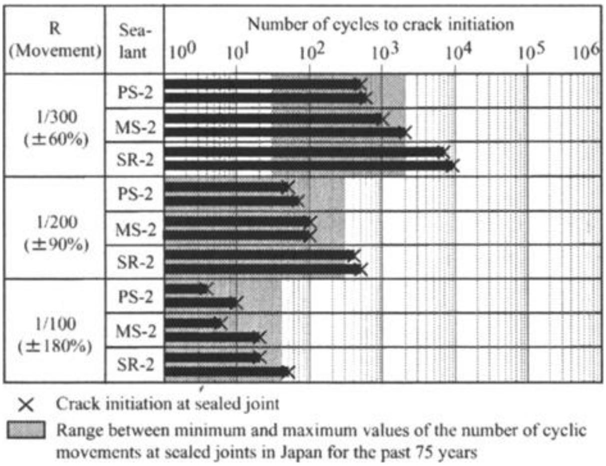

FIG. 10—*Number of cycles to crack initiation under rocking motion at intersection of sealed joints.*

Test Results and Discussion of Rocking-Type Curtain Wall Panel Fixing System—The number of cycles to crack initiation at the intersection of sealed joints under rocking motion is shown in Fig. 10. For all story drift with MS-2 and PS-2, the number of cycles to crack initiation is lower than the maximum values of the number of cyclic movements at sealed joints in Japan for the last 75 years. In contrast, fatigue resistance of SR-2 is higher than with other sealants, however, crack initiation occurred at tens of cycles for amplitude of ±180 % (R = 1/100). The fatigue test with $F/W_p = 1$ is very severe for the sealants, thus fatigue resistance of sealants is higher when F/W_p is smaller.

Process of Design Method Providing Optimal Sealed Joint Performance

Concept for Sealed Joint Design

The design method for the linear section and intersection of sealed joints was proposed on the basis of an idea described in our study and experimental data. This process of sealed joint design considered the relationship between the number of cyclic movements in service life and the number of cycles to crack initiation of sealed joints obtained by the fatigue test shown in Fig. 11.

Evaluation of Sealed Joint Performance Using Miner's Rule

"This proposed sealed joint method is divided to two-stages. Namely, it is judged whether the performance of sealant is sufficient to the target service life of sealed joint to relative story displacement by expression of Miner's rule, expressed by the number of cyclic movements occurring in service life and the number of cycles to crack initiation of the sealed joint, and expresses the accumulated damage level of the sealed joints."

During the first stage, the targeted service life of sealed joint is decided upon and is converted into a relationship between story drift and the number of cyclic movements occurring at the sealed joint during its service life. The number of cyclic movements to relative story displacement occurring during service life for each story drift R = 1/100, 1/200, and 1/300, is calculated. During the second stage, the number of cycles to crack initiation of the sealed joint is evaluated for the linear joint and the intersection of sealed joints for R = 1/300, 1/200, and 1/100. However, it is difficult to obtain data for the crack initiation number because of the number of parameters. The calculation of the number of cycles to crack initiation of the sealed joint was proposed as shown in Fig. 12. This figure shows the relationship between the number of cycles to crack initiation of the sealed joint and other factors, namely, story drift; sealant types;

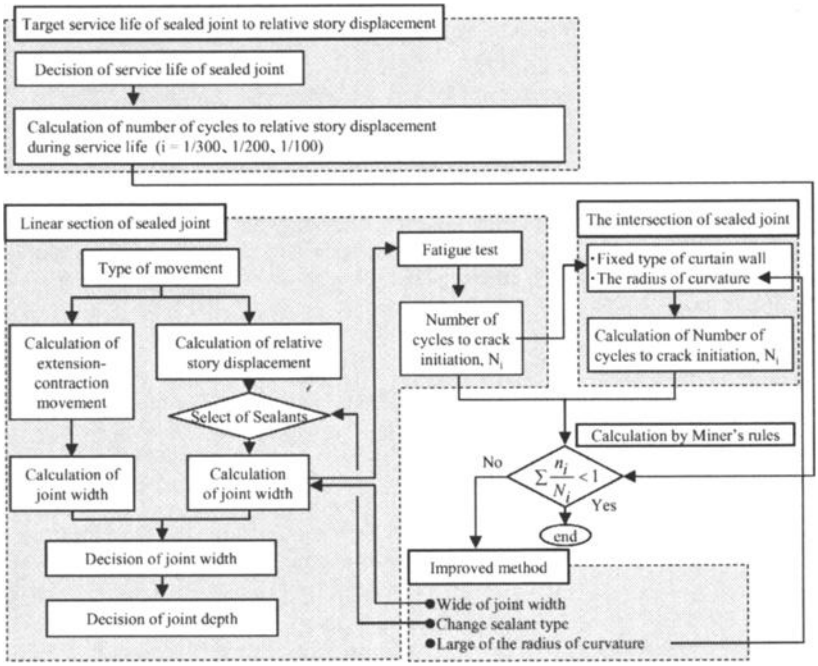

FIG. 11—*Flow of sealed joint method proposed in the current study.*

width of joint; radius of curvature at intersection of sealed joints; and distance between the upper and lower floor fixation of curtain wall panel. The radius of curvature at the intersection of sealed joints, and the distance between the upper and lower floor fixation of a curtain wall panel was calculated and described in our previous papers [13,14]. During the third stage, the accumulated damage level at the sealed joint was calculated using Miner's Rule [15–18]

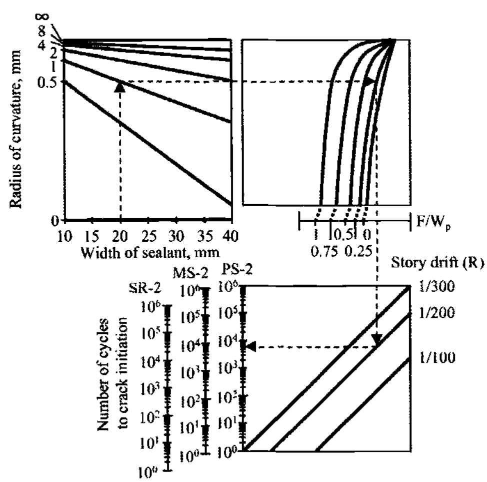

FIG. 12—*Figure to calculate number of cycles to crack initiation of sealant.*

$$M = \sum \frac{n_i}{N_i} = \frac{n_{1/300}}{N_{1/300}} + \frac{n_{1/200}}{N_{1/200}} + \frac{n_{1/100}}{N_{1/100}} \tag{3}$$

where:

M = accumulation damage level at the sealed joint (For M = 1, the crack initiation occur at the sealed joint),

$n_{1/300}, n_{1/200}, n_{1/100}$ = number of cyclic movements occurring in service life,

$N_{1/300}, N_{1/200}, N_{1/100}$ = number of cycles to crack initiation of the sealed joint.

To satisfy the targeted service life of the sealant, the result of Eq 3 must be lower than 1. If the accumulation damage level at the sealed joint is larger than 1, the fatigue resistance of the sealed joint must be improved by making the joint wider or by changing the type of sealant; furthermore, for the intersection of sealed joints, the radius of curvature must be increased.

Example of accumulation damage level calculation in a sealed joint

The accumulated damage level of a sealed joint was calculated using the factor conditions shown in Table 5. The accumulated damage level at a sealed joint can be calculated using Miner's Rule, according to Eq 3. The resulting accumulated damage level for the linear section of the sealed joint is 0.05, and is 0.28 for the intersection of the sealed joint. Both accumulated damage levels for the sealed joint sections are smaller than 1 and the fatigue resistance of the sealed joint is sufficient for a service life of about 25 years. However, the sealed joint design method proposed in our study does not consider weathering, and the accumulated damage level of sealed joints is actually greater than the value calculated in this study.

TABLE 5—*Factor conditions.*

Target service life of sealed joint		25 years
Sealant		MS-2
Width of joint		20 mm
Type of sealed joint	Linear section of sealed joint	. . .
	Intersection of sealed joint (Fixed type)	Rocking motion type (F/W_p=0.25)
The radius of curvature		1 mm

Conclusions

1. The relationship between the story drift and the number of cyclic movements at the sealed joint in Japan was calculated to clarify the service life of a sealed joint. The number of cyclic movements at a sealed joint occurred several thousand times at R = 1/300, several hundreds times at R = 1/200, and tens of times at R = 1/100.
2. It was obvious that the fatigue resistance of sealed joints was lower for the intersectional area than for the linear sections of the joints, and was lowest when the same movement occurred in both, vertical and horizontal, joints.
3. The fatigue resistance of sealants to relative story displacement became higher in the order, PS-2, MS-2, and SR-2.
4. The fatigue resistance of sealed joints to relative story displacement movements caused by earthquakes was studied for their linear sections and for the intersection of sealed joints, and a new joint design method providing the necessary sealed joint performance was proposed, which considers the service life of sealed joints. This process of method design took into consideration the relationship between the number of cyclic movements in a service life and the number of cycles to crack initiation of sealed joints obtained using a fatigue test.
5. The service life of a sealed joint was evaluated using Miner's Rule.

References

[1] Architectural Institute of Japan, "Japanese Architectural Standard Specification JASS 8 Waterproofing and Sealing," Japanese Standard Association, *AIJ*, 2000.

[2] Architectural Institute of Japan, "Symposium on Performance Design Method for Civil Engineering Designer," *Structural Technical Research Committee, Kanto Chapter of AI Japan Report*, 1998.

[3] Architectural Institute of Japan, "Estimation Method of Performance of Architectural Materials, Member and Part," *Architectural Materials Working Group, AIJ Report*, 2000.

[4] Architectural Institute of Japan, "Performance Specification View and Problems," *Architectural Materials Working Group, AIJ Report*, 2003.

[5] Architectural Institute of Japan, "Performance Design Method of Steel Construction," *Steel Construction Committee, AIJ Report*, 2003.

[6] Tanaka, Kyoji, Miyauchi, Hiroyuki, and Hirai, Takayuki, "Effect of Cross-Sectional Shapes of Polysulfide Sealants on Shear Fatigue Resistance to Sliding Joint Movement; Science and Technology of Building Seals," *Sealants, Glazing and Waterproofing, ASTM STP 1334*, 7th Vol., ASTM International, West Conshohocken, PA, 1998, pp. 43–50.

[7] Tanaka, Kyoji, Miyauchi, Hiroyuki, and Hirai, Takayuki, "Effect of Cross-Sectional Size and Shape on Fatigue Resistance of Sealing Joints by Shear Movement," *Durability of Building and Construction Sealants, Proceedings of the Third International RILEM Symposium*, 2000, pp. 87–96.

[8] Tanaka, Kyoji, Miyauchi, Hiroyuki, and Hirai, Takayuki, "Effect of Cross-Sectional Size and Shape on Fatigue Resistance of Sealant by Shear Movement," *Journal of Structural and Construction Engineering*, Architectural Institute of Japan, No. 511, 1998, pp. 47–52.

[9] Miyauchi, Hiroyuki and Tanaka, Kyoji, "Evaluation of Fatigue Resistance of Sealant to Shear Movement at Cross Area of Sealed Joint," *Journal of Structural and Construction Engineering*, Architectural Institute of Japan, No. 554, 2002 pp. 9–14.

[10] Miyauchi, Hiroyuki and Tanaka, Kyoji, "Evaluation of Fatigue Resistance of Sealant to Movement at Cross Area of Sealed Joint to Rocking Motion of Curtain Wall," *Journal of Structural and Construction Engineering*, Architectural Institute of Japan, No. 558, 2002, pp. 31–38.

[11] Architectural Institute of Japan, "Japanese Architectural Standard Specification JASS 14 Curtain Wall," Japanese Standard Association, *AIJ*, 1996.

[12] Japanese Meteorological Agency, http://www.jma.go.jp/JMA_HP/jma/indexe.html

[13] Miyauchi, Hiroyuki and Tanaka, Kyoji, "Estimation of the Fatigue Resistance of Sealants to Movement at Intersections of Sealed Joints and Improvements in the Joint Design Method, Symposium on Durability of Construction Sealants and Adhesives," *ASTM STP 1453*, Andreas T. Wolf, Ed., ASTM International, West Conshohocken, PA, 2004.

[14] Miyauchi, Hiroyuki and Tanaka, Kyoji, "Proposal of Sealed Joint Method for the Curtain Wall Panel Corners," *Journal of Structural and Construction Engineering*, Architectural Institute of Japan, No. 573, 2003, pp. 21–28.

[15] Miner, M. A., "Cumulative Damage in Fatigue," *Journal of Applied Mechanics*, Vol. 12, *Trans. ASME*, 67, A159–A164 (1945).

[16] Marco, S. M., and Starkey, W. L. "A Concept of Fatigue Damage," *Trans. ASME*, 76(4), 627–632 (1954).

[17] Collins, J. A., *Failure of Materials in Mechanical Design*, Wiley-Interscience, New York, 1981.

[18] Tamotsu, Watanabe and Tadashi, Ono, "Estimated Method on Life of Sealants in Building Joint (Part 8. Investigation of Cumulative Damage.)," *Summaries on Technical Papers of Annual Meeting Architectural Institute of Japan*, Architectural Institute of Japan, pp. 1297–1298, 1995.

Journal of ASTM International, Vol. 3, No. 6
Paper ID JAI13122
Available online at www.astm.org

Andreas T. Wolf,[1] *Shigeki Sugiyama,*[2] *and Fred Lee*[3]

Use of Optical Imaging/Image Analysis System for the Quantitative Analysis of Surface Changes Induced by Outdoor Weathering on Sealants

ABSTRACT: Six sealant samples that had been weathered outdoors for 6.8 years in Japan were evaluated using an Optical Imaging/Image Analysis System, Atlas VIEEW™. The specimens were first visually evaluated with aesthetic ratings assigned. These ratings were then used as the reference for the optical image analysis. Image analysis was carried out on sealant images taken under optimized diffuse illumination at a constant illuminance. Two sets of images were captured per specimen, first the weathered surface for deterioration evaluation, and second the unweathered surface as a control (reference) image. Four distinct surface defects are quantifiable in the samples. These are cracking (crazing), visual color change, spatial uniformity of deterioration (due to dirt pick-up and uneven color change, or both), and overall surface texture. Chalking and dirt pick up, as rated visually prior to this evaluation, could not be accurately assessed with the digital imaging technique. The analysis shows that surface cracking and crazing generally can be well characterized using the automated VIEEW™ system. Judging color changes visually is problematic, since cracking and crazing interferes with color judgment. Further investigations are needed to develop an automated surface characterization method for sealants.

KEYWORDS: aesthetic appearance, sealant, cracking, crazing, color change, dirt pick-up, chalking, optical imaging, image analysis

Introduction

The appearance of any building changes with time as a result of complex processes generally summarized under the term "aging." While sealants can contribute to these processes, many aesthetic issues will appear on a building facade over time with or without the presence of a sealant. Aesthetic issues raised by sealants may be classified into two groups: those that affect the sealant itself and those that affect the adjacent building substrates. Aesthetic issues that fall within the first category are blooming, dirt pick-up, microbial growth, chalking, surface crazing, change of color, and change of gloss. Aesthetic issues, which affect the adjacent building substrates, are fluid migration and fluid streaking.

In 1995, the International Standardization Committee TC59/SC8 (Building Construction, Jointing Products) formed a Work Group (WG10) to assess the need for developing test standards on aesthetic issues caused by sealants. In its inauguration meeting in 1997, WG10 prioritized the development of test standards for aesthetic issues as follows:

High Priority:	Fluid Migration (Substrate Staining)
	Dirt Pick-up
	Chalking
	Surface Crazing
Medium Priority:	Mold/Algal Growth
	Fluid Streaking

Manuscript received May 5, 2005; accepted for publication March 13, 2006; published online April 2006. Presented at ASTM Symposium on Durability of Building and Construction Sealants and Adhesives on 15–16 June 2005 in Reno, NV; Andreas Wolf, Guest Editor.

[1] Scientist and Convener of ISO TC59/SC8 WG10, Dow Corning GmbH, 65201 Wiesbaden, Germany.

[2] Senior Chemist and Member of Technical Committee of Japan Sealant Industry Association, Dow Corning Toray Silicone, Ichihara-Shi Chiba 299-0108, Japan.

[3] Standards Program Manager—Weathering Instrumentation Products, Product Specialist—Analytical Division, Atlas Electric Devices Co., Chicago, IL 60613.

Low Priority: Blooming
Change of Color
Change of Gloss

Good progress has been made by WG10 in the meantime on the issue of fluid migration, which had been rated as the highest priority work item, with an International Standard published: ISO 16938 Building Construction—Determination of the Staining of Porous Substrates by Sealants Used in Joints—Part 1: Test With Compression, and Part 2: Test Without Compression.

Concepts for a qualitative or semi-quantitative rating of aesthetic surface changes (dirt pick-up, chalking, and crazing) were developed within WG10 based on pictorial references for general comparison to allow a classification of the severity of a sample's defects. These methods, while admirably compensating for our visual limitations, did not meet the requirement for observer-independent ratings, since they do not fully eliminate the perceptual and psychological biases of the observer.

Therefore, the need was identified for an objective, quantitative method of rating the aesthetic surface changes occurring on weathered sealants that eliminates the bias of an inspector's judgment. This paper describes an early attempt at investigating the feasibility of such a method based on a digital Optical Imaging/Image Analysis System that initially had been developed for the detection of defects in automotive topcoats.

Definition and Description of Aesthetic Surface Changes

Dirt Pick-up

The term dirt pick-up describes the soiling caused by foreign material other than microbiological organisms that is deposited on or embedded into a sealant surface. The soiling is generally caused by the accumulation of airborne particulates on the sealant surface.

Microbial Growth

The term refers to the accumulation and colonization of microorganisms on a sealant surface.

Surface Cracking/Crazing

The term refers to cracks formed on a sealant surface as a result of environmental ageing. Surface crazing is only observed with organic sealants.

Chalking

The term refers to the whitening of some organic sealant surfaces with weathering. The whitening is caused by the degradation and erosion of organic polymer, which leads to increased roughness or porosity of the sealant surface. The early stages of chalking are marked by a loss of surface gloss and color. Some sealant formulations weather so badly that all organic material leaches from the surface, leaving behind nothing but the inorganic fillers, typically calcium carbonates, hence the term.

Change of Color

This term is self-explanatory, however, there are several mechanisms, which can cause changes in color. First, there are mechanisms that are inherent in the sealant. For example, a change in color can be caused by the insufficient color fastness of one of the pigments used in the sealant formulation. A darkening of a sealant may be simply the first stages of dirt pick-up or microbial growth, as the whitening of the sealant may be the first stages of chalking. Second, there are a number of mechanisms that are induced by factors external to the sealant. Probably the most important example of these is the incompatibility with other building materials, such as backing materials, building substrates, or the remnants of a failed building sealant in a resealed joint. Incompatible materials then migrate from the other building material into the sealant and cause it to change color. Examples of such incompatible materials are low molecular weight polymers, plasticizers, antioxidants, bitumen, or tar.

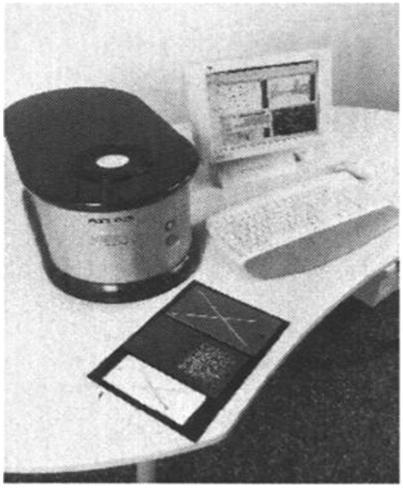

FIG. 1—*Atlas VIEEW™ digital image analyzer.*

Experimental

Optical Imaging/Image Analysis System

The VIEEW™ (Video Image Enhanced Evaluation of Weathering) digital image analyzer, developed by Atlas Electric Devices Company, is an integration of digital image capturing and processing technologies (see Fig. 1). The system is capable of capturing digital images of samples under various lighting schemes optimized for the sample surface, of digitally processing the images to highlight and enhance surface defects, and of measuring and counting defects such that each sample is defined by a comprehensive statistical profile.

Initial applications of the VIEEW™ system were primarily focused on the evaluation of automotive exterior coatings defects, such as chipping, marring, and corrosion [1,2], but the technique can also be applied to the evaluation of the scratch resistance of molded and extruded plastics [3,4]. A first attempt at applying this new technique to the analysis of surface defects in weathered sealants has been undertaken with the objective of quantifying the degree of aging induced by various artificial accelerated laboratory and natural outdoor weathering schemes [5].

The system incorporates two different illumination methods: diffuse, chromatic (color) lighting for the detection of variations in chromatic contrast; and direct lighting to measure variations in geometric reflection (gloss) and its textural characteristics.

Diffuse illumination is employed to accurately measure surface abnormalities resulting from chromaticity (color) difference. The sample is illuminated by a diffuse chromatic source where each color component—red, green and blue, or RGB—may be independently adjusted to maximize contrast on the sample surface.

Direct illumination is employed to provide the most accurate measurement of the reflectance, or gloss, of a surface, which also reveals surface irregularities such as scratches, chips, orange peel, etc. In direct illumination, the light strikes the sample normal (perpendicular) to its plane.

Two categories of surface defect analysis dominate the computerized image analysis: defect characterization and identification of surface texture properties. The former category includes defect size, shape, and distribution while the latter entails a determination of the change in surface appearance. The image analysis software exploits both binary (two-bit black and white) and gray scale image types to perform these characterizations.

TABLE 1—*Sample ratings based on visual inspection.*

Label	Type	Components	Crazing (1–5)[a]	Dirt Pick Up (1–5)[a]	Chalking (0–3)[b]	Visual Color Change (0–3)[b]
PU1-1	PU	1	3	1	3	1 (lighter)
PU2-3	PU	2	5	1	2	1 (lighter)
MS2-11	MS	2	3	3	0	1 (darker)
PS2-13	PS	2	2	5	0	3 (darker)
SR2-17	SR	2	1	4	0	0
SR1-20	SR	1	1	3	0	0

[a]1: low/good, 5: high/poor
[b]0: no/good, 3: high/poor

Visual Rating of Weathered Sealant Samples

Six sealant samples that had been weathered outdoors for 6.8 years in Japan as part of the SOPRO project (10-year outdoor exposure of 22 sealant samples at Hokkaido, Tsukuba, and Kyushu) were obtained from the Japanese delegation to ISO TC59/SC08. The samples were one-part polyurethane (PU1-1), two-part polyurethane (PU2-3), two-part silicon-modified polyether (MS2-11), two-part polysulfide (PS2-13), two-part silicone (SR2-17), and one-part silicone (SR1-20) sealants. The sealant samples were visually inspected and rated by experts of the Japanese delegation for crazing, dirt pick-up, chalking, and color change. A scale of 1 (low/good) to 5 (high/bad) was applied for crazing and dirt pick-up, while a scale of 0 (no/good) to 3 (high/bad) was applied for chalking and color change. The perception of the direction of color change on the grayscale (darker or lighter) was also indicated. Table 1 shows the sample ratings based on the visual inspection.

Figure 2 shows photos of the sealant samples (strips) obtained from the Japanese delegation.

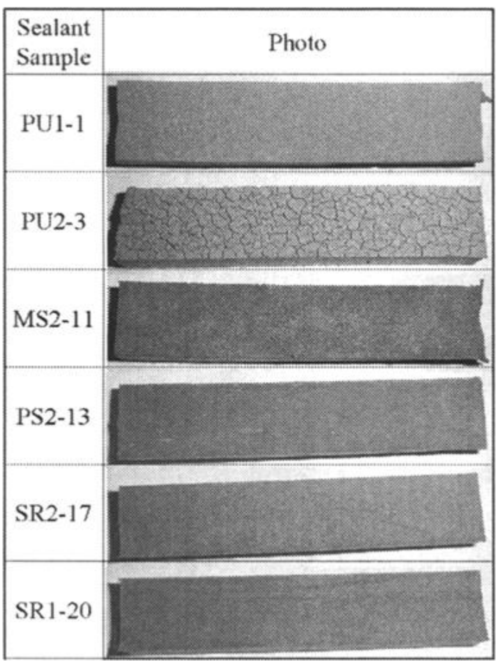

FIG. 2—*Photos of sealant samples (strips) obtained from the Japanese delegation (length of strip: ca. 50 mm, width: ca. 10 mm).*

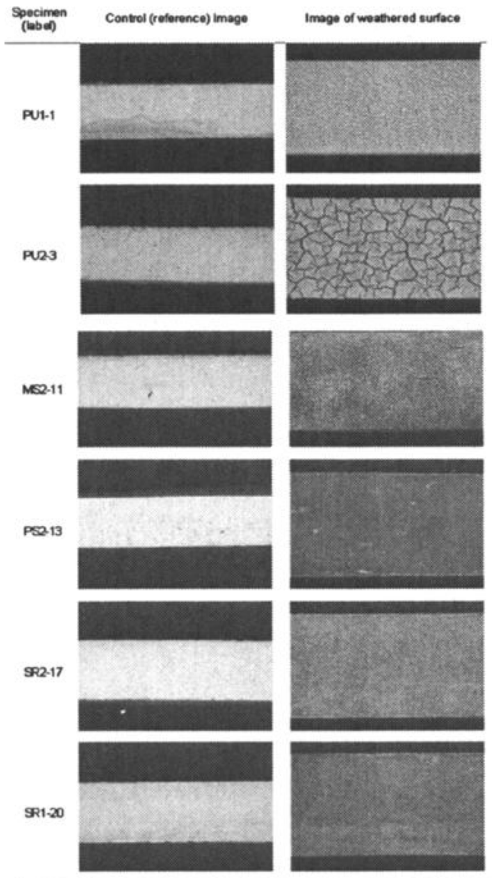

FIG. 3—*Raw digital images of sealant samples (weathered and unweathered surfaces). Note: Width of sealant strip in Figs. 3–6 and 9: ca. 10 mm, thickness of sealant strip in Fig. 3 (left): ca. 5 mm.*

Image Capturing and Analysis

Raw Digital Images (Gray Scale)—Images of the sealant samples were taken under an optimized diffuse illumination at a constant illuminance. This type of illumination enhances the chromatic differences of the sealant surfaces. Two sets of images were captured per each specimen: the weathered surface for deterioration evaluation and the unweathered surface on the lateral sample side for control (reference) image. While the use of an original unexposed specimen as the control image is desirable, this method was chosen, as no other reference sample was available. Figure 3 shows the raw digital images of the reference (unweathered) and weathered surfaces of the sealant samples.

Overall Surface Texture Change—This property is a quick, yet robust, means of measuring the overall surface deterioration. It is measured based on tonal variations caused by surface defects in digital images. For example, surface cracks and their interaction with incident light cause severe tonal variation in the captured image.

Cracking (Crazing) Analysis—Generally, the severity of cracking or crazing can be characterized in several ways, e.g., by determining density of cracks (amount of cracks shown in a given surface), nor-

Specimen (label)	Specimen Image	Overall Surface Texture (rating)
PU1-1	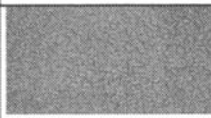	6.1
PU2-3	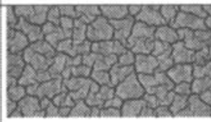	5.4
MS2-11		5.5
PS2-13		1.0
SR2-17	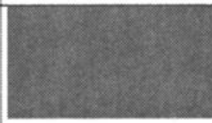	2.3
SR1-20	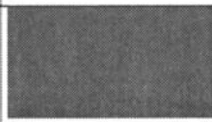	2.0

FIG. 4—*Digital images of weathered sealant samples and overall surface texture change index.*

malized crack density (based on skeletonized crack structure), crack thickness (width of crack), crack orientation (direction of cracks), etc. In sealants, density of cracks and crack thickness combined appropriately describe cracking severity in a quantitative manner.

Cracks, or other defects that are defined by boundaries, require that the images be converted to a black and white format. In the black and white image, cracks are shown as black pixels and the background as white pixels. In describing crack width, the term "main crack width" is used. This parameter is calculated as average crack width plus standard deviation. Figure 5 shows the binary (black and white) image of the weathered sealant samples and the calculated crack density and main crack width.

Visual Color (Tonal) Change—The visual color change is measured with respect to the average gray level of an image. With constant illumination condition, the gray level of the specimen surface depicted in a digital image corresponds to the specimen's visual color on the gray scale. In order to assess the changes from the original condition, the lateral side unweathered surface was used as the gray scale reference. For the specimens with a cracked surface, cracks were subtracted from the image, because the cracks and their interaction with light make the entire specimen surface appear darker than the actual surface color.

Average gray level values of control specimens and exposed specimens were used to calculate the change in visual color—see Fig. 6 for inverted gray images of weathered and unweathered sealant surfaces. Figure 7 illustrates the actual changes in gray levels, while Fig. 8 illustrates the color change, which is calculated based on gray levels of control surfaces minus the gray level of exposed surfaces.

Uniformity of Deterioration and Virtual Human Visual Evaluation—Digital images of a specimen surface often contain more data points than the human eye perceives. Human perception often averages the

Specimen (label)	Specimen Image (processed)	Crack Density (%)	Main Crack Width (mm)
PU1-1	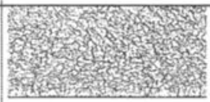	24.3	0.0142
PU2-3	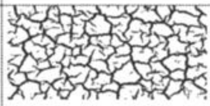	23.5	0.0377
MS2-11	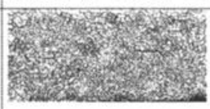	23.5	0.0138
PS2-13	Some crazing shown, but instrumentally not detectable.	N/A	N/A
SR2-17	No crack	N/A	N/A
SR1-20	No Crack	N/A	N/A

FIG. 5—*Binary image, crack density and main crack width for weathered sealant samples.*

details of a specimen surface and provides an overall judgment of the surface condition. This overall judgment is mostly based on the uniformity of surface deterioration based on their tonal variations. For example, cracked surfaces are by far the most severe damage in materials and their visual tonal variations result in highly nonuniform surfaces. With proper processing of digital images, surface images can be simplified in the same manner as is done by human perception. With the simplified (processed) images, one can digitally mimic human judgment of a surface condition and provide quantitative data that correlate

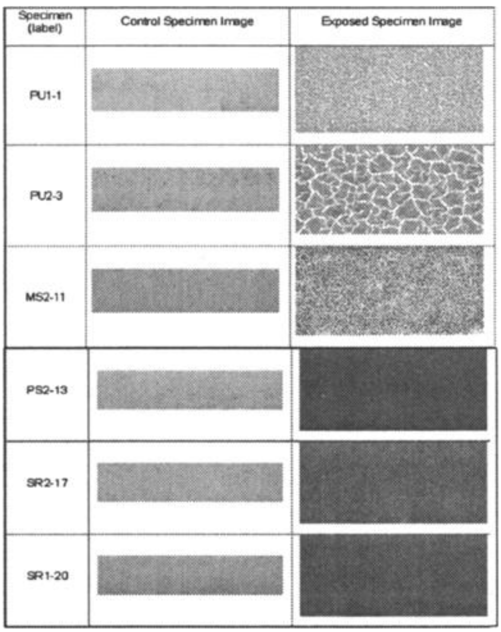

FIG. 6—*Inverted gray images of weathered and unweathered sealant surfaces used in the calculation of color changes.*

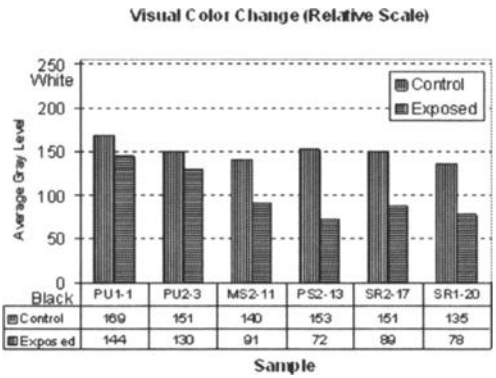

FIG. 7—*Average gray levels of unexposed (control) and exposed sealant surfaces.*

with human visual judgment (see Fig. 9 for enhanced and processed images of weathered sealant surfaces).

The images in the left column of Fig. 9 represent "enhanced specimen images." This enhancement amplifies surface damage and thus the tonal variation is superior to the original images. The images in the right column of Fig. 9 are further processed in order to mimic human perception of surface condition. In this process, similar gray level neighboring pixels are combined to represent simpler images. From these images, the uniformity of surface deterioration is measured based on tonal variation.

Results and Discussion

Four distinct surface defects are quantifiable in the weathered sealant samples. These are cracking (crazing), visual color change, spatial uniformity of deterioration (due to dirt pick-up and uneven color change, or both), and overall surface texture. Chalking and dirt pick-up, as rated visually prior to this evaluation, could not be accurately assessed with the digital imaging technique.

Overall Surface Texture Change

The cracked sealant surfaces of samples PU1, PU2, and MS2 show the highest ratings for overall surface texture change. The values for the silicone sealants, SR1 and SR2, indicate that their surfaces do have some variations. Visual observation of these two specimens indicates heavy accumulation of dirt particles.

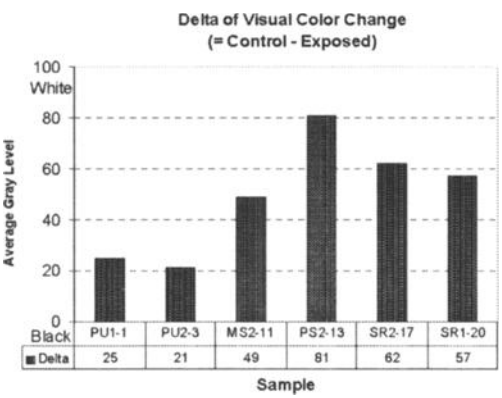

FIG. 8—*Visual color change of samples calculated on the basis of change in average gray levels.*

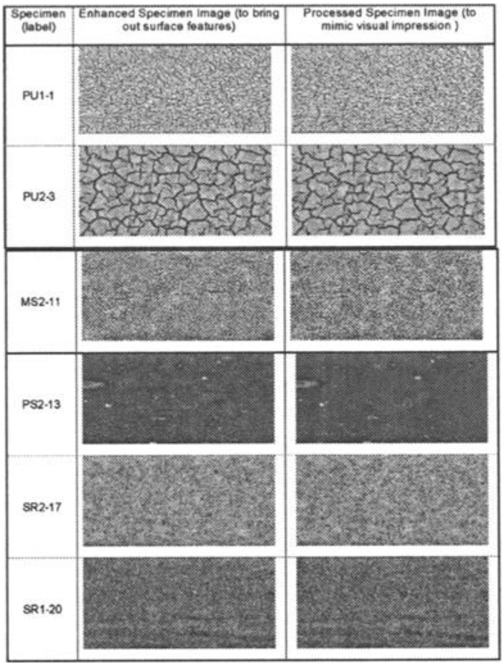

FIG. 9—*Enhanced and processed images of weathered sealant surfaces.*

Cracking/Crazing

PU1, PU2, and MS2 have apparent cracks and their severity is measured based on crack density and crack width. It is notable that all three specimens show comparable crack density values. The crack width measurement indicates that PU2 displays the most severe cracks in terms of crack width. The PS2 specimen shows some crazing; however, automatic detection of the crazing on this sample was not feasible.

Visual Color (Tonal) Change

Based on the tonal color changes determined in the automated analysis it is apparent that cracks do interfere with the visual color judging capability of humans. Because the cracks entrap light, the entire surface appears visually darker than the color of the unspoiled surface. Image analysis reveals that the PU1 and PU2 specimens have the least visual color change compared to other specimens. Contradictory to the visual ratings, where whitening was detected, digital images show that these specimens had darkened slightly. Specimens SR1 and SR2 were rated visually as no change in color; however, digital image analysis shows that these specimens had darkened quite a bit. This is probably due to dirt pick-up on the specimen surface. While it is possible to subtract the effect of dirt particles on color change, if the surface is not completely covered with dirt, an effective removal of dirt particles on the sealant surface prior to digital image capturing is not feasible. Microscopic examination of sealant surfaces typically reveals that dirt particles are embedded in the sealant surface. Because of this incorporation of dirt particles into the sealant polymer matrix, it is generally not possible to clean samples after exposure even by extensive brushing. While the authors of the earlier study of sealant surface degradation using the VIEEW™ system [5] were able to subtract the dirt particles from the images, due to a high difference between their color and the color of the sample background, this option did not prove feasible in the current study. The reason may be that in the earlier study, sealant samples were weathered outdoors for a maximum of three months, thus, displayed only a limited amount of dirt pick-up, while in the current study, sealant samples had been exposed for 6.8 years and in general showed much stronger dirt pick-up.

The limitation in the capability of the system of separating dirt pick-up and color change is especially

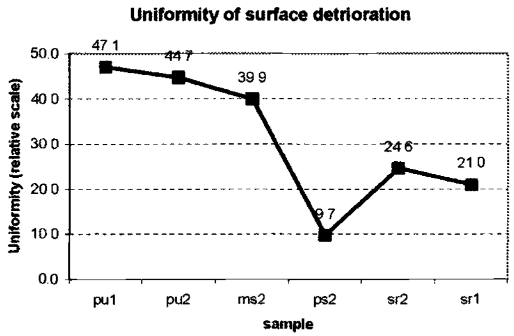

FIG. 10—*Uniformity of surface deterioration of weathered sealant samples.*

obvious in the analysis of dark colored sealants, especially those pigmented in black or dark bronze. Another limitation comes from the fact that dirt particles are normally not all black but composed of white and gray particles. Some of these particles, depending on the color of sealant, will not be recognized (e.g., white particles on a white sealant). This limitation does not affect comparative studies where relative performance is important and dirt composition is standard for all specimens.

Uniformity of Deterioration and Virtual Human Visual Evaluation

As shown in Fig. 10, the cracked sealant surfaces display the least surface uniformity. Specimens with severe dirt pick-up rated lower than the cracked specimen in surface uniformity, but higher than other samples with less dirt pick-up. It is obvious that the retained dirt particles render nonuniformity. It should be noted that this analysis yields different ratings than the overall surface texture discussed earlier.

Conclusions

The perceptual biases and limitations inherent in evaluations conducted by the unaided human eye may be overcome through the use of optical imaging and software analysis technologies that are available today. The application of such technologies can provide improved accuracy and objectivity in evaluation results across the entire field of visual evaluation. The current study of weathered sealant samples that had been exposed for a relatively long period of time (6.8 years in Japan) showed that an Optical Imaging/Image Analysis System, Atlas VIEEW™, is capable of quantifying four distinct surface defects in the samples. These surface detects are cracking (crazing), visual color change, spatial uniformity of deterioration (due to dirt pick-up and uneven color changes, or both), and overall surface texture. Chalking and dirt pick-up, as rated visually prior to this evaluation, could not be accurately assessed with the digital imaging technique.

The analysis shows that surface cracking and crazing generally can be well characterized using the automated VIEEW™ system. The study also confirms that judging color changes visually is problematic, since cracking and crazing interferes with color judgment. Further investigations are needed to develop an automated surface characterization method for sealants.

References

[1] Pourdeyhimi, B., Wang, X., and Lee, F., "Evaluation of Scratch and Mar Resistance in Automotive Coatings: Nano-Scratching by Atomic Force Microscope," *European Coatings Journal*, Vol. 3, 1999, pp. 72, 73, 76, 78, 79.

[2] Pourdeyhimi, B., Wang, X., Lee, F., and Schoff, C., "Evaluation of Scratch and Mar Resistance in Automotive Coatings: Surface Reflectivity and Texture," *Proceedings of the RETEC 98, September 27-29, 1998, SPE Color & Appearance Annual Conference*, Cleveland, OH, Society of Plastics Engineers (SPE)—Color and Appearance Division, Brookfield, CT, 1998, pp. 1–24.

[3] Lee, F., Pourdeyhimi, B., and Adamsons, K., "Analysis of Coatings Appearance and Surface Defects Using Digital Image Capture/Processing/Analysis (Chapter 14)," *Proceedings, The International Symposium on a Systems Approach to Service Life Prediction of Organic Coatings*, Breckenridge, Colorado, September 14–19, 1997, American Chemical Society, D. R. Bauer and J. W. Martin, Eds., Washington, DC, 1997, pp. 207–232.

[4] Lee, F., Pourdeyhimi, B., and Martin, J., "Comparative Study of Standard Weathering Test Methods Using Image Analysis," *Durability 2000: Accelerated and Outdoor Weathering Testing, ASTM STP 1385*, J. D. Evans and W. D. Ketola, Eds., ASTM International, West Conshohocken, PA, 2000, pp. 15–34.

[5] Wypych, G., Lee, F., and Pourdeyhimi, B., "Comparative Study of Sealants Durability—Surface Changes," *Proceedings, Durability of Building and Construction Sealants*, February 2–3, 2000, RILEM Publications S.A.R.L., A. T. Wolf, Ed., Cachan, France, 1999, pp. 173–197.

Journal of ASTM International, Vol. 3, No. 8
Paper ID JAI13136
Available online at www.astm.org

Daniel Huff[1]

Nondestructive Field Testing of Installed Weatherproofing Sealant Joints—Questions and Answers

ABSTRACT: With current expectations for building exteriors to prevent all air and water entry into the building interior, the need for a near perfect seal of weatherproofing sealant joints has reached new levels of intensity. The need for better field tests has increased accordingly. To reach these goals, ASTM Standard C-1521-02a [1] has been developed and adopted. The practice outlines a nondestructive procedure. This procedure provides an examiner of the joint the option of inducing an artificial strain to the sealant bead using a blunt instrument so that the sealant is subjected to a stress at the bond line typical to the anticipated cyclic movement endured by the sealant during the normal service life of the joint. The advantage of this methodology is that it allows an unlimited amount of testing to be conducted. While the procedure does not specify a specific instrument to induce the strain, a device able to accomplish this procedure in a uniform, controlled, and calibrated fashion has been developed. The paper outlines a description of the device and its capabilities. The paper also provides a discussion of the use of statistical sampling when the option of 100 % testing is not feasible or required. The author believes that the future of field testing of installed weather proofing sealant joints should include enhanced nondestructive procedures. Continued field use, research, and development are essential in the quest for a near perfect building seal.

KEYWORDS: sealant, adhesion, nondestructive, testing device, field testing, toxic mold, ASTM Standard C 1521

Introduction

The following discussion is directed toward barrier wall construction (face sealed) utilizing a single line of sealant joint as the only defense against the exterior climate. For the purpose of this discussion, failures are defined as loss of sealant adhesion. Adhesion failure is easily defined—the sealant either sticks to the joint or it pulls away free and clear. Joint geometry is not as easily defined with a pass/failure criterion, but it is discussed below. While the information provided may be useful in other areas of consideration, the author makes no assertions beyond those stated here. The stated goal of the testing advocated here is to find and fix failures of the sealant with the net result of producing a durable and complete building seal.

The current paper is a follow up to a previous paper by the author [2]. That paper began with the following comment: "A durable building seal requires full and continuous adhesion of the weatherproofing sealant in all joints at all locations." This comment coincides with the fact that the expectation for building exteriors to prevent all air and water entry into the building interior has reached a new level of intensity. In the case of toxic mold litigation, it has simply become too costly to expect anything less. It is the intent of this paper and the research it shares to assist the industry in achieving this goal. To that end, ASTM committee C-24 has taken the step of adopting ASTM Standard C-1521-02a, "Standard Practice for Evaluating Installed Weatherproofing Sealant Joints" [1].

The standard advocates a nondestructive procedure that provides the examiner of the joint the option of inducing an artificial strain to the sealant bead using a blunt instrument so that the sealant is subjected to stress at the bond line typical to that produced during the cyclic movement of the joint during normal service life (ASTM Standard C-1521 at 1.4, 6.1, and 7.1.2). This procedure validates the previously conceptual testing method of application of external pressure to the installed weatherproofing sealant joint.

The advantage of nondestructive testing is obvious; the quantity of sealant joint available for test is limited only by the needs of the specifying authority and access to the joint. A device able to accomplish

Manuscript received May 3, 2005; accepted for publication May 16, 2006; published online August 2006. Presented at ASTM Symposium on Durability of Building and Construction Sealants and Adhesives, Second Symposium on 15–16 June 2005 in Reno, NV; A. T. Wolf, Guest Editor.

[1] Associate Consultant, Construction Consulting Laboratory, 4751 West State Street, Suite B, Ontario, California 91762.

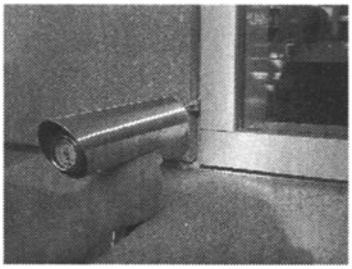

FIG. 1—*Photo of pressure-controlled inspection device.*

this nondestructive procedure in a uniform, controlled, and calibrated fashion has been developed. The paper outlines a description of the device and its capabilities and provides a discussion of the use of statistical sampling when the option of 100 % testing is not feasible or required.

Description of Controlled Calibrated Constant-Pressure Device

The newly developed apparatus is a handheld instrument able to exert pressure in a controlled manner to the sealant joint. Extending from the housing at the front of the device is an armature with a roller at the tip. Behind the armature is a piston charged with compressed gas delivered from a pressurized tank. The amount of pressure behind the piston translates directly into the amount of force that is applied to a surface to which the roller probe is engaged. The amount of gas pressure delivered from the pressurized tank is adjusted with a regulator. Pressure within the device and behind the piston is monitored from a gage visible at the rear of the housing. Within the housing the gas pressure is manipulated in such a way that the pressure is constant within the entire stroke of the piston. Pressure in the apparatus as derived from the gas source resulting in strain at the probe contact point is maintained provided that the armature is somewhere within the stroke of the piston. The user pushing in or pulling from the joint with the device during operation cannot alter the pressure at the probe contact point. This means that the pressure that the test probe exerts on the sealant remains constant. To maintain constant pressure, the piston must simply be kept within its stroke range.

The bottom line is that pressure applied to the joint for the purpose of testing is not dependant on adjacent surfaces (as in the case of a backer rod placement style device) or the judgment of the user (as in the case of a screen roller or similar device) when using the pressure controlled device (see Fig. 1).

The ability to maintain consistent controlled strain coupled with infinite adjustability provides the opportunity for calibration. This was described in detail in the above referenced paper [2].

Field Use and Statistical Sampling

When approaching a building with the intention of assessing the quality of the sealant joints, the question arises, "Does the entire building need to be tested?" Under many circumstances, the answer is yes. This may be due to a specification, a warranty requirement, or any variety of other conditions that we need not discuss here. The question to address here, based upon experience in the field, is what constitutes an adequate sample that will provide quantifiable data for statistical relevance?

Where Should Sampling Occur?

The first consideration is where should the sampling take place? In northern latitudes, a southern exposure is an obvious first location to sample, with the converse logic applying in southern latitudes. This allows the sampling to occur where the greatest thermal joint movement takes place.

The next best place to sample is the "weather side" of the building. The reason for this is that difficulties during construction in obtaining dry substrates to apply sealant tend to be on the weather side. However, at times the difficulties may occur on the "dark" (shaded) side of the building where there may be a reduced ability for the substrate to dry out.

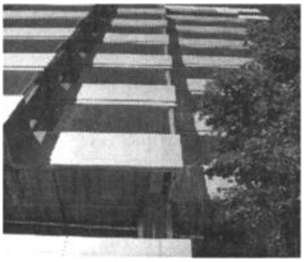

FIG. 2—*Weather side of a building not much affected by moisture problems ("Specimen A").*

Of course, historically verifiable problem areas take first place in order of importance. Without historical data, the tester must take many thoughtful considerations into account when deciding on sampling locations. Dictating this is not appropriate here or in any document due to the uniqueness of every building both in its construction and circumstance. As an example, Fig. 2 shows a building where the weather side was not as much affected by moisture problems as the "dark" (shaded) side since on the weather side the joints were able to dry out. This building façade side is considered "Specimen A" for the subsequent discussion.

How to Take the Sample

The next question to address in the sampling is how to take the sample. Again, every building is unique and subject to specific circumstance, therefore the following example is offered for the purpose of illustrating such distinctive characteristics and what may be done to address them: On a recent project the entire building exterior (13 stories) utilized fixed standing scaffolding. After interviewing the sealant applicator it was learned that a team of applicators working together in assembly line fashion (one cleaner, one backer rod installer and primer, and one sealant installer) had worked in a horizontal configuration around the building. The result was that the sampling was conducted vertically as an effort to sample potential changes in the crew's application procedure over the installation time period. Historical information such as that obtained in this case is not ordinarily available, but the example is offered to illustrate the strategy one may use to obtain the most accurate sample.

If suspended power staging was the method used during construction, it is important to sample at least two separate areas to allow for possible variations resulting from different crews working on different locations. Since staging crews typically move the suspended power staging horizontally from one grid to the next, it can be assumed that sampling two grid areas side by side would not be as effective as sampling at completely different areas of the building. If knowledge of the construction access is not available, it nevertheless is logical to sample in the method suggested here.

Figure 3 shows as a further example an 18-story condominium project where balcony access allowed for comprehensive statistical sampling. In this case, balconies were accessed at random on all floors on every elevation.

FIG. 3—*Condominium project allowing balcony access for a comprehensive statistical sampling.*

TABLE 1—*Statistics generated from sealant testing (Specimen A).*

Parameter	Statistics
Linear length of sealant joint	10 668 m (35 000 feet)
Number of adhesive failures	427
Average length of failure	50 mm (2 in.)
Failure rate in linear length of joint	one in 25 m (82 feet)
Total linear length of sealant failure	21.6 m (71 feet)
Percentage rate of sealant failure	0.2 %
Percentage rate of sealant success	99.8 %

How Much Should be Sampled?

The next question is how much sampling should take place. Experience has demonstrated that if at least 5 % to 10 % of the building is sampled, the results are usually representative of the entire sealant installation.

For example, on an 11-story building, with 24 grid locations for suspended scaffolding, two grids were sampled. This represented an 8.3 % sampling rate. The inspection revealed 14 adhesion failures on one grid section, and 20 on the other, for an average of 17 failures per grid section. From this sample, it was predicted that 408 failures would be found on the entire building if testing was conducted at a 100 % rate. A complete 100 % inspection of the building revealed a grand total of 427 adhesive failures. This result indicates that statistical sampling forms a solid basis for obtaining a realistic view of the sealant installation on a building.

How Much Additional Testing Should Occur After Initial Sampling?

As a final consideration, one should ask, "How much of the building is to be tested after the initial sampling is completed? To what level should the testing ascend? What should be the recommendation to the authority that specified the sampling?" These are questions that may be considered in the future by ASTM Committee C-24. However, using what typically is a pass/fail criterion in a façade mock-up testing laboratory may provide some guidance.

We will next make that comparison in terms of a pass/fail criterion. First, using the example of the 11-story building described above to review the resultant data from testing, we will establish a theoretical basis from which we may begin discussion in order to answer this question. Let this referenced test data be referred to as project Specimen A.

Statistical Interpretation of Data Obtained on Specimen A

In the case cited here as Specimen A, the sealant applicators participated in the testing process and fixed the failures immediately after they were found. The entire process took a total of six days (see Table 1).

Discussion Regarding Specimen A and Acceptable Rates of Failure

These numbers illustrate that the failure rate on the Specimen A wall grid was approximately four failures for every 90 m^2 [1000 ft2]. The average size of a wall specimen tested in a mock-up laboratory prior to construction is around 90 m^2 [1000 ft2]. For example, Fig. 4 depicts a wall section prior to testing at

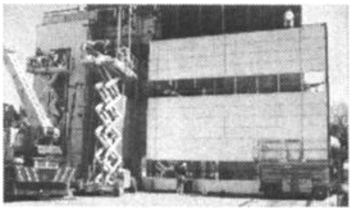

FIG. 4—*Mock-up wall section prior to testing at Construction Consulting Laboratory West, Ontario, California.*

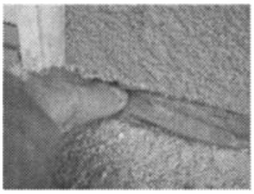

FIG. 5—*"Tag and fix" approach to sealant testing.*

Construction Consulting Laboratory West, Ontario, California. This mock-up wall section was approximately 1000 ft2 [90 m2] when completed. The number of leaks allowed in the laboratory to pass the wall test is zero. It is the author's opinion that a zero seal failure rate is the best assurance that a wall will not allow water entry, this opinion is based on what is typically found during laboratory mock-up testing.

Joint Geometry

When this paper was initially conceived, it was felt that joint geometry should be discussed. Why? With a pressure-constant strain device, the joint geometry is easily visualized because the strain on the sealant does not fluctuate by any action of the tester meaning that when the sealant thins, the probe goes deeper into the joint, and when the sealant thickens, the probe stays closer to the surface of the joint. This observation has been demonstrated with sealant manufacturers representatives present during the testing process. To verify what was visually discernable on the surface during the test, locations with what appeared to be radical deviations were marked, cut into, and examined by the sealant manufacturer's representatives. In nearly every case, the anticipated geometry was confirmed.

However, assuming no failure in adhesion had yet occurred at the location, the information was noted as verification that the pressure-constant device is able to provide that kind of information, not as a pass/fail criterion for the test. At no time was this information reported upon. Before that type of information is deemed necessary to collect and report, sealant manufacturers must define the pass/fail criterion. Put another way, it is the opinion of the author that the purpose of sealant testing in a nondestructive testing system should primarily be focused on finding adhesion failures, the main purpose of this discussion as stated in the Introduction, and additional information derived from testing may or may not be relevant.

Conclusions

Nondestructive field testing of installed weatherproofing sealant joints using a pressure-controlled, constant, and calibrated testing device provides valuable information. Much attention has been paid in development to make the device independent of the user to regulate and maintain the contact probe pressure. The calibration of the device to the property of various sealants allows the user to refer to a calibration chart, dial up the correct pressure, and let the device do the rest. This means that no matter the user, when identical pressures are dialed into the test device system, the pressures applied to the test specimens are consistent. Our initial studies indicate that this approach provides a reproducibility potential that may not be available from less controlled or uncontrolled test devices. However, other devices can provide information, too. For example, one may use a three pronged roller assembly known as an "adjustable backer rod placement device" which offers limited pressure control potential to the center roller from the side by side rollers moving over adjacent surfaces. Also, a window "screen roller" where pressure is uncontrolled, or rather is controlled by the arm of the person using the device, may be used. Additional research in comparing various devices to determine significant differences affecting outcome is under way. In the meantime, no matter what device is used, the author would suggest that the focus of any testing should be directed toward uncovering adhesive sealant failures with the intent to tag and fix the failures. This is because even a very small failure rate (defined in the Introduction as "loss of sealant adhesion") in terms of total installation of sealant can pose substantial problems for the building. Figure 5 illustrates the "tag and fix" approach to sealant testing. Since in the example shown the sealant was silicone, the documenting consultant used survey ribbon and a construction grade stapler to fix the "flags" into the sealant bead at the failure locations making it easy for the sealant installer to make repairs.

The Future of Sealants in Barrier Wall (Face Sealed) Construction

An associate of the author made the following comment when presented with the data included in this paper [3]: "Even with above average workmanship, there will always be a failure rate. Even if sealant joints on any given project are as good as 99.5 % successful (an extraordinary achievement in any human endeavor), the remaining 0.5 % can cause significant damage. Submarines have bilge pumps to catch the leaks from the 0.5 %. There needs to be a second line of defense. Nothing we do is perfect enough to rely on a sealant joint 100 % of the time, and in my opinion, this is a foolhardy approach to building design."

The problem is that the majority of constructed buildings in the United States and throughout much of the globe rely on face sealed technology. Due to the high cost of rain screen technology, this situation will likely remain unchanged in the immediate future.

In the meantime, water is promiscuous and has all the time in the world. How long does the industry have to take appropriate action to address the problem of less than adequate building seals? When does "zero tolerance" start to enter our mentality?

Ultimately, will sealants be relegated to a position of irrelevance in exterior building construction? Will barrier wall systems (face-sealed) disappear? In the opinion of the author, despite the cost, the rain screen wall system may well become the gold standard unless enhanced field testing of sealants is adopted by the industry as a recommended and encouraged activity.

References

[1] ASTM Standard C-1521-02a, "Standard Practice for Evaluating Adhesion of Installed Weatherproofing Sealant Joints," *Annual Book of ASTM Standards*, ASTM International, West Conshohocken, PA.

[2] Huff, D., "Non-destructive Field Testing of Installed Weatherproofing Sealant Joints," *Durability of Building and Construction Sealants and Adhesives, ASTM STP 1453*, A. T. Wolf, Ed., ASTM International, West Conshohocken, PA, 2004, pp. 335–345.

[3] Gallant, P. E. and B. Arch, *MAIBC, MRAIC, Morrison Hershfield, Ltd.*, Canada, & Morrison Hershfield Inc., Atlanta, GA, personal communication.

www.astm.org

ISBN: 978-0-8031-3414-0

Stock #: STP1488